FH Vorarlberg
Vorarlberg University of Applied Sciences

Development of an Active Knee Rehabilitation Device

Master's in Mechatronics

A Thesis Presented in Partial Fulfilment
of the Requirements for the Degree
Master of Science
Dornbirn, 2011

Submitted by
Sebastian Bereuter BSc

[Accomplished at
Arizona State University
Human Machine Integration Laboratory]

Abstract

The "Development of an Active Knee Rehabilitation Device" allows a large variety of possible topics and directions for the thesis. The goal of this work is the realization of a device capable of supporting the user for knee rehabilitation. The term "active" indicates that active elements such as motors, or active damping devices are used to vary the forces, torques or resistance felt by the user.

In the USA up to 250,000 annual Anterior Cruciate Ligament (ACL) injuries occur and approximately 175,000 ACL reconstructions are accomplished every year. Most knee injuries occur in popular sports such as soccer, skiing, American football and basketball. State of the art rehabilitation and gym machines use largely weights to generate forces or torques, which can be varied by changing the number of weights, but they are not capable of changing the torque between concentric contraction (weight lifting) and eccentric contraction (weight lowering) and the generated torque has a fixed torque-knee angle characteristic (e.g. a constant torque at all knee angles). An active device makes it possible to actively change torques for different angles and movement directions and thus provides the possibility of a more effective rehabilitation program.

A wide literature review describes existing knee devices and the ongoing research in the field of knee orthoses and rehabilitation devices followed by a focus on the human knee including anatomic structure, biomechanics in closed kinetic chain exercises and a description of knee movement and torques during gait. A new way to investigate stiffness at the knee during gait is included which, to the knowledge of the author, has never been described before for the knee.

A wide design study evaluates different design concepts and after a decision in favor of replacing the weights of an existing training device, several design proposals are studied in detail. A concept of using a motor to power concentric movements and the same motor as a brake to resist eccentric movements is chosen because it can fulfill all requirements. A bench type prototype was built and tested. The prototype is a proof of concept and shows that the chosen direct attachment of a motor/generator via gearboxes at an existing leg extension/curl bench is capable of providing the desired variable torque-angle characteristics during exercising.

Abstract - German

Die Bezeichnung "Entwicklung eines Aktiven Knie Rehabilitations-Geräts" lässt eine weite Bandbreite an möglichen Entwicklungen offen. Ziel ist es ein Gerät oder eine Maschine zu entwickeln, die den Patienten bei der Knie Rehabilitation unterstützt. Der Begriff "aktiv" deutet dabei an, das aktive Elemente wie Motoren oder aktive Dämpfer benutzt werden um entstehende Kräfte und Drehmomente aktiv zu variieren.

Jährlich treten in den USA bis zu 250.000 Verletzungen des vorderen Kreuzbandes auf und davon werden 175.000 operativ behandelt, was immense volkswirtschaftliche Kosten nach sich zieht. Die meisten Verletzungen treten in populären Sportarten wie Fußball, Schi fahren, American Football und Basketball auf. Standard Rehabilitations- und Trainings-Geräte nutzen meist Gewichte um Kräfte und Drehmomente zu erzeugen, die dann vom Benutzer überwunden werden müssen. Je nach Benutzer kann die Intensität der Belastung mit der Anzahl der Gewichte variiert werden, allerdings ermöglichen diese Geräte keine Veränderung während einem Zyklus zwischen konzentrischer Belastung (Gewicht heben) und exzentrischer Belastung (Gewicht wieder hinunterlassen). Zusätzlich ist die Drehmoment-Winkel Charakteristik fix vorgegeben (z.B. konstante Belastung für alle Positionen/Winkel). Genau hier setzt der Ansatz dieser Arbeit an. Es soll ein Gerät entwickelt werden, das flexible Belastungen während der Ausübung ermöglicht.

Eine breite Literatur Recherche zeigt existierende Knie-Apparaturen, den aktuellen Stand der Forschung und zeigt wichtige Aspekte um Knie Rehabilitation. Es werden die menschliche Knie Anatomie, Muskel- und Knochen-Strukturen sowie auftretende Kräfte und Drehmomente im Knie gezeigt. Eine neue Art Knie-Steifigkeit während dem Gehen zu analysieren wird gezeigt, die nach dem Wissen des Authors nie zu vor für das Knie beschrieben wurde.

Mit Drehmoment-Winkel Charakteristiken aus der Literatur-Recherche als Basis, werden verschiedene Realisierungsmöglichkeiten grob analysiert. Für den Ersatz der Gewichte an einem existierende Trainingsgerät werden detaillierte Design-Vorschläge ausgearbeitet und derjenige mit dem besten Realisierung-Potential wird in einem Realisierungsteil getestet.

Der Realisierungsteil ist als Konzeptstudie aufgebaut und zeigt, dass die gewählte Variante, bei der ein Motor/Generator über zwei Getriebe direkt an rotierende Achse einer Bein Trainingsbank befestigt wird, funktioniert und mit Hilfe von zwei verschieden Reglern die gewünschten variablen Drehmoment-Winkel Charakteristiken zur Verfügung stellen kann.

Contents

List of Figures

List of Tables

1 Introduction

1.1 Needs and Motivation for this Work

In knee rehabilitation the Anterior Cruciate Ligament (ACL) has a very crucial role because it can be torn easily. In the USA up to 250.000 annual ACL injuries occur and approximately 175.000 ACL reconstructions are accomplished every year, which makes the ACL the most commonly injured ligament in the human body and causes annual costs of more than $ 2 billion and these numbers are still rising [11] [12] [45]. According to a study at West Point 3.5 % of women and 3.2 % of men of the US population suffer an ACL tear within four years [27].

A 10-year study in Switzerland and Germany by Majewski et al. investigated the epidemiology of athletic knee injuries [28]. Sports like snowboarding, inline skating, mountain biking and the use of carving skies has become more and more popular, where the lower extremities and especially the knee is involved. Within the class of internal knee injuries, ACL injuries account for 45.5 % the most common knee injuries, followed by injuries of the medial meniscus with 24 % [28].

Approximately 50 % of the injuries happen to persons between the ages of 20 to 29 years old. In total numbers, the most knee injuries happen while performing soccer with 35 % and skiing with 26 % share of all knee injuries. If the injuries are related to the number of people who are performing the sport, squash (active traumas / active members = 2.39 %), American football (1.46 %), skiing (1.08 %) and ice-hockey (0.83 %) are the most dangerous sports. Soccer has a "risk-coefficient" of 0.32 %, a lower risk of getting injured, but as it is very popular, most injuries in this study happened in soccer because of the larger number of players multiplied by 0.32 % [28]. Other studies by Holzach showed that the number of knee injuries caused in sports activities is double the number of knee injuries caused by traffic accidents in Switzerland [25].

Especially in sports like American football, soccer, skiing and basketball, many ACL injuries occur due to involving high pressure and twisting stress on the knee and physical contact [18]. Besides ACL injuries, knee structures like Meniscus (medial and lateral) and Articular Cartilage are common knee injuries [45]. All of these injuries involve rehabilitation exercises for the knee muscle groups (hamstrings and quadriceps).

Ideally, knee rehabilitation starts immediately after an injury with rest, ice cooling, and elevation of the injured leg. Two to four weeks after the injury, surgical reconstruction is performed if needed but already before the operation and immediately after it moderate rehabilitation exercising should be performed. Professional equipment like continuous passive motion (CPM) machines

or the Biodex Isokinetic Dynamometer are able to run different exercise patterns to allow flexible, rehabilitation training, but unfortunately such devices are very expensive and thus only available for a low percentage of the injured population.

The goal for this research is the development of an active knee rehabilitation device, which is capable of applying different exercise patterns for the knee muscles and also log e.g. moment-angle dependencies for the different training sessions to document the rehabilitation progress.

Additionally to rehabilitating the muscles, the same device could be used for strength training e.g. for professional sport coaching. The only change is a different exercise pattern e.g. with higher knee torques during movement. Also of interest is the fact, that additionally with other risk reducing factors, strength training of knee muscles reduces the risk of an ACL injury in sports up to 40 % [45].

2 Literature Review on existing Knee Devices

2.1 Commercially Available Active Knee Devices

2.1.1 C-Leg

Variable damping prostheses are able to vary the damping of the knee device according to the actual phase of gait. An available variable-damping prosthesis is the C-leg shown in Figure 2.1 from Otto Bock Inc, which uses microprocessors to control the damping of the knee joint.

Figure 2.1: C-Leg Prosthetic. A variable damping prosthesis controlled by a microprocessor. The system provides support to the user for walking down stairs or slopes, but cannot provide active power for walking up [2].

The C-Leg was introduced in 1997 and was the first commercial microprocessor controlled prosthesis. The microprocessor-based hydraulic system adapts the stiffness according to the actual phase of gait. To control the device, strain gauges in the tube adapter and a knee angle sensor are sampled every 20 ms. Whereas the variable stiffness is a big advantage to conventional prostheses especially when walking down slopes or stairs, it cannot support the user with positive power for walking up slopes or stairs [2].

2.1.2 Variable Damping Orthoses

The commercially available knee orthoses are mostly passive or variable damping devices, which are able to vary the damping of the knee device according to the phase of gait. During the stance phase, the knee is locked and is released during the swing phase. Figure 2.2 shows such devices provided by the companies Otto Bock Inc and Ossur Inc.

Variable damping orthoses have the same advantages as the C-leg described before. They are

Figure 2.2: Variable damping orthoses, Left: Free Walk orthosis by Otto Bock Inc , Middle: E-MAG Active orthosis by Otto Bock Inc [3] Right: CTi Custom by Ossur Inc [4].

able to support the user for walking down slopes or level walking, but cannot provide positive power need for walking up slopes or ascending stairs.

2.1.3 Active Knee Orthoses

Horst et al. introduced a knee exoskeleton developed at the company Tibion Inc. The orthosis is capable of supporting patients up to 100 kg for movements like sit-to-stand, ascend, descend and horizontal walking and was developed for rehabilitation and mobility enhancement. It is basically an active knee orthosis with additional support for the ankle. To keep the weight low, it is constructed of carbon fiber. In the exoskeleton, the actuator, motors, battery, electronics and user interface are integrated and the active elements are located on the thigh. The quite bulky looking device shown in figure 2.3 is the bionic leg called PK100.

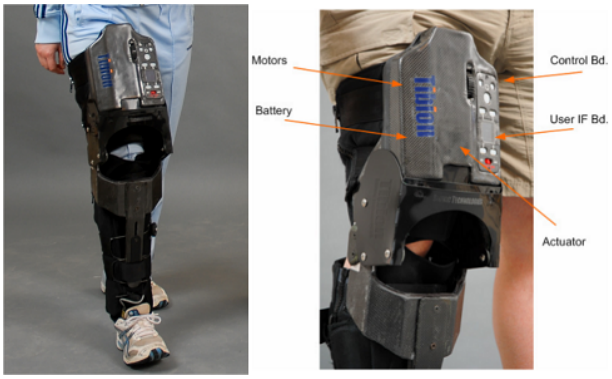

Figure 2.3: Tibion's active knee orthosis capable of supporting patients up to 100 kg for movements like sit-to-stand, ascend, descend slopes and stairs, and horizontal walking. It was developed for rehabilitation and mobility enhancement [26].

For the controlling of the device, foot-sensors are used to measure the pressure on the foot and also information about the knee angle and applied forces by the actuator are collected. Different

modes like auto, passive and a therapy mode can be selected by the user.

According to the author, significant improvements in walking speed can be achieved after four weeks. The system is already in a testing phase at hospitals and videos show the device working well [26].

2.2 Power Exoskeletons

2.2.1 RoboKnee

Pratt et al. introduced an active knee orthosis which is shown in figure 2.4. The device is designed to increase the power of the wearer and is fabricated from a commercial knee brace combined with a motor in series with a spring, which shows similarities to the Robotic Tendon introduced by Hollander [24]. The actuator is located between the upper and lower portions of the knee brace and thus can generate a torque about the knee.

Figure 2.4: Active knee walking orthosis (RoboKnee). The batteries in the backpack allow heavy usage up to 60 minutes [8].

A computer system and 4 kilograms of Nickel-Metal-Hydride batteries in a backpack allow up to 60 minutes of heavy usage. For the control algorithm, the ground reaction forces are measured and the necessary motor torque is calculated [34]. The system shows promising results and worked well in videos. However the weight of the system is more than 6 kg quite heavy and movements like sit-to-stand are not possible. Although the RoboKnee was already introduced in 2004, the project still is in a prototype status and no commercial variant of the RoboKnee is available. Further funding is needed to commercialize the device.

2.2.2 Berkeley Lower Extremity Exoskeleton

The Berkeley lower extremity exoskeleton (BLEEX) which is shown in figure 2.5 is designed to increase strength and endurance of the wearer in the field. It allows the user to carry major loads up to 75 kg on long marches.

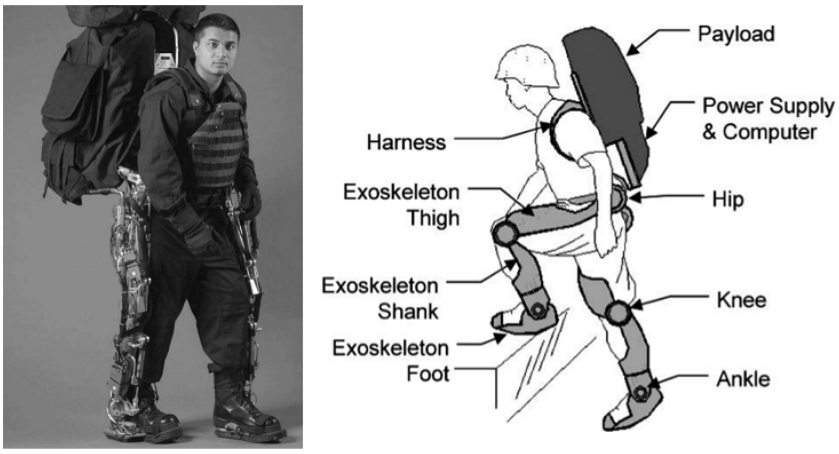

Figure 2.5: Berkeley lower extremity exoskeleton (BLEEX) is designed to increase strength and endurance of the wearer in the field. For controlling the system, no sensors are integrated to measure contact forces between the the wearer and the exoskeleton. Instead forces, accelerations and positions in the exoskeleton are measured [46].

For controlling the exoskeleton, no direct measurements of the human contact with the exoskeleton are used such as force sensing resistors. Instead, the forces on the exoskeleton are measured with sensors in the exoskeleton and every actuated joint has an encoder and linear accelerometers to determine the joint angle, angular velocity, and angular acceleration. Also inclinometers and force sensors are integrated in the exoskeleton. Foot switches are used to measure how the weight is distributed on each foot.

In order to save energy not all of the seven degrees of freedom (DOF) of the exoskeleton are actuated. The actuated joints are the hip, knee and ankle where always only one DOF is actuated. The knee joint of the exoskeleton is able to flex up to 121 degrees which allows more complex movements in the field than only horizontal walking which needs a knee flexing angle of 74 degrees. The actuators used in this system are linear double acting hydraulic actuators which have very high specific power, but they need a constant supply pressure of 6.9 MPa which results in a constant energy consumption of the hydraulic supply system. The resulting efficiency of the hydraulic actuation is low due to the pressure drop in the pipelines, valves and the efficiency of the hydraulic supply. The total efficiency of 14 % is very low compared e.g. to an electrical actuation system. Thus, for mechanical power of 165 W at the joints, an input power of 1143 W is necessary [46].

BLEEX is a remarkable project and is the first exoskeleton which allows one to carry an additional payload and is supported by the Defense Advanced Research Projects Agency (DARPA).

2.2.3 Hybrid Assistive Limb - HAL

Sankai et al. introduced the Hybrid Assistive Limb (HAL) which is an active exoskeleton for legs and arms. There are different prototype versions of HAL. HAL-1 to HAL-4 are for the lower body and HAL-5 assists legs and arms. The system is designed to assist disabled and elderly people in their daily life. Figure 2.6 shows HAL-1, HAL-3 and HAL-5 exoskeletons.

(a) HAL-1(1999). (b) HAL-3(2001). (c) HAL-5(2005).

Figure 2.6: Hybrid Assistive Limb - HAL. HAL-1 and HAL-3 support the legs and HAL-5 the legs and the arms. [38].

The actuators consist of DC motors. In the HAL-1 system the motor is connected to a ball screw and the newer systems have rotational actuators including a DC servo motor with a harmonic drive gearbox.

The HAL system uses electromyography for assisting a healthy person and the EMG signal also provides an input to an intention based controller e.g for a paraplegia patient. As there are two different control algorithms integrated into the system, it leads to the notation "hybrid" controller. The intention based controller uses information like the shift of the center of gravity from one leg to the other or a leaning into the front or the back of the structure to estimate the users intention (a paraplegia patient still needs walking assistive devices such as a walking frame or a cane for balance).

The exoskeleton consists of power units, sensors, a controller and an exoskeletal frame. Potentiometers are used to measure the angular position of the joints and also the floor reaction forces are measured by pressure sensors in the the sole of the foot part for intention estimation [38]. The weight of the system is approximately 15 kg for the HAL-3 and 23 kg for the HAL-5, and as the DC motors with very high gear ratios are directly connected to the human body without any compliance, safety aspects must be a concern. The HAL system is a remarkable achievement

with a big potential as e.g. the elderly assistance, a growing population in many countries such as Japan and the U.S.A.

2.3 Devices for Knee Rehabilitation

2.3.1 Active Knee Rehabilitation with an Electro Rheological Damper

An electro-rheological fluid-based variable damper combined with an active torque actuator was introduced by the "Dinos Mavroidis" Lab at Northeastern University. Figure 2.7 shows a prototype called “Active Knee Rehabilitation Orthotic Device (AKROD)”. An electro-rheological fluid increases its viscosity if an electrical field, which is acting on the fluid, is increased. Thus, it is quite easy to control the stiffness of a damper built with this fluid. A disadvantage of this damper type is a constant need of energy to control the viscosity especially if the electrical field is held constant over a long time.

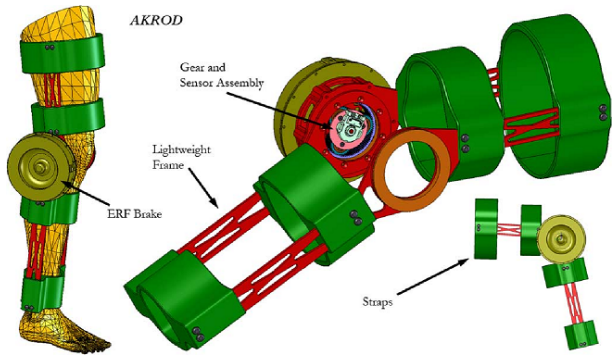

Figure 2.7: Active Knee Rehabilitation Orthotic Device (AKROD) introduced at Northeastern University. An electro-rheological fluid-based variable damper combined with an active torque actuator [32].

The active torque actuator, called a gear bearing drive, is basically a DC motor within a sun gear. It was developed for rehabilitation purposes and provides approximately 30 Nm. A possible disadvantage of this system is the direct linkage of the actuator to the knee via the sun gear bearing which supplies no compliance. To measure the knee angle, velocity and acceleration, an optical sensor is located in the sun gear. An additional torque sensor measures the torque applied by the wearer which is used for closed loop control [32].

2.3.2 Active Knee Orthosis for Gait Rehabilitation with Pneumatic Muscles

At the IWT-Vlaanderen in Brussels an active knee orthosis for gait rehabilitation was introduced by Beyl et al. It is powered by pneumatic artificial muscles and is intended to prove the possibility

of powering an active knee orthosis with pneumatic muscles. As a pleated pneumatic muscle is only capable of supplying a contracting force, two pneumatic actuators in an antagonistic configuration are integrated. The antagonistic pneumatic muscle configuration is connected to a four bar mechanism which is shown in figure 2.8.

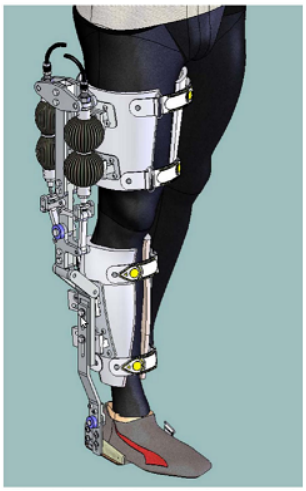

Figure 2.8: CAD drawing of an active knee orthosis for gait rehabilitation consisting of an antagonistic configuration based on a four bar mechanism [13].

A disadvantage of pneumatic muscles is their nonlinear force-contraction characteristic which has to be considered in the design. Especially if two or more pneumatic muscles work together, the control of this non-linearity is a difficult challenge. On the other hand, pneumatic muscles have a compliant behavior and are very light.

The prototype of this pneumatic system shows the possibility of such a system, but the challenging control of the artificial muscles, an integration of the electronic controls, and safety all need further research [13].

2.3.3 Backdrivable Knee Actuator for Investigating Gait in Stroke

Sulzer et al. introduced a knee actuator to investigate gait in stroke which is capable of assisting knee flexion just as the foot leaves the floor during gait (toe off) or during swing phase but it does not affect the knee during the rest of the gait cycle (stance). They call their actuator a "Series Elastic Remote Knee Actuator", which uses a cable transmission and is backdrivable. With a mass of 1.2 kg (without motor), it is very light and can provide a torque up to 41 Nm. Figure 2.9 shows the design of this active knee orthosis which is mounted to a commercial knee brace.

In order to achieve a compliant behavior, a torsional spring is used in series with a cable. To measure the spring displacement a goniometer is used, and for measuring the knee angle an

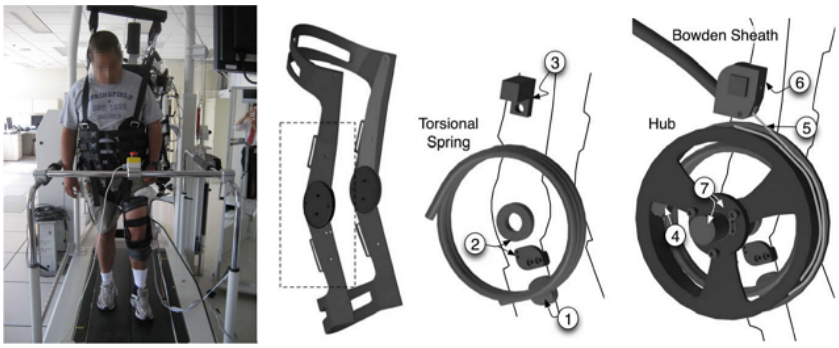

Figure 2.9: Backdrivable knee actuator for investigating gait in stroke consisting of a commercial brace, torsional spring, and a cable system. The free end of the cable is connected to a motor mounted to a bench and not on the person. The motor activates the system by pulling on the torsional spring [37].

annular magnet in combination with a Hall sensor is integrated. As the system is designed for treadmill walking a three-phase 230 V DC servomotor is used which is mounted away from the user to a fixture which drives a hub and anchors to the cable. For the motor, a torque controller is used, which either provides the desired assisting torque during toe off at the start of swing phase or zero torque during the rest of the gait circle. Orthosis tests with stroke patients showed promising results as a more natural gait could be achieved [37]. The most interesting parts of this design are the very light weight design due to the motor mounted on a fixture and the backdrivable behavior from the torsional spring.

2.3.4 Lower Extremity Powered Exo-Skeleton (LOPES)

Van der Kooij et al. from the University of Twente, Netherlands introduced the Lower Extremity Powered Exo-Skeleton (LOPES) which is a compliant actuated exoskeleton for gait training. The exoskeleton, shown in figure 2.10, is designed for the rehabilitation of post-stroke patients.

The exoskeleton is fixed to the treadmill at the pelvis which makes it possible to compensate the weight of the exoskeleton. The three actuated degrees of freedom are the hip, the knee and the pelvis. To keep the weight of the exoskeleton low, the joints are driven by motors via cables. The motors are in series with springs and thus the system is compliant and safer. Advantages of this system are its light weight because the motors are fixed to the base and the compliant behavior due to springs. The range of impedances varies from free walking (no assistance by the exoskeleton) to fully passive walking (the exoskeleton does all the work) [39].

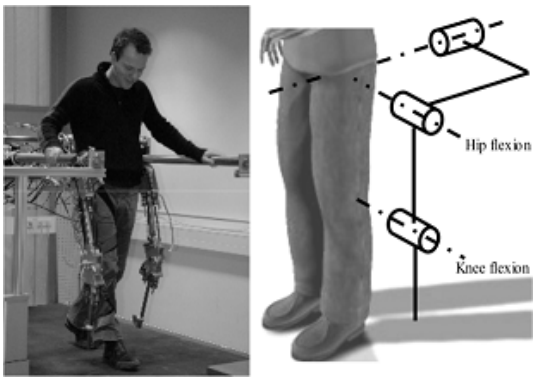

Figure 2.10: Lower Extremity Powered Exo-Skeleton (LOPES). The exoskeleton is fixed to the treadmill at the pelvis and is driven by motors via cables. To achieve a safer and compliant behavior, springs are integrated in series to the motor. The three actuated degrees of freedom are the hip, the knee and the pelvis [39].

2.3.5 Biodex Isokinetic Dynamometer

The Biodex Isokinetic Dynamometer is a professional rehabilitation device used for multi joint rehabilitation and strength enhancement. The electrically controlled servomechanism is used in clinical and research areas. The system provides different modes of operation like isokinetic, passive, isometric (concentric and eccentric), isotonic and reactive eccentric mode for various joints like the ankle, knee, hip, shoulder, elbow and wrist. An included software allows advanced data logging of the training improvements.

Figure 2.11: Biodex System 3 Isokinetic Dynamometer. In this figure, the Biodex system is used for knee extension/flexion. Different modes of operation like isokinetic, passive, isometric (concentric and eccentric), isotonic and reactive eccentric mode for various joints are supported [5].

Figure 2.11 shows the Biodex system used for knee extension and flexion. A knee angle from 0 to 135 degrees is possible. The possible speed ranges from 0 to 500 deg/sec and the torque can be varied from 0 to 677 Nm. Additionally to the open kinetic chain activities, which allow isolated

joint movements, also closed kinetic chain activities are possible with the biodex system, which is an important part of a complete rehabilitation program [5] [10].

As described, the Biodex system offers a large variety of professional operations and data logging. However prices for such a system are very high which makes it only available for clinics or professional gyms.

2.4 Energy Harvesting at the Knee

2.4.1 Quasi-Passive Knee exoskeleton to Assist Running

The power curve during a walking or running gait cycle is consisting of regions with positive and negative power (described in more detail later). The knee exoskeleton introduced by Dollar et al. tries to store energy during negative power regions with springs and releases the energy again in positive power regions. According to Dollar the human body is less efficient during running than during walking. The exoskeleton is designed to increase the efficiency of human running. The design shown in figure 2.12 consists of a spring carriage which is connected to a brushed DC motor via a belt drive and a ball screw.

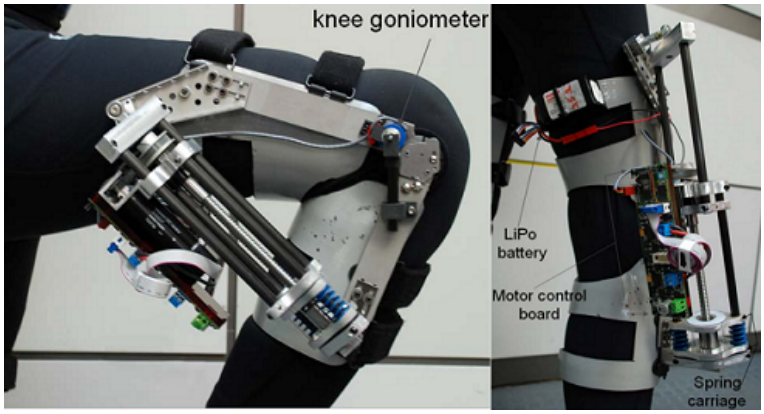

Figure 2.12: Quasi-passive knee exoskeleton to assist running. The device consists of a spring carriage which stores energy during negative power regions and releases the energy again when needed. When storing energy in the spring, the motor is stalled to support the force. [16].

When storing energy in the spring, the motor is stalled to support the force applied by the spring. During the swing phase, the spring carriage has to be removed quickly to allow free flexing of the knee. The actuator does not add energy to the system, but it moves the position of the springs. Thus Dollar calls it quasi-passive. The whole exoskeleton has a total mass of 2466 g including the very light commercial braces. To sense the knee for controlling the device, an optical encoder on the motor, a rotary potentiometer and foot-switch-sensor are used.

According to Dollar, the the prototype has possible design pitfalls with misalignment of joints between the wearer and the exoskeleton and the connecting of the exoskeleton with the wearer itself. Also there are undesired lifting forces to the user's leg and a resistance against motion is felt during swing [16]. If the prototype is working with the desired behavior, metabolic cost can be evaluated by measuring the oxygen consumption of the wearer with and without the exoskeleton during running. The effectiveness of the device is currently unknown.

2.5 Knee Assisting

2.5.1 Wearable Walking Helper

At the Tohoku University, Nakamura et al. introduced a wearable walking support system for elderly people which they call Wearable Walking Helper. The Wearable walking helper, shown in figure 2.13, takes into account that the human knee consists of two joints and thus the human knee joint generates rotation and flexion.

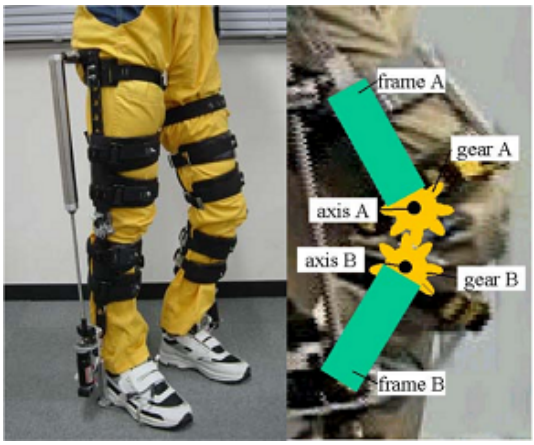

Figure 2.13: Wearable Walking Helper consists of geared dual hinges, a DC motor connected to a power screw and potentiometers mounted at the hip, the knee and the ankle joint. The system takes into account that the human knee consists of two joints [31].

The system consists of geared dual hinges, a linear actuator and potentiometers mounted at the hip, the knee and the ankle joint. The knee joint fabricated from geared dual hinges is also often used in commercial braces. The actuator consists of a DC motor and a power screw which is backdrivable. The controller tries to estimate the user's intentions with a model based control algorithm. With angular information at all of the joints and the ground reaction forces, the supporting joint moment is calculated from the user's posture.

According to Nakamura this method allows, in contrast to electromyography methods, one to calculate the necessary motor torque in real time, and also no EMG electrodes need to be fitted

to the human body directly. The signals measured by electromyography are a result of muscle contraction and thus a controller reaction based on this information is always delayed. Also EMG signals are very sensitive to placement of the device. The prototype of the Wearable Walking Helper showed promising results but more research needs to be completed [31] [30].

2.5.2 Limb Exoskeleton using Electromyography

Fleischer et al. introduced an active leg exoskeleton using electromyography (EMG) to control the system which is developed at the Berlin University of Technology. Fleischer focused in his work on the analysis of data collected with electromyography. The exoskeleton is shown in figure 2.14. The linear actuator consists of a DC motor which drives a ball screw. A force sensor is integrated to measure the actuator's force on the exoskeleton and the joint angle is measured with a Hall effect sensor.

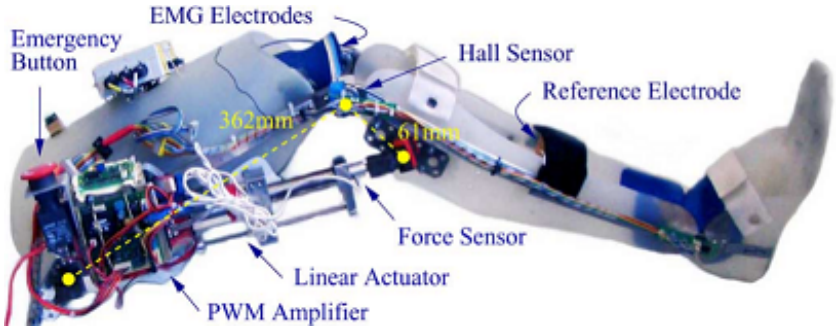

Figure 2.14: Limb exoskeleton using electromyography. The exoskeleton consists of a DC motor driving a ball screw, a force sensor to measure the actuator's force on the exoskeleton, a Hall effect sensor to measure the joint angle and several differential electrodes to measure the muscle activity [17].

For measuring the muscle activity several differential surface electrodes are integrated. The exoskeleton weighs approximately 5 kg without a PC and power supply. Evaluating signals collected with electromyography is a challenging task. In experiments with one healthy person, the system worked, but no experiments with other persons or with people who suffered a stroke were made [17].

It can be expected, that the signals look quite different from person to person and for stroke patients the signals will look very different as their muscles do not move in the correct manner with neuropathy. We believe that electromyography is not an interesting possibility to estimate the user's intention in stroke rehabilitation.

2.5.3 Assistive Knee Brace with Magnetorheological Fluid

Chen et al. introduced an active knee orthosis with a magnetorheological actuator which is shown in figure 2.15 at the Chinese University of Hong Kong. The actuator consists of a DC motor in combination with a brake/clutch which uses the magnetorheological effect. Active power is provided by the motor e.g. for walking upstairs and the magnetorheological brake acts when negative torque is needed.

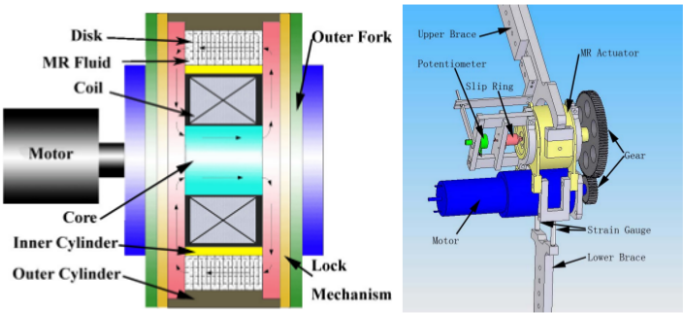

Figure 2.15: Assistive knee brace with magnetorheological fluid. The actuator consists of a DC motor in combination with a brake/clutch which uses the magnetorheological effect. Active power is provided by the motor. The left picture shows a schematic of the actuator with magnetorheological fluid and the the right picture shows the actuator in combination with the motor and the braces [15].

When a magnetic field is applied to a magnetorheological fluid, the magnetic particles in the fluid line up along the magnetic field and a stress is necessary to disrupt this connection. Thus it is possible by varying the magnetic field to vary the damping characteristics of a damper constructed with such a fluid.

If no magnetic field is applied to the fluid, the joint can rotate freely. When a magnetic field is applied, the torque of the motor is acting on the brace and thus also on the knee. By varying the applied magnetic field, the system can be used as controllable variable damper, when negative power at the knee is needed. The weight of the actuator is approximately 1 kg and it is capable of generating a torque up to 30 Nm. To measure the angular position of the joint, a potentiometer is used and for the measurement of force and torque about the knee joint of the brace strain gauges are used [15].

2.6 Previous Projects at the Human Machine Integration Laboratory

2.6.1 Powered Ankle Foot Prosthesis

Hitt et al. introduced a powered ankle foot prosthesis called SPARKy (Spring Ankle with Regenerative Kinetics), at Arizona State University. Hitt used the work of Hollander as a basis and introduced a working and tested powered ankle foot prosthesis. In SPARKy, a Robotic Tendon actuator is implemented. Figure 2.16 shows an isometric and side view of the powered ankle foot prosthesis described by Hitt.

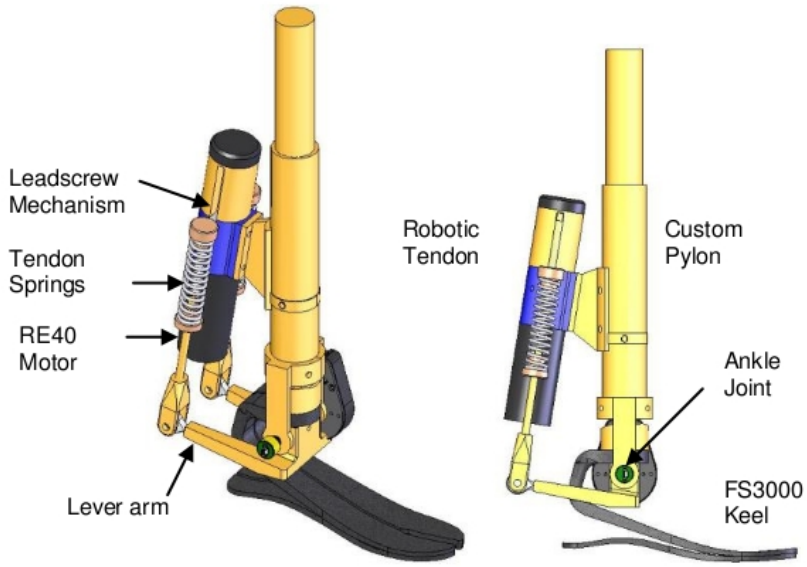

Figure 2.16: Isometric and side views of the SPARKy design. The motor coupled with the spring provides a dynamic moment about the ankle joint [22].

In his research Hitt presented modeling, design, analysis and testing of SPARKy. In an analysis, the behavior of the system was simulated with models and with this information the design of SPARKy was optimized. SPARKy was built using the optimized design and it withstood six months of rigorous testing and provided a lot of test data. This data shows that the prosthesis is able to provide 100 % of the ankle power and ankle joint movement similar to able-bodied gait. The longevity and durability are very important because only ten minutes of walking require more than 8.000 revolutions of the lead screw nut and 34.000 revolutions of the motor [22].

The spring stiffness and lever arm of SPARKy can be adjusted "offline" to the person (weight) and the walking conditions (walking, running, stair climbing,..). To get the best possible power amplification of the helical spring in series with a motor, the spring stiffness has to be adjusted. Power amplification is the ratio of the ankle peak power to the required motor peak power. A

power amplification of over 3 was achieved. Thus, it was possible with a small 150 W motor, to fully power walking gait, which typically requires 200 W to 400 W for an 80 kg person. The difference is due to the capability of the spring to store energy and release it when demanded.

Another important area of the SPARKy project was maximizing the efficiency. A resulting overall system efficiency of 43 % was achieved, which is doubled compared to the value before the optimization. This is only possible because of the power amplification described before and a rigorous energy optimization. For controlling the complex system, Real Time Workshop and Simulink from Mathworks are used. A Simulink model is compiled and downloaded to an embedded target PC on which a xPC Target operating system is running. Optical sensors in the bottom of the prosthesis and position sensors at the ankle joint and motor give the necessary information to control the system [22]. At the time of writing this literature research, the SPARKy project has passed the prototype state and the development of a commercial product is going on at the company Springactive Inc. [9].

2.6.2 Powered Ankle Foot Orthosis

Another project using Sugar's and Hollander's work as a foundation is the robotic ankle foot orthosis for stroke rehabilitation called PAFO (Powered Ankle Foot Orthosis) which is described by Boehler [14]. The device was developed to assist stroke patients in rehabilitation, which is a quickly growing population in need. Also, the support of elderly people who are not able to walk securely over different ground conditions or stair climbing is a possible application area of this device. Figure 2.17 shows the powered ankle foot orthosis described by Boehler.

The PAFO also uses a Robotic Tendon to reduce the mass and the energy consumption of the system. Thus the peak power requirements are reduced from 3.1 W/kg to 1.55 W/kg. This is due to the ability of the spring to store and release energy. Thus it is possible to use a 0.8 kg device instead of a 6.5 kg motor and gearbox combination. After the robotic ankle foot orthosis was constructed, test trials were started and showed the capability of the system to fulfill all requirements. It is constructed to provide 50 % of the required ankle moment. Boehler focused in his work on the optimization of the already existing robotic ankle foot orthosis and on the controlling of the PAFO and the electronic package of the system [14].

Figure 2.17: Powered ankle foot orthosis. The arrow indicates the degree of freedom of the device. It uses a Robotic Tendon to generate a torque about the ankle [14].

2.6.3 Wearable Robot to Actuate the Knee

In a previous project at the Human Machine Integration Laboratory at ASU, Bellman described an active knee orthosis [35]. He investigated the changing torque if a helical spring, which is used as a Jack Spring, is bent 90 degrees. The number of active coils is varied and thus different torques are obtained. If a spring is bent, a bending torque is created by the spring. Secondly, if the bending radius is controlled by a curved path, the length of the spring is increased and an additional torque is generated by the spring. The torque increases with an inverse relationship to the number of active spring coils.

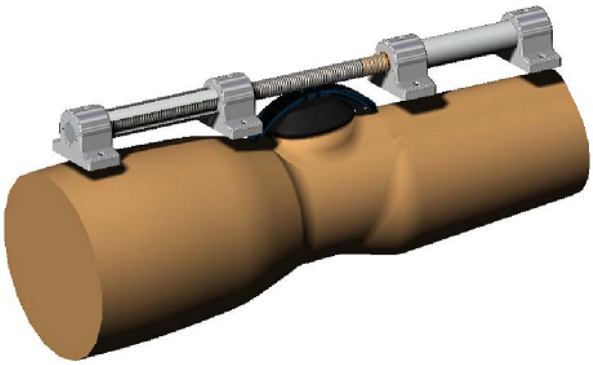

Figure 2.18: Orthosis with an extension spring spring used to create a torque about the knee. The number of active coils is varied which causes the tensile force to increase or decrease (unpublished data [35]).

Bellman started with an orthosis only supported by an extension spring to investigate if such a device is capable to perform a sit to stand operation. The results were promising as the orthosis was capable of providing the necessary torque to hold the body weight of a person when the knee is bent 90 degrees. Figure 2.18 shows the design of such a device. The device is mounted to a commercial brace. The orthosis consists of an extension spring used to create torque about the knee. The number of active coils is varied which causes the tensile force to increase or decrease (see Jack Spring Concept 4.3.2). By varying the number of active coils during knee movement, it is possible to reach different torque-angle-relationships, which are shown in figure 2.19 (unpublished data [35]).

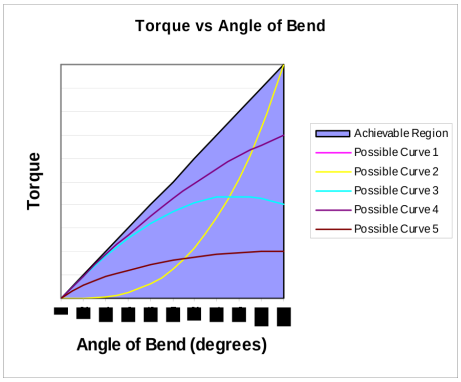

Figure 2.19: By varying the number of active coils during knee movement, it is possible to reach different torque-angle-relationships (unpublished data [35]).

2.7 Conclusion

The large number of fabricated active knee devices underlines the need for knee orthosis development. A research gap for the development of an active knee orthosis for ACL rehabilitation, which was the original goal for this project, is the design of a simple robust system. The building and testing of an active knee orthosis would not be possible to finish within the six month research program in the USA. It was decided to focus on a knee rehabilitation device which is not attached to the body reducing the complexity and weight of the system.

3 The Human Knee

3.1 Anatomic Structure

The human knee consists of the respective bone structures: the Tibia, Femur and Fibula and supporting soft tissue such as ligaments, tendons and cartilages. The ligaments hold the bones together and give the knee both it's flexibility and stability. Figure 3.1 shows a frontal view of a partially flexed right knee.

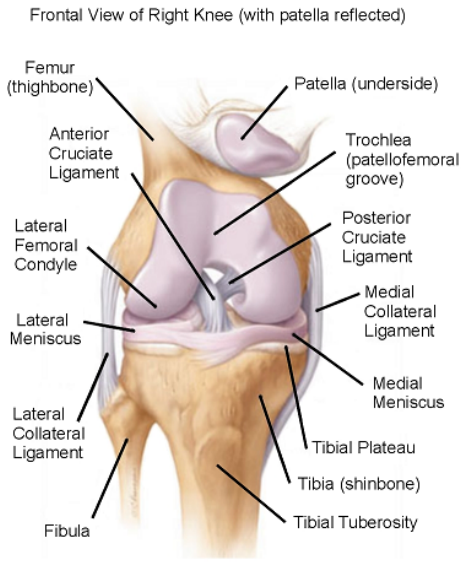

Figure 3.1: Anatomy of the human knee, frontal. Frontal view of a partially flexed right knee with all major components labeled. The patellar tendon has been cut, and the patella has been reflected proximally [19].

The ligaments reduce the degrees-of-freedom, but as they extend under tension there is still a small movement in their respective direction. The Lateral Collateral and the Medial Collateral Ligament prevent the knee from rotating about the Anterior-Posterior axis and moving along the Proxima-Distal axis shown in figure 3.2. The Anterior Cruciate and the Posterior Cruciate Ligament prevent the knee from moving along the Anterior-Posterior axis and rotating about the Proximal-Distal axis. These ligaments are affected most often by injuries.

Figure 3.2 shows the three important axes at the knee: the Medial-Lateral, the Anterior-Posterior and the Proximal-Distal axes. The knee is capable of moving both in rotational direction and translational direction about the three axes, but of course, the most important and the highest range of motion is rotation about the Medial-Lateral axis, which is called Extension and Flexion.

Figure 3.3 shows the anatomy of a right human knee while flexing and extending. For knee

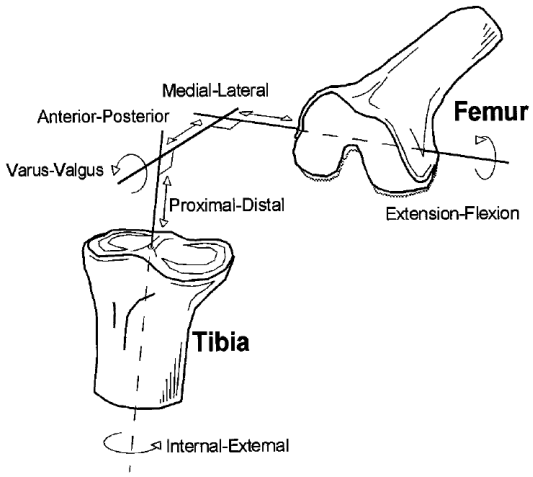

Figure 3.2: Knee Degrees of Freedom. The human knee is capable of six degrees-of-freedom. Both rotational movements and translational movements about the three axis are possible [44].

extension the Quadriceps muscles are contracting and for flexion the Hamstring muscles are contracting. To generate a torque at the knee, muscle forces are transferred via tendons creating a pulling force. The pulling forces combined with a lever arm result in a torque at the knee.

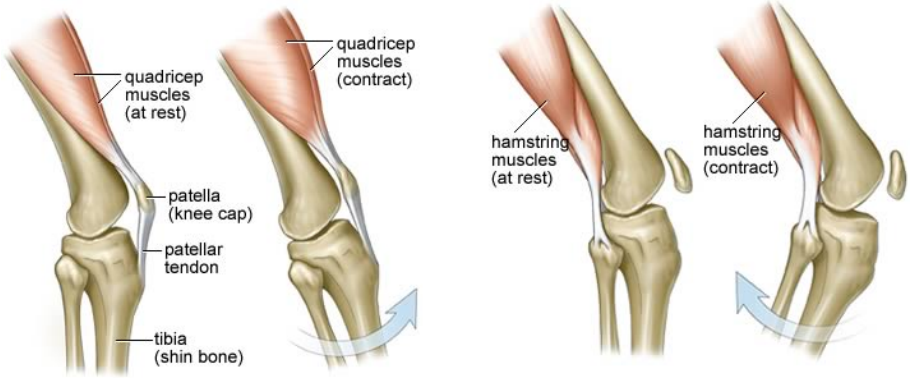

Figure 3.3: Anatomy of the right human knee, flexion, extension. Left: Flexion of the knee, Right: Extension of the knee [19].

From the literature research, a very good summary of the knee movements during flexing and extending by Nakamura et al. was found:

"The human knee joint consists of two joints, the patella-femur joint and the femur-fibula joint. The human knee joint generates flexion and rotation. In ordinary, flexion is generated on the sagittal plane, and the joint moves from 0 degree (extension) to 135 degrees (flexion), which is generated by rolling and sliding of femur on the fibula. Bending knee joint from completely extended position occurs as follows; First the femur only rolls on the fibula, gradually the femur rolls and slides on the fibula, and finally the femur only slides on the fibula. As a voluntary motion,

rotation is occurred in the flexed position and when ligaments are relaxed such as sitting on the chair." Nakamura et al. page 61 "Human Knee" [30].

The fact that the knee consists of two joints needs to be considered if a knee exoskeleton or a knee orthosis is designed which is explained in more detail in section 2.5.1 "Wearable Walking Helper".

3.2 Biomechanics of Muscles

3.2.1 Muscle Mechanics

Muscles are the actuators of the human body. They consist of many muscle fibers which can be separated in filaments in parallel and sarcomere elements in series. They build the contractile elements, which are controlled by nerve endings. The muscle endings are connected via tendons to the bone structure. This combination of muscles, controlling nerves, tendons and bone make complex movements e.g. like human gait possible.

Electrical signals control the motor units, and these signals can be measured with electrodes on the skin. The measurement of these signals is called Electromyography (EMG). If a motor unit is stimulated by a firing nerve end, it starts to contract and the muscle tension rises. From the start of firing to the maximum muscle tension a time delay occurs. Typical "turn-on" times are approximately 200 ms and "turn-off" times are 300 ms. The response behavior of the muscle contraction to the input signal (nerve firing) can be modeled as an impulse response of a second-order critically damped system [43].

There are many factors influencing the time delays including the training state and temperature of the muscles. A lower muscle temperature causes longer delay times and thus slower reactions, which is one reason, besides reducing the risk of injuries, that it is so important e.g. for sprinters to warm up before competitions.

3.2.1.1 Force-Length Characteristics

In the resting state, the number of cross bridges between the filaments are at a maximum value which makes a maximum force possible. If the muscle is lengthening or shortening, the number of the cross bridges is decreasing and thus the resulting force is reduced, which is shown in figure 3.4 marked with Fc in picture (a). The contractile elements are surrounded by connective tissue, which acts as an elastic band and is referred to as a parallel elastic component. If the muscle is in a resting state, no tension is applied on the elastic components. As the length of the muscle is

increasing, the tension of these elastic components is rising in a non-linear behavior. The resulting tension caused by the parallel connective tissue is shown in 3.4 marked with Fp in picture (a). The overall force-length characteristics are a summation of Fc and Fp shown in 3.4 as Ft in picture (a) [43].

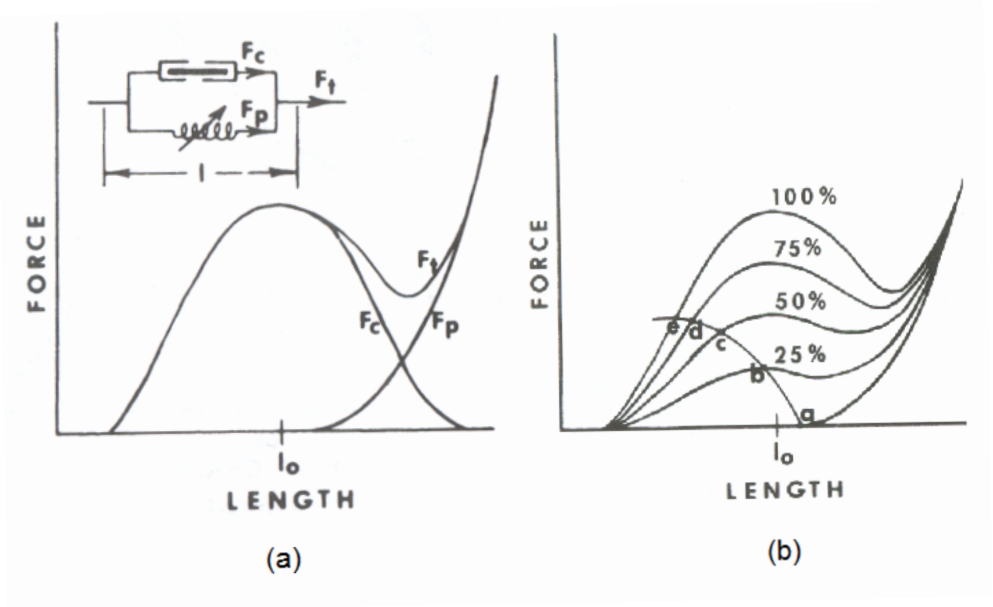

Figure 3.4: Force-length characteristics: (a) shows a curve resulting from the reduced number of cross bridges between the filaments during muscle lengthening or shortening marked as Fc. The Fp curve shows the increasing force caused by extending the parallel elastic component during muscle lengthening. The resulting force-length characteristics is curve Ft. (b) shows tensions caused by different levels of muscle activation. The muscle characteristics combined with the load characteristics of a flexing elbow against a gravitational load results in different equilibrium points [43].

Picture (b) in figure 3.4 shows tensions caused by different levels of muscle activation. In addition, the load characteristics of a flexing elbow against gravitational load showing different equilibrium points during the movement marked with characters [43].

3.2.1.2 Force-Velocity Characteristics

The previous discussion focused on isometric tensions (constant position). When the muscle moves while generating a force additional factors have to be considered. For **concentric** contraction (shortening), the muscle force is reducing as the velocity of the movement is rising which is shown in figure 3.5. The two main reasons for the reduction in force are firstly a breaking of the cross bridges in the contractile element and reforming in the shortened position and secondly a fluid viscosity in the contractile and connective tissue, which can be modeled as a fluid damper and considered as friction. The force-velocity characteristics can be described mathematically in the

Hill model [43].

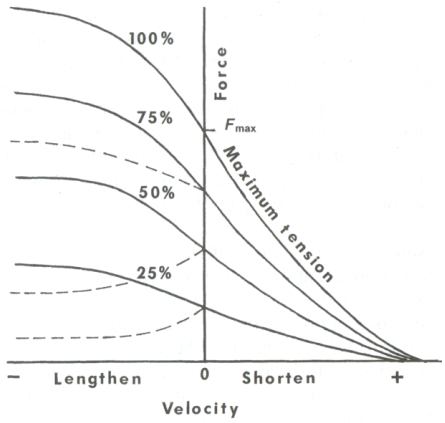

Figure 3.5: Force-velocity characteristics: For concentric movements (shortening), the resulting maximum tension is reduced by a recurring breaking and reforming of the cross bridges in the contractile element and the fluid viscosity in the contractile and connective tissue which can be considered as friction. The knowledge for eccentric movement (lengthening) is not well understood and the reasons for this behavior are not well described. The solid lines appear during isotonic movements but for isokinetic movements the dotted lines occur [43].

For **eccentric** movements (lengthening), the knowledge about the force-velocity curve is not well understood. The solid lines appear during isotonic movements but for isokinetic movements the dotted lines occur. Normal human movement usually consists of both concentric and eccentric movements in an equal distribution [43].

3.2.1.3 Combination Length and Velocity Characteristics

Natural movements e.g. like reacting to an external disturbance are often a combination of static and dynamic movements which is a navigation on the surface plot shown in figure 3.6 which is a combination of the length and velocity characteristics of the muscle force.

If force and movement have the same direction, the power and work of the muscle are positive. If they have a different sign, the power is negative and work must come from outside the muscle (energy is flowing in the muscle).

3.2.2 Torque Angle Characteristics

Figure 3.7 shows the torque at the knee for extension and flexion. The blue curves show the torque-angle dependency for the Quadriceps muscles (extensors) for concentric, eccentric and isometric contractions and the red curves show the same dependencies for the Hamstring muscles (flexors). These knee torque angle characteristics are the basis for all following design and realization

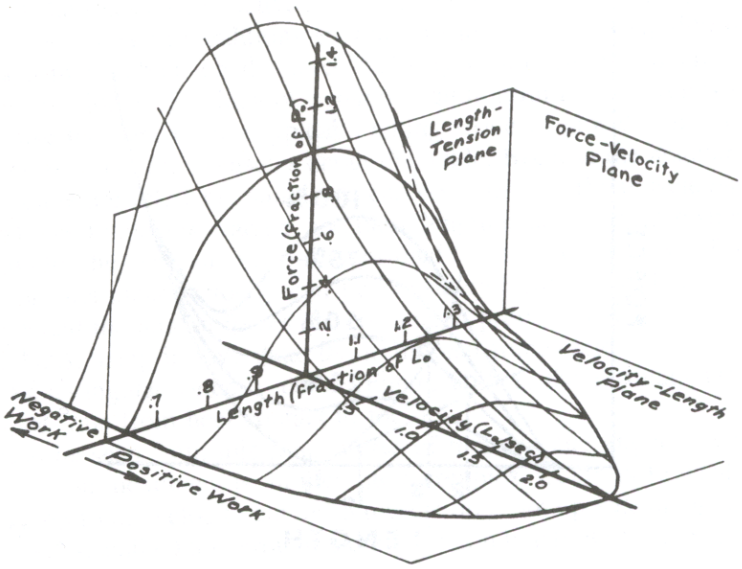

Figure 3.6: Combination of length and velocity characteristics. Three dimensional plot which shows the change of the contractile element respectively the force is a function of length and velocity. A natural movement is often a change of length and velocity at the same time, which is a navigation on the surface of the plot. The influence of the parallel elastic elements are not shown [43].

considerations. Thus, the realized knee device is designed to meet these characteristics.

It is interesting to see that for both muscles much higher torques are possible for eccentric contractions than for concentric contractions. For the Quadriceps, a maximum torque of 116 Nm for eccentric and 90 Nm for concentric contractions are possible for an 80 kg person. For the Hamstrings, 54 Nm is possible for eccentric and 43 Nm for concentric contractions [36]. Most of the available exercise training devices apply a combination of concentric contraction (weight lifting) and eccentric contraction (weight lowering), but they don't take in consideration, that both the Hamstrings and the Quadriceps are capable of different torque levels for concentric and eccentric contraction and changing values for different angles of the knee.

Especially during extension movement (Concentric Quadriceps and Eccentric Hamstrings) a so called "stairstep" phenomena can be observed, which consists of sudden decreases in torque followed by a fast increase [36].

3.2.3 Force Angle Characteristics

The torque at the knee is caused by forces generated by the Hamstrings and Quadriceps muscles times the perpendicular distance to the axis of rotation (lever arm). Figure 3.8 shows a rough knee model. The Quadriceps/Hamstring muscle groups generate a pulling force which generates

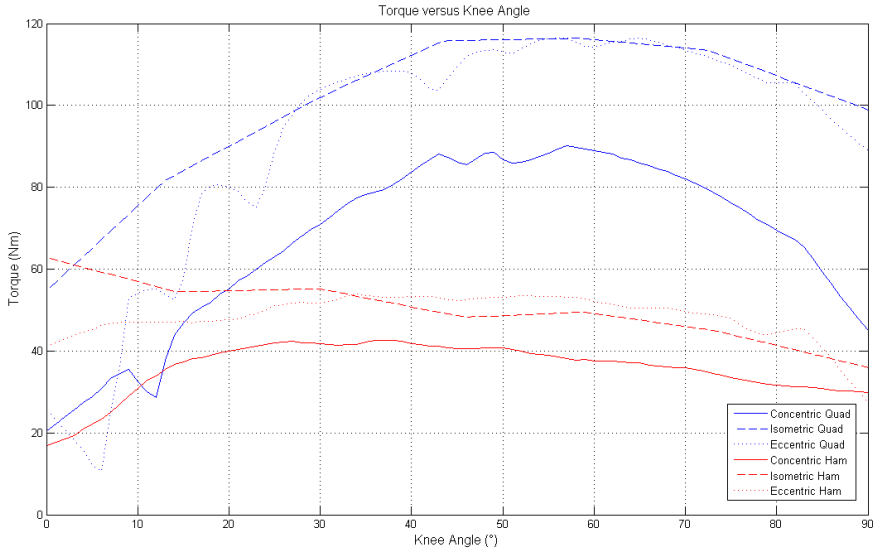

Figure 3.7: Knee Flexion Extension Torque. For both muscle groups much higher torques are possible for eccentric contractions than for concentric contractions. These torque-angle relationships will be used for later design considerations. Redrawn from Smidt [36].

an extension/flexion torque at the knee.

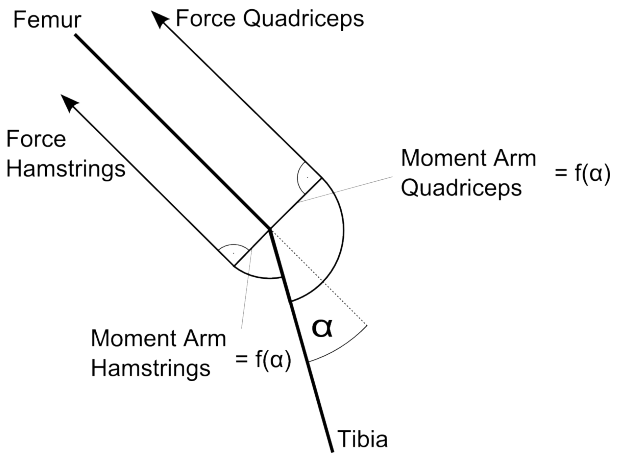

Figure 3.8: Knee Model. An extension or flexion torque is generated by a pulling force generated by the Quadriceps or Hamstring muscle groups.

The line of action respect to the Tibia is changing during extension and flexion, which is taken into consideration by calculating a lever arm as a function of the knee angle, which was investigated by Herzog et al. [21].

One of the results of Hergog's work is shown in table 3.1. To calculate the lever arm for Hamstrings and Quadriceps the coefficients in table 3.1 are used in equation 3.1. For the model, it

is assumed that the the tension in the patellar tendon and the Quadriceps tendon are equal [36].

$$Leverarm = A_0 + A_1\alpha + A_2\alpha^2 + A_3\alpha^3 + A_4\alpha^4 \tag{3.1}$$

In order to calculate the lever arm of the Hamstring muscle group, the average of the Biceps Femoris, Semimembranosus and Semitendinosus was calculated.

Table 3.1: Quadriceps and Hamstrings Lever Arm Coefficients [21]

Coefficient	A_0	A_1	A_2	A_3	A_4
Patellar/Quadriceps tendon	4.71E-02	4.20E-04	-8.96E-06	4.47E-08	0
Biceps Femoris	1.46E-02	-9.26E-05	8.55E-06	-8.78E-08	2.38E-10
Semimembranosus	2.84E-02	-1.61E-04	6.81E-06	-8.80E-08	2.77E-10
Semitendinosus	-4.11E-03	5.86E-04	6.90E-06	-5.31E-08	0
Hamstrings Tendon average	1.30E-02	1.11E-04	7.42E-06	-7.63E-08	1.72E-10

The change of the lever arm length versus the knee angle is shown in figure 3.9. Whereas the lever arm for the Patella of the Quadriceps muscle is relatively constant, the lever arm for the Hamstring muscle is varying quite strongly. This is caused by a relatively non-ideal line of action of the Hamstring muscles when the knee is fully extended [21].

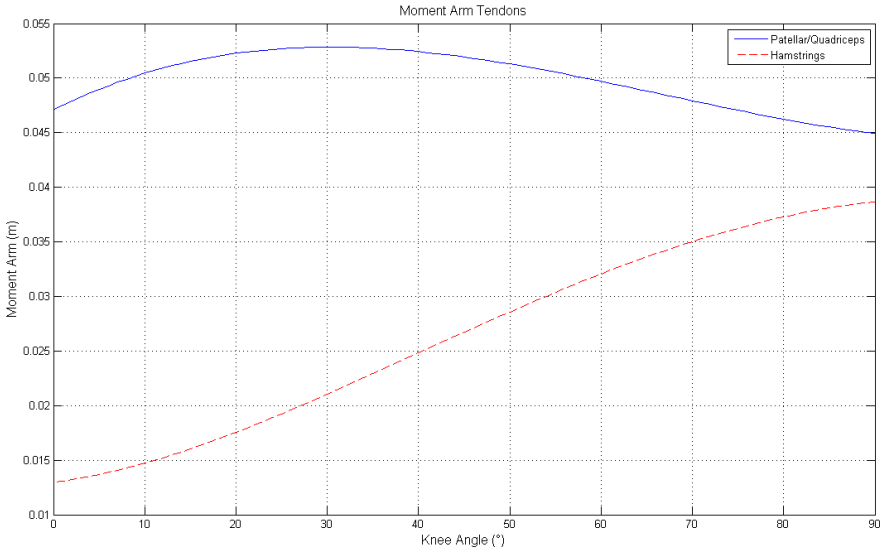

Figure 3.9: Knee lever arm. The blue curve shows the lever arm for the Patella of the Quadriceps muscle. The red dotted curve shows the lever arm for the Hamstring muscle which is varying much more than the lever arm of the Patella. Redrawn from [21].

Studies of the human knee often only focus on the torque at the knee, but also the forces in the

muscles are interesting as no rotational actuators exist in the human body. The muscles generate, as described before, a force-length change which acts via the tendons to generate a torque at the knee.

With the knowledge of the torque and the lever arm for Hamstrings and Quadriceps the necessary force of the muscles can be calculated as shown in equation 3.2, where F is the force of the muscles, T is the torque and ma the lever arm. Both the torque and the lever arm are changing as a function of the knee movement.

$$F = \frac{T}{ma} \tag{3.2}$$

Figure 3.10 shows the forces of the knee muscles calculated with equation 3.2. Because of the short lever arm at small bending angles (from 0 to 10 degrees), the Hamstring muscle must have much higher forces although the torques are more or less the same for both the Hamstring and Quadriceps muscle groups.

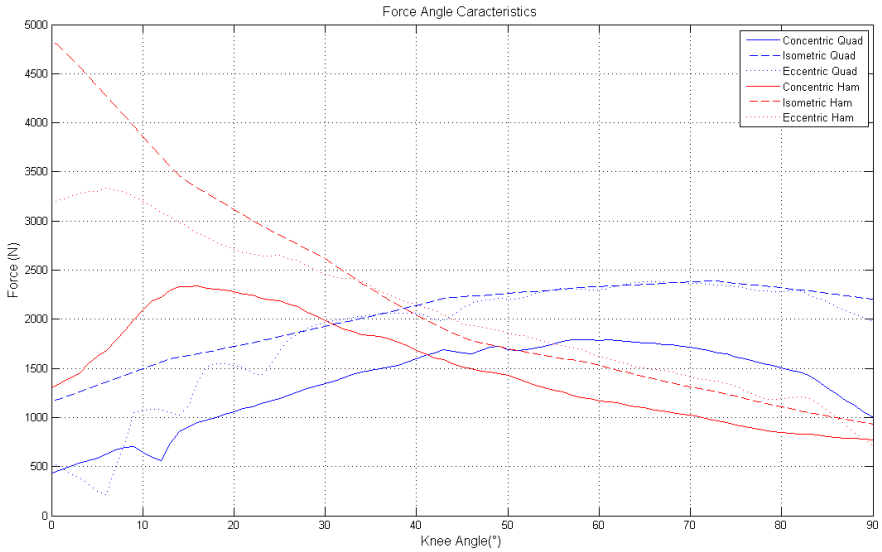

Figure 3.10: Knee Flexion Extension Force Angle. Because of the short lever arm at small bending angles (from 0 to 10 degrees), high forces of the Hamstring muscles are necessary. Calculated with data from [21] and [36].

3.2.4 Force Length Characteristics

In order to evaluate the actual force-length characteristics of the hamstring and quadriceps muscle groups, additionally to the force one needs to know the length change of the muscles during knee

extension and flexion. Unfortunately no information about this dependency could be found in this literature review. Nevertheless these dependencies are modeled roughly to get an idea of the actual force-length characteristics:

$$\begin{aligned} \Delta l_{quad} &= \overline{ma}_{quad} \cdot \alpha \cdot \frac{\Pi}{180} \\ \Delta l_{ham} &= \overline{ma}_{ham} - \overline{ma}_{ham} \cdot \cos(\alpha) \end{aligned} \tag{3.3}$$

For these calculations, it is assumed that the attachment points of the tendons at the tibia are moving on circular path for knee extension and flexion. This approximation is not exact and shall only give a rough impression of the force-length dependency of the hamstring and quadriceps muscle groups. Figure 3.11 shows the force-length dependency at the human knee for knee extension and flexion. As high forces occur for Hamstring actuation at 0 degree knee angle, it can be assumed that this model is not accurate for small knee angles, but the model can give an idea how the actual force length characteristics at knee can look like.

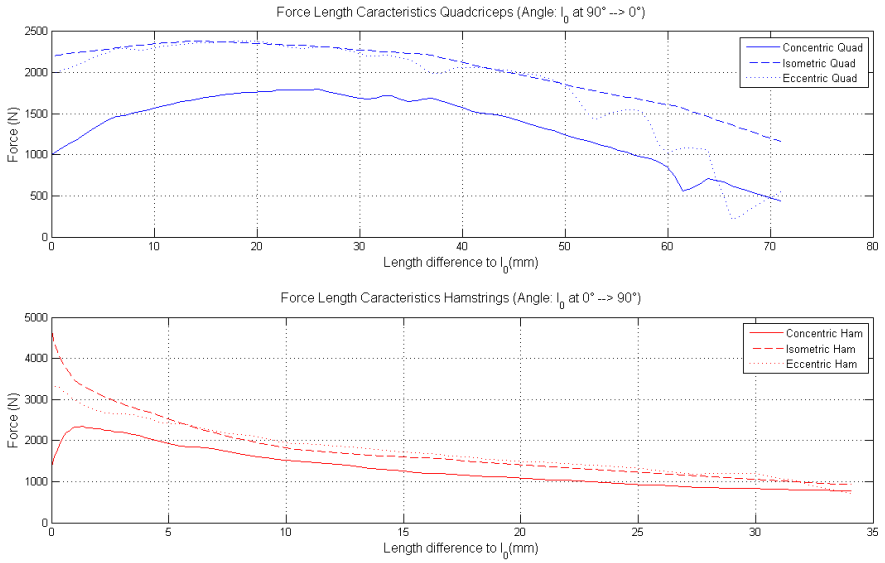

Figure 3.11: Knee flexion extension force length dependency. For the Quadriceps actuation length zero (l_0) represents a knee angle of 90 degrees and for the Hamstrings actuation the contraction starts at a knee angle of 0 degrees. A positive length change represents a contraction of the muscle. Calculated with data from [21] and [36].

For the Quadriceps actuation, length zero (l_0) represents a knee angle of 90 degrees and for the Hamstrings actuation the contraction starts at a knee angle of 0 degrees. A positive length change represents a contraction of the muscle.

3.3 Human Gait and the Knee

3.3.1 Horizontal Walking

For the design and testing of wearable devices, it is necessary that one has enough knowledge about human movement. Information about kinetic and kinematic profiles such as the necessary peak power need to be studied in detail. A common way to describe human gait is by its gait cycle. One gait cycle is the period of time between one contact of a foot with the floor to the subsequent contact of the same foot. The gait data is usually evaluated by motion capture systems and ground reaction forces. Using inverse dynamic calculation methods, the forces and joint angles are used to calculate the angles and torques needed at the ankle, knee and hip of the human body during gait. Figure 3.12 shows a single human gait cycle.

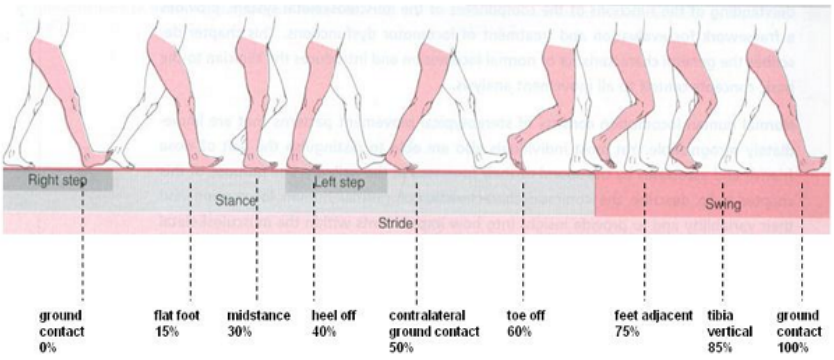

Figure 3.12: A single human gait cycle [22].

Figure 3.13 shows the knee angle and required knee torque over one gait cycle for a typical 80 kg person with a cycle time of 1.25 s. The knee angle shows the flexing and extending of the knee joint during one gait cycle. The torque graph shows positive and negative torques. Human muscles and tendons are able to generate and absorb power. Positive work is done during a concentric contraction.

The required power necessary for this normal walking cadence can be calculated as shown in equation 3.4. to be consistent with common gait literature the power calculation is inverted:

$$P = -T \cdot \omega \tag{3.4}$$

Where P is the power, T is the torque and ω is the angular velocity.

The calculated power during one gait cycle is shown in figure 3.14. If the muscle torque and the direction of the angular velocity have the same direction the power is positive and energy is

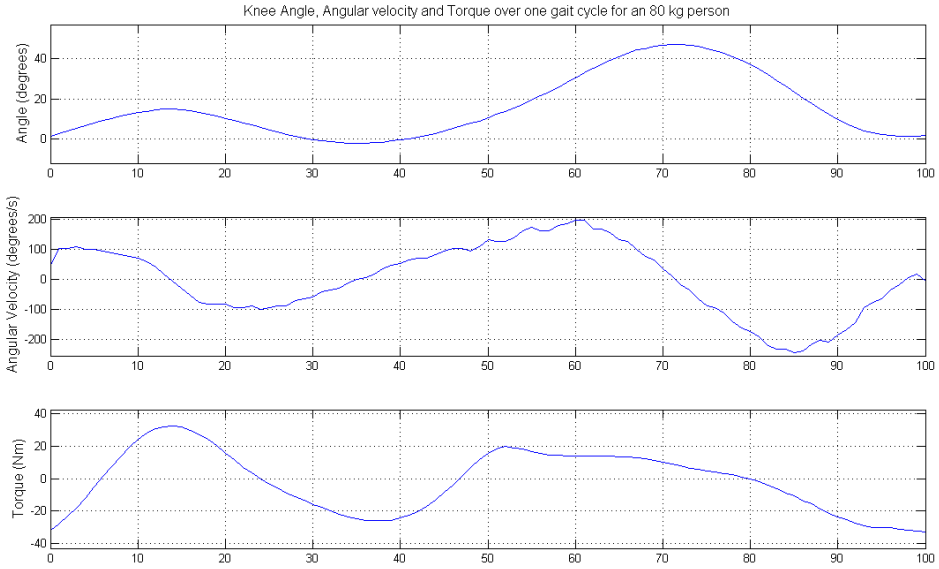

Figure 3.13: Knee angle and torque for level walking over one gait cycle. Typical values for knee angle and torque over one gait cycle for an 80 kg person with a cycle time of 1.25 s. Digitalized from Whittle [41].

generated by the muscles. If the torque and the angular velocity are in opposite directions, power is absorbed by the muscles and tendons.

The Power curve in figure 3.14 is marked with numbers at different areas and shows distinct phases of absorption and generation. From 0 % to 15 % stride, the knee is flexing, caused by the knee extensors which is a region of negative power. From 15 % to 40 % gait cycle, the knee extends partially corresponding to concentric knee extensor activity during mid-stance, requiring positive power. At 40 % of stride the knee is flexing again until early swing, which is at 70 % stride. Here negative power acts at the knee. At 60 % of stride the knee starts to extend again and the muscles have to absorb energy caused by converting potential energy to kinetic energy [42].

Peak knee torque values are about 32 Nm for a typical male weighing 80 kg which results in a required peak power of 51 W for generated power and 78 W for absorbed power with a cycle time of 1.25 s as shown in Figure 3.13 and 3.14. The knee peak power is much lower than the 250 W peak power in the human ankle joint [22] and thus an orthosis or a prosthesis with lower peak power is necessary for a knee device.

The energy during one gait cycle is defined in equation 3.5. Where E is the calculated Energy, P the power and i the percentage of the gait cycle. The calculated energy at the knee for one

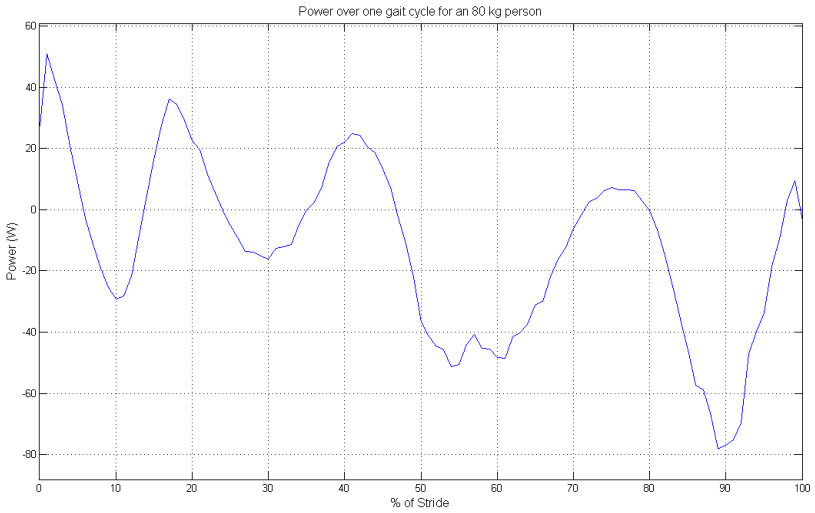

Figure 3.14: Knee power over one gait cycle. Typical values for knee power over one gait cycle for an 80 kg person with a cycle time of 1.25 s. Calculated with digitalized values from Whittle [41].

gait cycle is approximately -15 J which means that energy is flowing into the knee during walking (absorbing energy).

$$E = \int_0^\infty P(t)\,dt \simeq \sum_{i=0}^{100} P_i \cdot \Delta t = \Delta t \cdot \sum_{i=0}^{100} Pi \tag{3.5}$$

E...Energy

$P(t)$...Power depending on time

P_i...i th power value

Δt...Time difference from one sample to the next

If e.g. the person is running or walking up/down stairs or slopes, the energy for one gait cycle becomes positive or negative which is described in the following sections.

3.3.2 Gait in walking Up and Down Slopes and Stairs

Gait data for level ground walking can be found in literature written by Winter [42] or Whittle [41]. For walking up and down stairs or slopes, data is available from McIntosh et al. [29]. Figure

3.15 shows the knee power for a ten degree incline walking up and down. It shows typical values for an 80 kg person at a cycle time of 0.88 s and stride length of 1.5 m for walking down and 0.94 s cycle time and 1.6 m stride length for walking up.

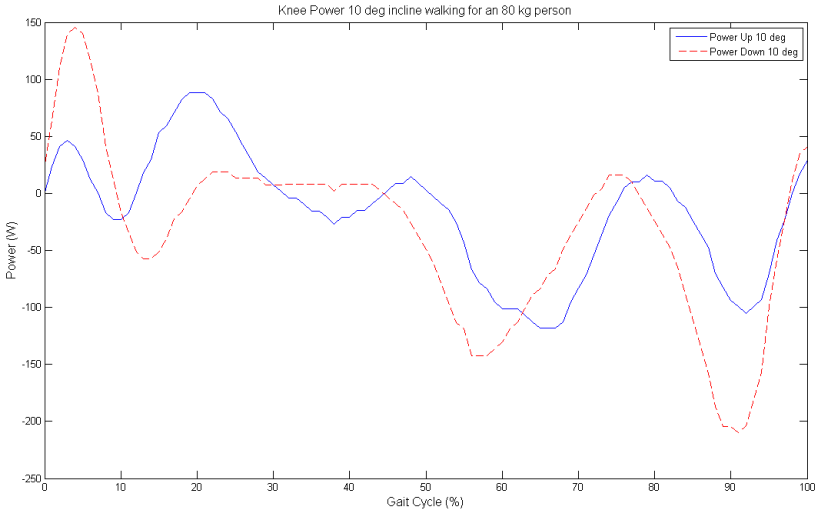

Figure 3.15: Knee power over one gait cycle for a ten degree inclined walking cycle. Typical values for knee power over one gait cycle for an 80 kg person for ten degree incline walking with a cycle time of 0.88 s and stride length of 1.5 m for walking down and 0.94 s cycle time and 1.6 m stride length for walking up. Digitalized from McIntosh [29].

If compared to horizontal walking power, the positive and negative amplitudes of the knee power are increasing for inclined walking. For walking up, the maximum power is 88.5 W and the minimum power is -118 W and for walking down, the maximum power is 146 W and the minimum power is -210 W. The knee energy over one gait cycle for walking down is -29 J and surprisingly also for walking up a negative value of -15 J is the outcome with the data from McIntosh. Thus for walking up, where the human body has to generate energy to move it's mass upward, energy is flowing from the hip and the ankle joint to the knee joint, but knee muscle power has of course both positive and negative power peaks.

As raw gait data was available, in this chapter, an additional evaluation of inclined walking and stair climbing was done. The power and energy at the knee are especially interesting for these situations. For these calculations gait data from four different test-persons was provided by the company Springactive Inc. [9], which is a spin-off from the "Human Machine Integration Laboratory" at Arizona State University. To get a detailed impression, data with more test-persons is necessary, but for getting a basic understanding, this data contains enough information.

The gait data is provided as mat-files and is analyzed with Matlab. The basic steps to analyze

the data are explained in the following section. The data is sorted in slopes up and down and stairs up and down, but different gait cadences are mixed as shown in figure 3.16.

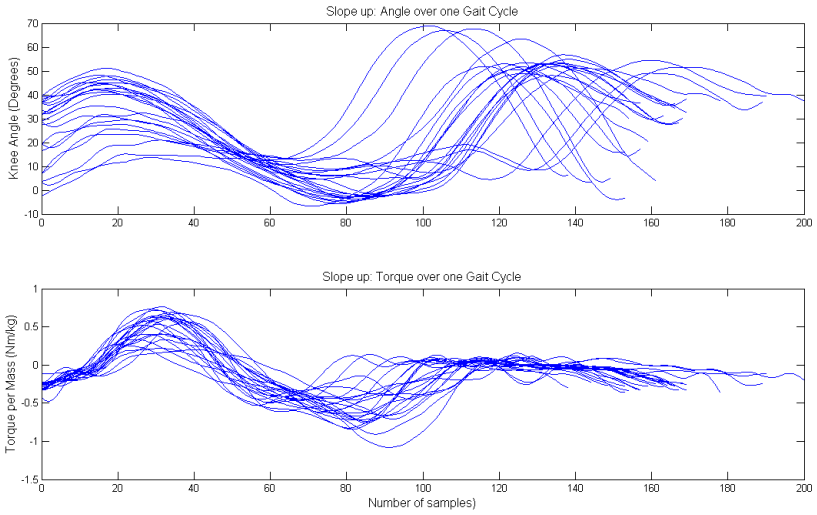

Figure 3.16: Gait Analysis: Slope Up unsorted. Different steps with varying duration of one test-person. The varying duration of one gait cycle depends on the number of samples which were recorded with a 200 Hz sampling rate [9].

The curves are separated according to their cycle duration. Every 0.1 second a new group starts (Group 1: 0 - 0.6 sec, Group 2: 0.6 - 0.7 sec, Group 3: 0.8 - 0.9 sec ...). This ordering is done for all four participants. For each group an average torque and angle curve is calculated. To calculate an average curve, values at every % of gait cycle for all curves are interpolated. With the interpolated points, an average value for every % of gait cycle can be calculated which is shown in figure 3.17.

In order to detect the existing outlier curves, the Standard Deviation of every point for every curve is calculated as shown in equation 3.6. For every curve in one curve group (0.1 sec cycle time group) the "Average Standard Deviation" for all all curves is calculated. If the Standard Deviation of one curve varies significantly from the "Average Standard Deviation" in this group (for this analysis 200 % are used), it is considered as an outlier and removed.

$$S = \sqrt{\frac{1}{N}\sum_{i=0}^{N}(x_i - \bar{x_i})} \tag{3.6}$$

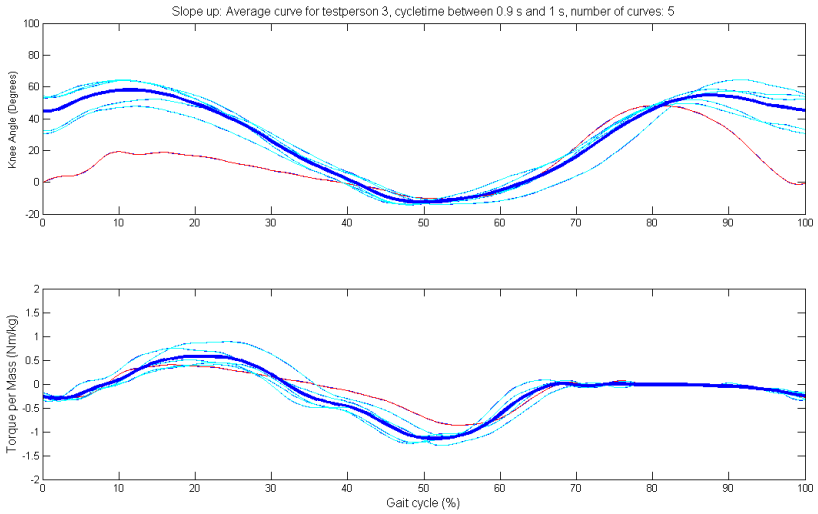

Figure 3.17: Gait Analysis: Slope Up Average Curve. Slope Up, Test-person 3, Steps with a cycle time between 0.9 s and 1 s. The group consists of 5 curves. Average Standard Deviation allows an automatically outlier detection which removed one red marked outlier. The calculated average curve is drawn in bold. The outlier curve has no influence on the average curve.

S...Standard deviation

N...Number of samples (101, 0 - 100)

x_i...i th sample value

$\bar{x_i}$...i th average value (mean)

In figure 3.17 a detected outlier curve is marked red. The outlier curve has no influence on the final average curve which is drawn as a bold line. The average curve calculation for the knee angle and knee torque is done for every cycle time group and all test-persons. With these average curves for each group and test-person, average curves over all test-persons can be calculated which is used for the further calculations.

3.3.2.1 Gait Analysis Stairs Up

The average curves over all testpersons are used for the power and energy calculations described in equation 3.4 and 3.5. Figure 3.18 shows the knee angle, angular velocity and torque for walking up stairs at a gait cycle time of 0.85 s (0.8 - 0.9 s group, 1,17 Hz). The depth of the stairs is 265 mm and the height of one step is 75 mm. In comparison to level ground walking higher peak

torques and higher angular velocities can be recognized, which results in higher power and energy. Also the shape differs from horizontal or decline walking, which has to be considered e.g. for an exoskeleton's control algorithm.

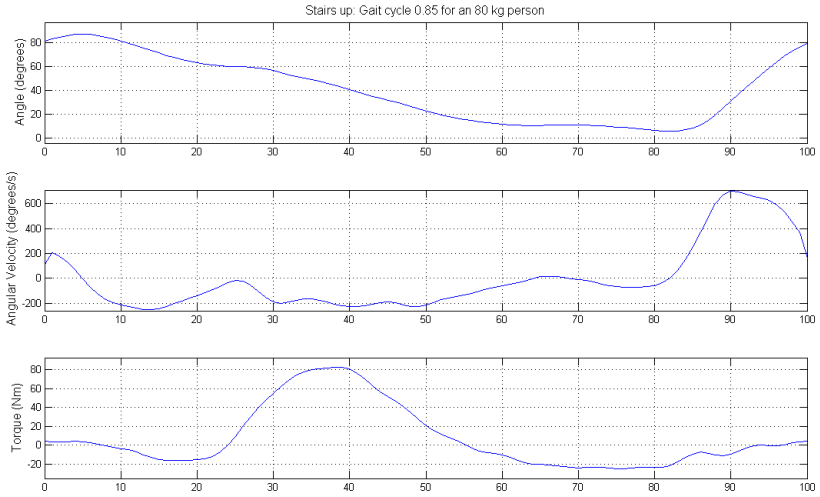

Figure 3.18: Gait Analysis: Angle, angular velocity, torque. Stairs Up 0.85 s cycle time (1.17 Hz). In comparison to level ground walking higher peak torques and higher angular velocities can be recognized, which results in higher power.

Figure 3.19 shows the calculated knee power over one gait cycle for climbing stairs with a 0.85 s cycle time. In comparison to level ground walking a significantly higher peak power with 321 W can be recognized which results in 39 J of energy flowing out the knee.

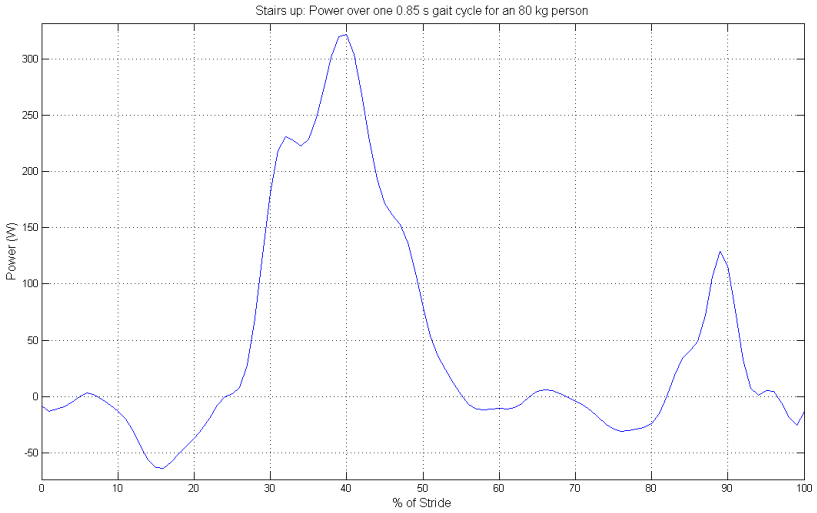

Figure 3.19: Gait Analysis: Power. Stairs Up 0.85 s cycle time (1.17 Hz). In comparison to level ground walking, a significantly higher peak power with 321 W can be recognized.

3.3.2.2 Gait Analysis Stairs Down

Similar to the stairs up analysis, the data for descending stairs was calculated which is shown in figure 3.20 which shows the knee angle, angular velocity and torque at a gait cycle time of 0.85 s (0.8 - 0.9 s group, 1,17 Hz).

Figure 3.21 shows the calculated knee power over one gait cycle for descending stairs with a 0.85 s cycle time. In comparison to level ground walking a significantly higher negative peak power with -450 W can be recognized which results in -84 J of energy flowing into the knee.

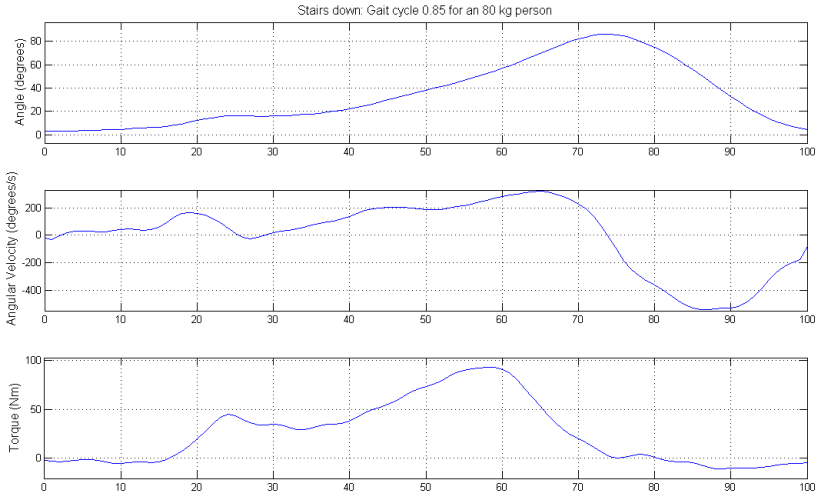

Figure 3.20: Gait Analysis: Angle, angular velocity, torque. Descending stairs at 0.85 s cycle time (1.17 Hz). In comparison to level ground walking, higher peak torques and higher angular velocities can be recognized, which results in higher power but the sign of the angular velocity has changed compared to ascending stairs.

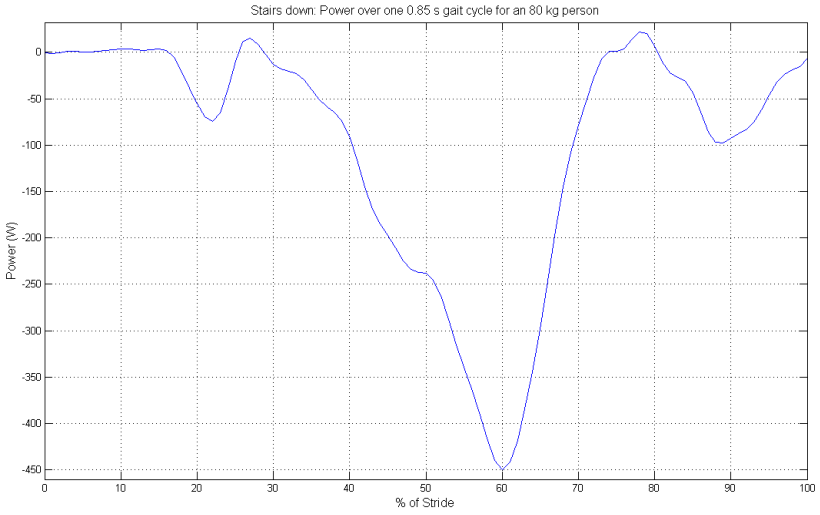

Figure 3.21: Gait Analysis: Power. Descending stairs at a 0.85 s cycle time (1.17 Hz). In comparison to level ground walking a significantly higher negative peak power with -450 W can be recognized.

3.3.2.3 Summary

The same calculations for walking up and down slopes were done. Table 3.2 shows a summary of the analyzed data. In order to get exact values for power and energy a greater sampling of more than four test-persons would be necessary, but with this amount of data it is possible to get an idea of the situation when walking up and down slopes or stairs.

Table 3.2: Summary Gait Data: Slope and Stairs up and down for an 80 kg person and a 0.85 s cycle time (1.17 Hz).

	Max Power	Min Power	Energy
	W	W	J
Slope Up	232	-37	28
Slope Down	15	-339	-86
Stairs Up	321	-64	39
Stairs Down	22	-450	-84

As originally expected and in contrast to the data of McIntosh, the overall knee energy over one gait cycle is positive for walking up and negative for walking down. Reasons for these differences in the results can be the too small test group and the big standard deviation in such an investigation. In contrast to level walking the values for maximum and minimum peak power are much higher for walking up or down. The data from Whittle [41] and the analyzed data in this chapter show that the Hamstring and Quadriceps muscles do not need to provide much power during level walking (max 51 W, min -78 W for 0.8 s cycle time, 80 kg), but as expected, when it comes to walking up or down slopes or stairs significantly higher peak power is necessary (max 320 W, min -450 W for 0.85 s cycle time, 80 kg).

3.4 Translational Potential Energy at the Knee

For calculating the stiffness in gait literature, it is usually assumed that the spring is fixed on one side, but this is not the case for knee and ankle muscles as both sides are moving back and forth. Ward et al. described this consideration for ankle gait data [40]. In this chapter the same considerations are made for knee gait data. If e.g. springs are used to store energy in prosthetic devices it is important to analyze a spring that allows both sides to move. To the knowledge of the author, the knee stiffness has never been described with this approach.

Important for the energy storage in a spring is the relative velocity between the input and output side. Additionally to this translational potential energy approach, Ward et al. defined

the spring stiffness not with the relationship between force and displacement, but through the derivative of force and velocity [40].

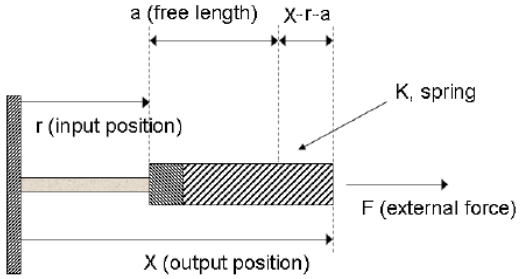

Figure 3.22: Robotic Tendon Model, a motor turning a nut back and forth adjusting r. The output position x and the external force F are the desired outputs. A spring, with the free length a and the stiffness K, is connected to the input and output position is capable of storing energy. Adapted from [40].

A model of a robotic tendon (spring in series with a motor) is shown in figure 3.22. The energy and the force depend on the free length a, the output and input position causing a spring deflection (x - r - a) and the spring stiffness K. The input position r is actively controlled by a motor and the output position depends on the position of the human body (the input variable is used to control the device).

The following calculations follow the calculations of Ward et al. [40]. With an ideal spring (no friction) the external force is:

$$F = K \cdot s = K(x - r - a) \tag{3.7}$$

Thus the output position x is defined by:

$$x = r + a + \frac{F}{K}$$

By differentiating the output position, we obtain the relative velocity v at the spring, which is the difference between the input and output velocity (spring stiffness is assumed to be constant):

$$\begin{aligned} \dot{x} &= \dot{r} + \frac{\dot{F}}{K} \\ v = \dot{x} - \dot{r} &= \frac{\dot{F}}{K} \end{aligned} \tag{3.8}$$

The spring power for a translational spring cannot be found in common literature when both

ends are moving. Usually, it is assumed that one side is fixed.

$$P_{out} = F \cdot v = F\frac{\dot{F}}{K} \tag{3.9}$$

The input position r is defined by the number of revolutions and the lead l, which is used for the calculation of the motor angular velocity:

$$\begin{aligned} r &= l \cdot n \\ \omega = \dot{\theta} &= 2\pi\dot{n} \\ \dot{\theta} = \frac{2\pi}{l}\dot{r} &= \frac{2\pi}{l}(\dot{x} - \frac{\dot{F}}{K}) \end{aligned} \tag{3.10}$$

The input power of the motor is the torque τ multiplied by the angular velocity. In standard gait literature, the power is inverted which is also done here to be consistent. The necessary motor position, motor angular velocity and input power depend on the output position, the output force and the spring stiffness:

$$\begin{aligned} P_{in} &= \tau\dot{\theta} = -F \cdot v \\ P_{in} &= -F \cdot \dot{r} = -F \cdot (\dot{x} - \frac{\dot{F}}{K}) \end{aligned} \tag{3.11}$$

During a gait cycle the input and output power are not always equal. The difference is energy flowing into or out of the spring.

$$E_{spring}(t) = \Delta P(t) \cdot t = (P_{out}(t) - P_{in}(t)) \cdot t \tag{3.12}$$

3.4.1 Stiffness at the Knee

Additionally Ward et al. studied the dynamic stiffness instead of the common static stiffness at the ankle joint:

$$K = \frac{\dot{F}}{\dot{x}} \tag{3.13}$$

Two different methods are used to calculate the stiffness at the knee. In standard literature Hooke's Law relationship is used. In order to investigate the stiffness at the knee, the relation

between force and position is not studied, but torque T and angle α are investigated:

$$K_{static} = \frac{T}{\alpha}$$
$$K_{dynamic} = \frac{\dot{T}}{\dot{\alpha}} \tag{3.14}$$

The static and dynamic stiffness over one gait cycle are calculated with equation 3.14 and are shown in figure 3.23.

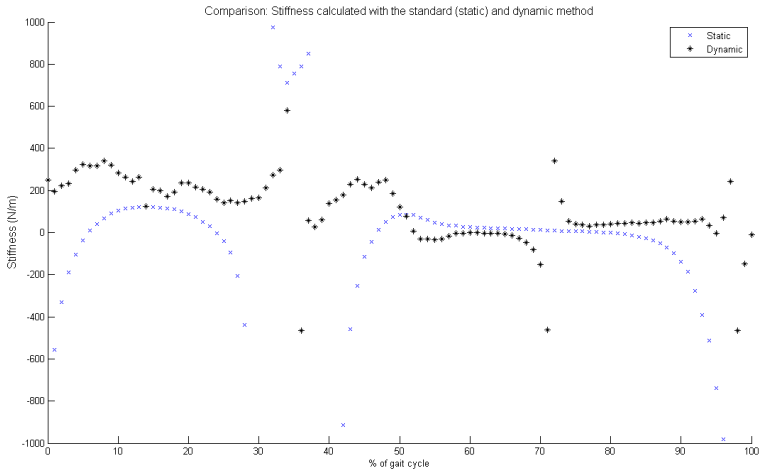

Figure 3.23: Knee stiffness over one gait cycle. Between 0 and 50 % and from 50 to 100 % of the gait cycle, the dynamic stiffness is relatively constant.

The static stiffness at the knee describes the torque angle relationship. The realized design for an orthosis or prosthesis is directly proportional to a force-length relationship at the motor, which is important for controlling the motor. On the other hand, a spring chosen for an orthosis or prosthesis depends on the dynamic stiffness. Therefore, it is more relevant to evaluate if there is a dependency between $\dot{M}$ and $\dot{\alpha}$ (a $\dot{F}/\dot{x}$ dependency). A series spring design that uses the dynamic stiffness will be able to store and release energy properly.

It is interesting to see, that between 0 and 50 % (stance phase of gait, foot has contact to the floor) of the gait cycle, a relatively linear dependency between $\dot{M}$ and $\dot{\alpha}$ is existing, which is shown in figure 3.24.

The linear fit is calculated with the following values, which is a constant stiffness of approximately 3.8 Nm/rad:

$$\dot{M} = 3.809\frac{Nm}{rad} \cdot \dot{\alpha} + 218.26\frac{Nm}{s} \tag{3.15}$$

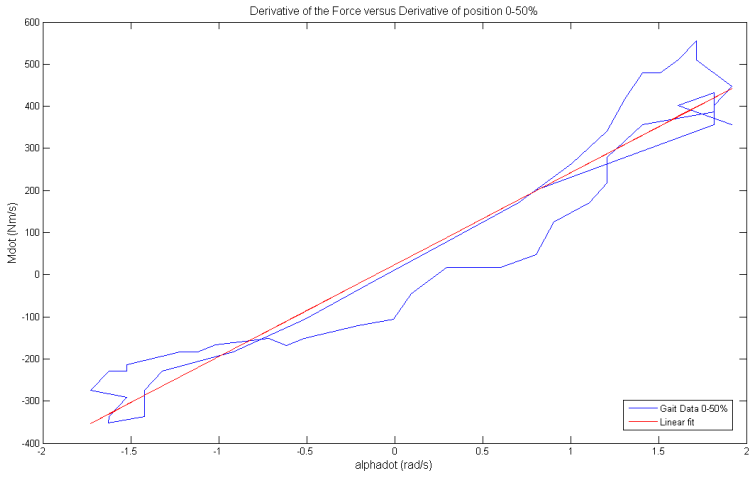

Figure 3.24: Dynamic Knee Stiffness between 0 and 50 % gait cycle. A linear fit of the dynamic stiffness shows a good approximation.

The linear regression shows a good approximation as the R^2 (German: Bestimmtheitskoeffizient), which is a measure for the goodness of the fit, is more than 92 % which is very high.

The R^2 is calculated by the following equation, where $\hat{y}$ is the estimator (linear fit) and y is the original knee data:

$$R^2 = \frac{\sigma(\hat{y})^2}{\sigma(y)^2} \tag{3.16}$$

For a linear regression the R^2 value is the square of the correlation.

$$R^2 = corr(\dot{M}, \dot{\alpha})^2 \tag{3.17}$$

If e.g. a robotic tendon is used as an actuator for an active knee orthosis, it is favorable to choose the spring stiffness K_{spring} of the actuator equal to the dynamic stiffness at the knee (3.8 Nm/rad), which results in a input velocity (motor velocity) which is no longer dependent on the output velocity ("knee velocity") and is a constant value for 0 to 50 % of the gait cycle. The following equations are calculated with values of Ward as a $\dot{F} - \dot{x}$ dependency is only available if

the whole design is known [40]:

$$\begin{aligned} \dot{r} &= \dot{x} - \frac{\dot{F}}{K_{spring}} \\ \dot{r} &= \dot{x} - \frac{49\frac{N}{m}\dot{x} + 1751\frac{N}{s}}{K_{spring}} \\ K_{spring} &= 49\frac{N}{m} \\ \dot{r} = \dot{x} - \frac{49\frac{N}{m}\dot{x} + 1751\frac{N}{s}}{49\frac{N}{m}} &= \dot{x} - \dot{x} \cdot \frac{49\frac{N}{m}}{49\frac{N}{m}} - \frac{1751\frac{N}{s}}{49\frac{N}{m}} \\ \dot{r} &= -\frac{1751}{49} m/s \end{aligned} \tag{3.18}$$

Using this information for the controlling of e.g. a knee prosthesis or orthosis leads to a constant motor speed during the first 50 % of the gait cycle which is desirable as DC motors are much more efficient, if their speed is constant and not changed every sampling period. Ward et al. simulated and tested their powered ankle foot orthosis with such a constant speed approach between 9 and 60 % of gait cycle and showed, that energy was reduced and peak power was reduced dramatically [40].

A lower peak power immediately leads to a smaller and thus lighter DC motor which is very desirable for wearable robots. If this translational potential energy approach is considered for the design of a knee orthosis or prosthesis, a similar peak power reduction could decrease the weight of the whole system significantly. As for this research no knee orthosis or prosthesis is developed, this interesting dependency is not relevant in the following design chapter, but it can be very relevant for future projects.

3.5 Knee Rehabilitation

In knee rehabilitation, there are two big areas with large populations. One is stroke rehabilitation, where the brain has to learn again how to control the intact knee. The second possibility is rehabilitation after injury and/or surgery of the knee.

The following information and considerations are based on the book "Rehabilitation of the Injured Knee" by Letha Y. Griffin [20]. The main goals of rehabilitation are restoring the knee physiologically, anatomically and biomechanically. Most of the rehabilitation exercises can also be used for strengthening and increasing the flexibility of a healthy knee, which can decrease the risk of future injuries. A weak knee puts extra stress on other links of the kinematic chain such as the

hip or ankle.

The reasons to do a professional rehabilitation program besides the much shorter duration of healing for the patient are a reduction of injury symptoms like swelling, pain, redness, knee instability, increased range of motion and an improvement of muscle strength and others. The goals for rehabilitation are restoring the knee-strength, -power, -flexibility and -balance. Also as mentioned before, reducing the risk for future injuries is important, especially for professional sportsman where the duration of rehabilitation and risk of injuries determine the whole career.

One needs to know about the healing of tissue in order to create an effective rehabilitation program. Minutes after an inflammation and destruction of the tissue, the disrupted vessels fill with blood and form a hematoma. Within the first 24 hours, proteins and water volume increase and the blood clots. After several days the new fibroblasts, capillary buds and the first collagen structures grow. In the second week DNA concentration rises and collagen builds a disordered connection structure. After three weeks the gap of the ligament closes and and the collagen fibers start to orientate longitudinally to the ligament. After three weeks the ligament gap closes, and the ligament is already capable of $2/3$ of a normal ligament stress [20].

Rehabilitation starts immediately after injury or surgery through ice or cooling packs and starts in form of continuous passive motion machines. If during the healing process controlled stress is applied to the tendons (muscle activation), the collagen fibers in the ligaments grow much faster and orientate themselves earlier to the ligament direction, which is a main reason why rehabilitation exercises shorten the healing time. A rehabilitation program can consist of temperature treating (heating or cooling), therapeutic ultrasound, muscle activation and many others.

The muscle activation training is consisting of endurance training and strength training. Different muscle activations like concentric (weight lifting), eccentric (weight lowering) and isometric (constant position) activation are used. These activations can be in the form of isotonic actuation where a constant force acts on the muscle, or isokinetic (constant speed) actuation, where the rehabilitation device sets the speed of the motion and the patient tries to resist against the movement (eccentric). Often a combination of these contraction types is used.

Different knee injuries like Patella-, Meniscal- and ligament injuries require different rehabilitation programs. The most common ligament injury is an Anterior Cruciate Ligament injury, which is under large stress if sudden forces combined with changing movement direction are acting at the knee, which happens e.g. in sports like Basketball, American Football, Soccer, Gymnastics

and others. Although the rehabilitation programs differ, all of them contain concentric and eccentric exercises of the Quadriceps and Hamstring muscle groups in closed kinematic chain and open kinematic chain exercises (one muscle group isolated) [20].

The device developed in this project is capable of providing open kinematic chain exercises and offers furthermore the possibility of varying the applied torque at the knee as desired during the movement, which offers the development of a more sophisticated and effective rehabilitation program. There are devices capable of these varied torque programs, like the "Biodex System 3 Isokinetic Dynamometer" described in chapter 2.3.5, but their high prices allow the access to these professional rehabilitation programs only for a few persons. We envision a simple take-home device that is robust and easy to use.

4 Design Study

4.1 Definition of the Design Specifications

To determine the necessary attributes for the development of a knee device, one has to define in which area it will be used. Figure 4.1 shows the focus of this work in the area of knee rehabilitation e.g. after surgery. If an orthosis respectively an exoskeleton shall be developed, there are different possibilities according to its usage. A power exoskeleton tries to increase the power of the wearer e.g. for carrying heavy backpacks on long distances such as the Berkeley lower extremity exoskeleton (BLEEX) described in chapter 2.2.2. Also, a focus on energy harvesting is a possibility which is realized by Dollar et al. described in chapter 2.4.1.

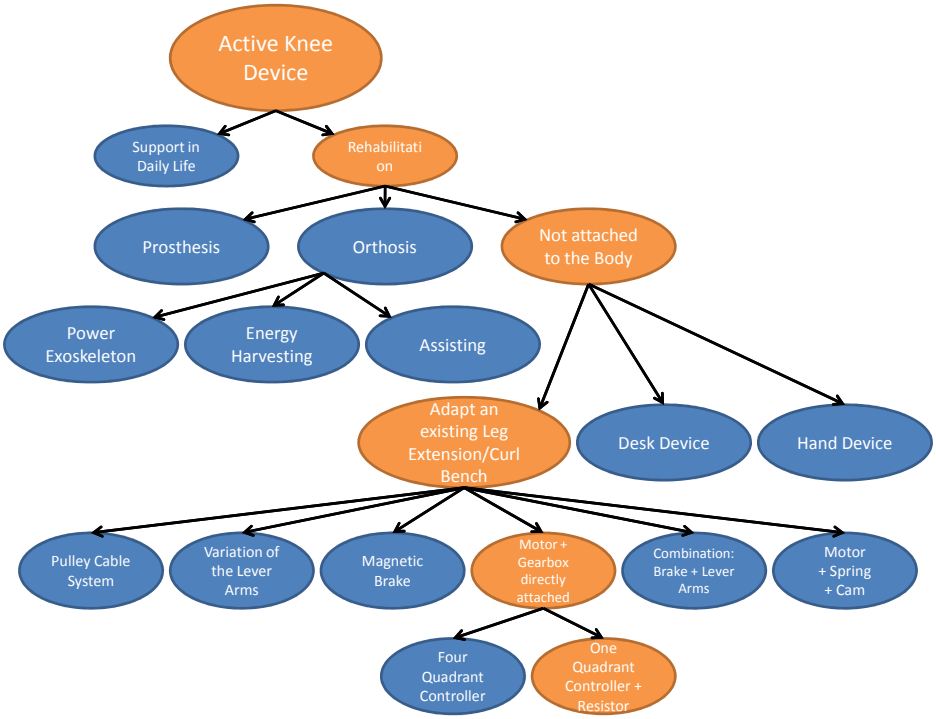

Figure 4.1: Possible topics for an active knee device. The chosen variant is marked orange. The focus of this work is in the field of knee rehabilitation and on adapting an existing device.

The third possibility is a focus on assisting weak or elderly persons during their daily life. This work will focus on the the fourth possibility, a knee rehabilitation device. In rehabilitation, different types of designs are possible. If the device is used for stroke rehabilitation it must be capable of guiding and assisting the patient to learn the movement in a proper manner with the aim of retraining a natural gait pattern. If the device is used for strength rehabilitation e.g. after

surgery, the goal is applying a resistance against the user the train and improve the strength of the muscles and tendons. Also automatic measuring and documenting of the patients force during the sessions could be desired to analyze the progress of the patient.

For a knee rehabilitation device, it is possible to realize a device for a treadmill usage or device where the patient is sitting during the exercise training program. In this work, a device for sitting or standing is developed and the focus will be on a leg flexion and extension device.

Also, the design requirements must specify which muscle groups are trained and what type of tension (e.g. concentric or eccentric) is applied to these muscle groups. For this project, the goal is a concentric and eccentric tension at the Hamstring muscles and Quadriceps muscles with the possibility of applying different torque profiles based on the angle of the knee.

4.2 Knee Muscles and Possible Tensions

In the section 3.1 Knee Anatomic Structure, the anatomy of a right human knee while flexing and extending is shown in figure 3.3. Figure 4.2 shows a rough model of the human knee and possible tensions during flexion or extension. If the muscle is shortening while it contracts, it is called a concentric contraction (weight lifting), and if the muscle is lengthening while it produces a tension (weight lowering), it is called eccentric contraction (from Whittle page 26 [41]).

The situation marked with A is a flexion movement of the knee. An external force F is acting against the movement and thus it is a concentric contraction for the Hamstring muscles. The difference from situation A to B is the direction of the external force. Now, it is acting in the direction of movement and thus it is an eccentric contraction for the Quadriceps muscles. During natural gait this situation is existing e.g. while walking down stairs. In situations C and D, the knee is extending. In situation C, the external force is acting against the movement which is a concentric contraction for the Quadriceps muscles and the movement applies in natural gait while walking up stairs. In situation D, the external force is acting with the movement direction which is an eccentric contraction of the Hamstring muscles.

If one wants to develop an active knee device for knee rehabilitation, it is important to define which of these tensions are part of the rehabilitation exercises supported by the device.

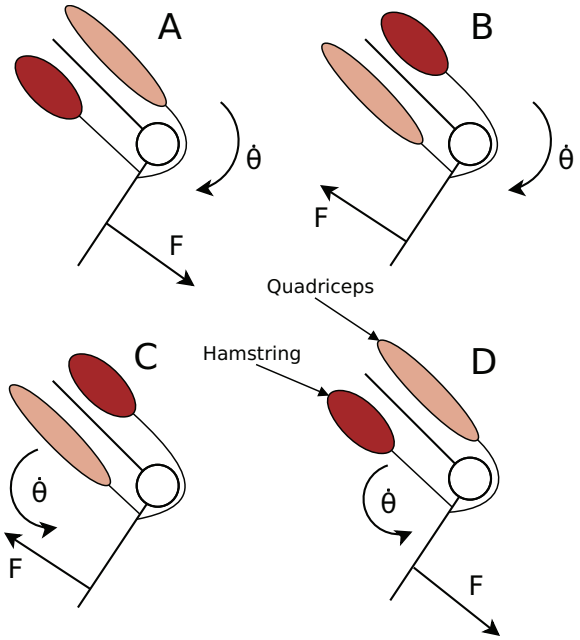

Figure 4.2: Knee Model: Different possibilities of muscle tensions. Actuated muscle is marked red.
A: Flexion, external force acting against movement, Hamstring muscles: concentric contraction
B: Flexion, external force acting with the movement, Quadriceps muscles: eccentric contraction
C: Extension, external force acting against movement, Quadriceps muscles: concentric contraction
D: Extension, external force acting with the movement, Hamstring muscles: eccentric contraction

4.3 Possible Actuators

4.3.1 Robotic Tendon

The Robotic Tendon is an actuator introduced by Hollander et al. It combines a lightweight motor in series with a helical spring. The spring is able to store and release energy and thus the energy and power requirements on the motor are reduced. Also, humans and animals use the elastic nature of their physiologic muscle tendon structure to store and release energy so that energy consumption is minimized.

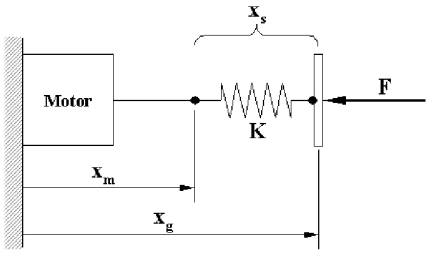

Figure 4.3: Robotic Tendon Model. The DC motor and the helical spring are in series [24].

Figure 4.3 shows a model of the Robotic Tendon. The DC motor and the helical spring are in series. The spring stiffness is tuned for proper gait. With a Robotic Tendon actuator it is possible to construct a device capable of supplying all of the power and energy necessary e.g. for normal human ankle gait with just a 0.95 kg package [24]. This package is almost seven times lighter than a standard DC Motor and gearbox combination for a direct drive system without properly tuned springs. Sugar et al. successfully realized an active ankle foot orthosis and active ankle foot prosthesis with a Robotic Tendon at the Human Machine Integration Laboratory at the Arizona State University [14] [23].

4.3.2 Jack Spring Concept

A spring is an ideal component for a wearable system because a spring stores and releases energy efficiently and is also lightweight and powerful. The power to weight ratio of a standard DC Motor is about 300 W/kg while a spring sized for wearable robotics is capable of 300.000 W/kg. In his work, Hollander introduced the "Jack Spring Concept", which uses a helical spring as a screw and a motor in series. This is a very simple and smart way to store energy in the spring. At the same time the spring can act as a gearbox, which reduces the mass of the construction significantly as a smaller motor and no additional gearbox is needed.

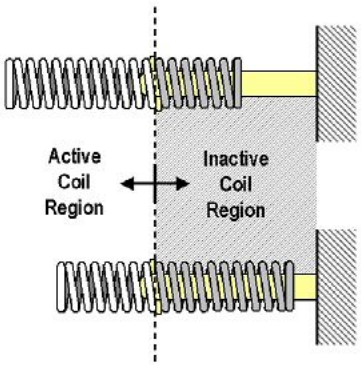

Figure 4.4: Jack Spring Actuator. Changing the active coils by turning the spring causes a change of the spring stiffness [24].

Figure 4.4 shows the concept of the Jack Spring. If the spring is turned, more or less coils of the spring are active and thus the spring stiffness can be adjusted as needed. The Jack Spring can also be used as a transmission converting rotary motion into linear motion. In a wearable robot, the Jack Spring can be used as a gearbox, compliant interface, energy storage device, and safety mechanism. The safety properties arise due to the compliant behavior of a spring which is a much safer attachment to the human body as compared to directly attaching a DC motor to a human

joint [24].

4.3.3 Stiffness Control with Elastic Bands

Similar to the Jack Spring approach, an approach with elastic bands is described in this section. The basic idea is to replace the elastic element in the system by an elastic band instead of the helical spring in a traditional Jack Spring device. In this approach, the length of the rubber band is changed adjusting stiffness similar to changing the number of active coils in the traditional Jack Spring device.

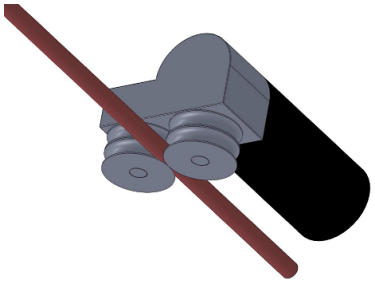

Figure 4.5: Jack Spring with rubber band. The active length of the red rubber band is actively changed by turning wheels driven by a DC motor varying the stiffness of the system.

Figure 4.5 shows a rough CAD design of such a concept. The active length of the red rubber band is actively changed by turning wheels driven by a DC motor. In contrast to the "traditional Jack Spring", the rubber band approach is only capable of providing a pulling force which needs to be considered. The following schematic design study uses this rubber band approach in some designs, but because none of these designes will be prototyped, this actuator is only described roughly. It could be an interesting variant for future projects. This actuator concept is a new variant on the work by Hollander.

4.4 Schematic Design Study

In this section, some rough CAD (Computer Aided Design) desings were considered during the progress of the project. The designs are a summary of possible alternative approaches. If the Hamstrings or Quadriceps actuation is mentioned, a concentric or eccentric tension applied to the regarding muscle is described.

4.4.1 Orthoses (Exoskeletons)

All exoskeleton approaches described in this section have in common that it is very challenging to attach the exoskeleton to the human body in a satisfying manner which is the most tricky part for developing an exoskeleton, which is one of the reasons, why in this project a decision against a realization of an orthosis or exoskeleton was made.

4.4.1.1 Jack Spring "Traditional"

The Jack Spring Approaches use a "traditional" Jack Spring, described in chapter 4.3.2 "Jack Spring Concept", either in a straight or bending mode. For the straight Jack Spring approach, two different configurations (mechanical attachment of the spring) are needed to exercise the Hamstring or Quadriceps muscles. For the bending approach, only Hamstrings activation is possible. If during the movement the number of active coils is varied, different torque-angle relationships are possible.

Jack Spring bending

Figure 4.6 shows an approach of a bending a Jack Spring which is similar to the approach of Bellman described in section 2.6.3. Note, only one of the two Jack springs (back or front) is used, but both configurations allow a Hamstrings actuation and no Quadriceps configuration is possible with this approach. The torque occurring at the knee is a combination of a spring bending torque and a torque generated by a spring extension force due to a defined bending radius as described by Bellman.

Figure 4.6: Jack Spring bending. There are two possibilities, but only one of the two actuators is attached. Only Hamstrings actuation is possible.

Jack Spring straight

Depending on the pre-tension (attachment of the open spring end to the limb) of the spring, it is possible to change the direction of the force. If the spring is compressed as shown in the left picture in figure 4.7, a Hamstrings actuation results. If the spring is extended as shown in the

right picture in figure 4.7, a Quadriceps actuation is achieved.

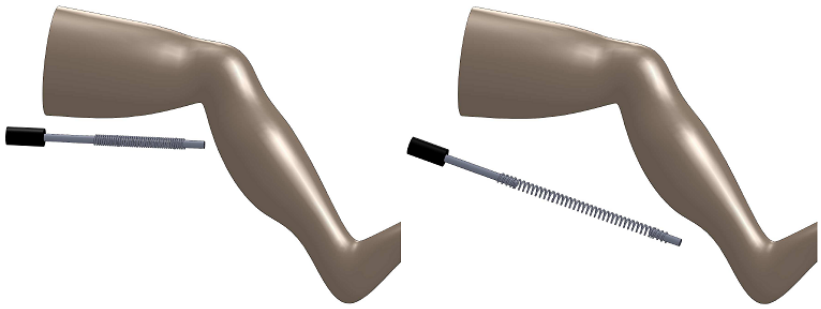

Figure 4.7: Left: Compressed Jack Spring straight device, Hamstrings actuation; Right: Extended Jack Spring straight device, Quadriceps actuation.

4.4.1.2 Jack Spring Rubber Bands

Instead of changing the number of active coils in the "traditional" Jack Spring, it is possible to change the active rubber band length and thus a change in the stiffness of the rubber bands is achieved. The rubber band Jack Spring actuator is described in more detail in chapter 4.3.3. A variable stiffness actuator using a rubber band in combination with a motor was to the knowledge of the author never described before. If such an actuator is used for the design, it has to be considered, that rubber bands are only capable of transferring tension and not compression loads, which causes different configurations needed for Hamstrings or Quadriceps actuation.

One Rubber Band

Figure 4.8 shows a design approach with one rubber band Jack Spring. Additionally, instead of using a rubber band for the whole tendon, a partly metal tendon is possible as it is e.g. difficult to determine the stiffness behavior while bending around a wheel. If the active length (length between the motor attachment and the leg attachment) is actively changed during the movement, the stiffness and thus the force and the torque at the knee are changed.

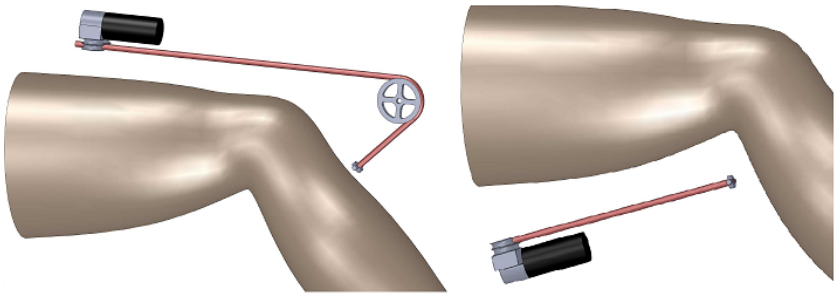

Figure 4.8: One Rubber Band Approach. Left: Hamstrings actuation; Right: Quadriceps actuation. If the active length is actively changed during the movement, the stiffness and thus the force and the torque at the knee are changed.

Two Rubber Bands Knee Wheel

Figure 4.9 shows a design with two rubber bands. The length of both rubber bands is changed symmetrically. In order to not end up with twisting torques around the leg, a symmetric design is favorable, which is the reason for the second rubber band. The second end of the rubber band is connected to a "knee wheel".

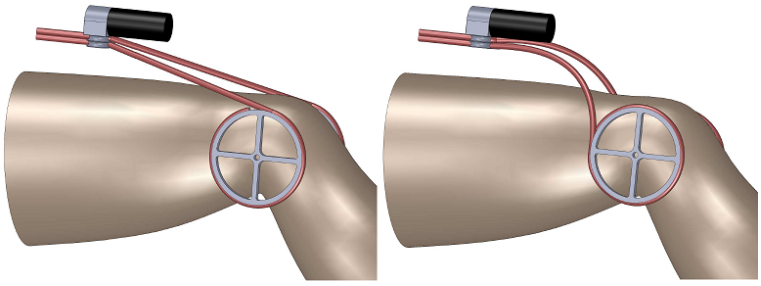

Figure 4.9: Two Rubber Bands Knee Wheel. Left: Hamstrings actuation, Right: Quadriceps actuation.

In the right picture, the knee rubber band is not straight between the motor connection and the wheel. An additional redirection of the bands is necessary because otherwise the rubber bands are colliding with the upper leg.

Two Rubber Bands Low Brace

Figure 4.10 shows an additional approach with two rubber bands, but here the rubber bands are attached to the leg at the lower brace instead of the knee wheel.

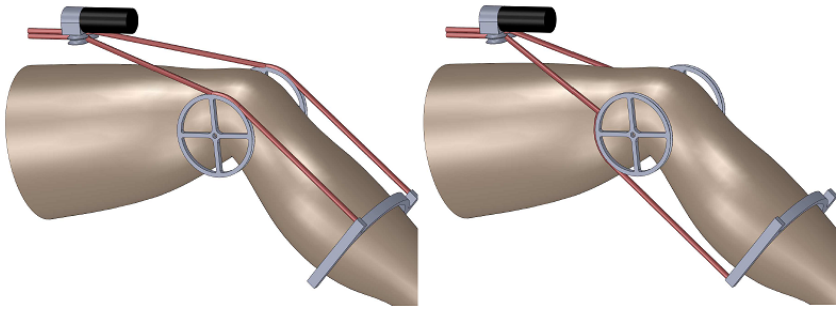

Figure 4.10: Two Rubber Bands Low Brace. Left: Hamstrings actuation; Right: Quadriceps actuation

4.4.1.3 Robotic Tendon

A robotic tendon is basically a motor in series with a spring, which is described in more detail in chapter 4.3.1. It is capable of generating positive and negative power which results in one configuration for both Hamstrings and Quadriceps actuation shown in figure 4.11. Two possible

configuration are roughly drawn.

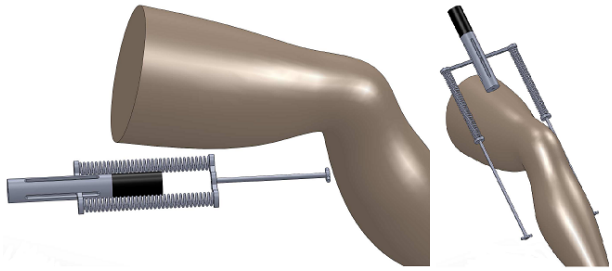

Figure 4.11: Robotic Tendon. Left: Lower attachment; Right: Upper attachment. With both configurations, it is possible to apply positive and negative torques at the knee and thus a Hamstrings and Quadriceps actuation is possible with both configurations.

4.4.2 Non Exoskeletons

4.4.2.1 Desk Device

The "Desk Device" approach illustrates a device which is e.g. attached to a table and the user can easily use it from a sitting position. The advantage of such a device in contrast to an exoskeleton is a much easier design and fewer problems with the attachment to the human leg. Thus, the design is less complex. As in the exoskeleton approaches, different actuator designs a like rubber band Jack Spring, Jack Spring or Robotic Tendon are possible. Figure 4.12 shows rough design drawings with a rubber band Jack Spring approach. Different configurations for Quadriceps and Hamstrings actuation are shown. Also it would be quite easy to change the device to ankle actuation, which is shown in the right picture.

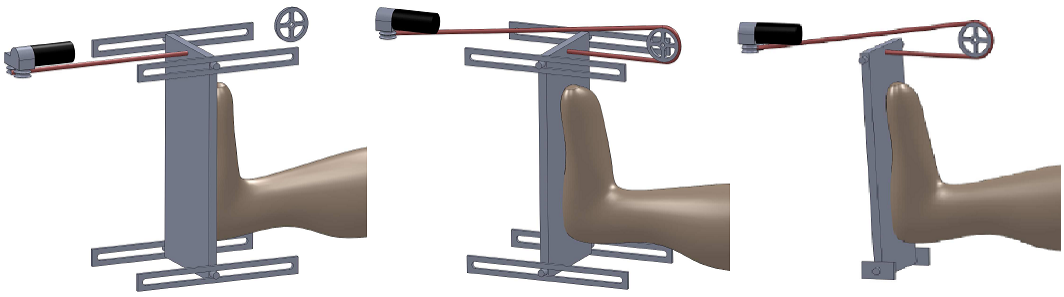

Figure 4.12: Desk device slide. Left: Slide, Hamstrings actuation; Middle: Slide, Quadriceps actuation; Right: Swing, ankle actuation

4.4.2.2 Hand Device

The idea of the hand device is a device which can be held by hand and thus is very easy to "wear" or start exercising, which makes the design even less complex. A schematic of the design is shown

in figure 4.13. Such a system is less complex and thus it has a low price which, can be an important factor if a device for home use is designed.

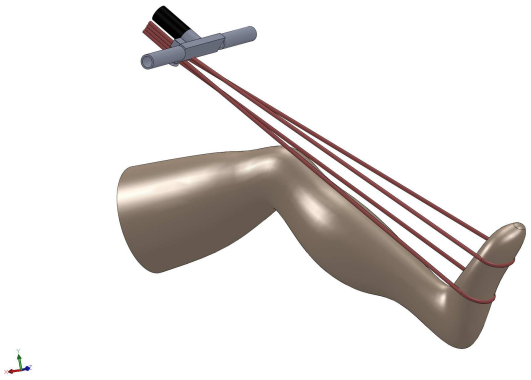

Figure 4.13: Hand Device. Very low complexity but it is difficult to define the forces/torques and safety issues such as slipping at the hand are possible.

The device is only capable of providing Hamstrings actuation which is big disadvantage. Also, it is difficult to accurately define forces/torques at the knee, as they depend on the user's hand forces. Lastly, a safety issue occurs if the device e.g. slips out of the user's hands.

4.5 Detailed Design Study: Commercial Leg Extension/Curl Bench with Active Elements

In order to reduce the complexity of this proof of concept, a decision in favor of a commercial knee extension/curl bench, where the weights are replaced by an active actuator, was made. Figure 4.14 shows a picture of the PLCE165X bench from the company Body-Solid Inc. [6].

Figure 4.14: Leg Extension/Curl Bench PLCE165X. Instead of using weights to generate a torque as shown in the figure, an active element is used. The left picture shows a Quadriceps and the right picture a Hamstrings actuation [6].

A big advantage of this device is, that the same mechanical design can be used to exercise the Quadriceps or Hamstring muscles. In figure 4.14, the left picture shows the device being used for Quadriceps exercises and the right picture shows Hamstrings exercises.

Figure 4.15 shows the two lever arms r_1 and r_2 which generate in combination with the mass a torque at the knee.

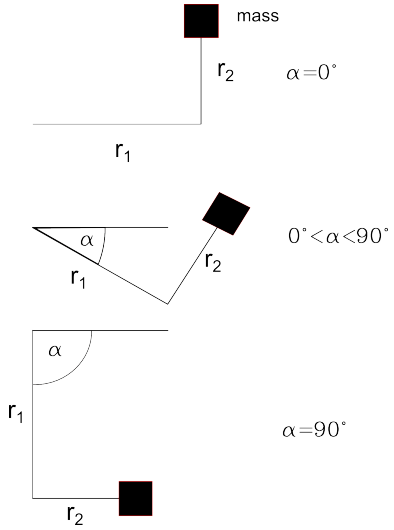

Figure 4.15: Leg Extension Curl Bench. Lever arms for different angles. At $\alpha = 0°$ only r_1 and is effective and at $\alpha = 90°$ only r_2 and the mass influences the generated torque.

The generated torque of the system can be calculated as shown in equation 4.1 where r_1 is the lever arm parallel and r_2 is the lever arm perpendicular to the leg in Quadriceps actuation; mass is the mass of the weights; g is the gravitational acceleration (9.81 m/s^2); and α is the angle of the device/knee (0 degrees is fully extended). The effective lever arms r_1 and r_2 both change as a function of the knee angle which makes it difficult to control the actual torque applied to the knee as a function of knee angle.

$$T = mass \cdot g \cdot (r_1 cos(\alpha) + r_2 sin(\alpha)) \tag{4.1}$$

Figure 4.16 shows the generated torque at the knee if a mass of 20 kg and lever arm r_1 of 0.3 m and r_2 of 0.25 m is used. Whereas the amplitude of the torque can be changed by changing the weights, it is impossible to vary the shape of the torque-angle curve as the two lever arms of the system are fixed. In figure 4.16, the actual generated torque and the optimal curves for concentric Hamstrings and Quadriceps actuation (additional optimal curves shown in figure 3.7) are plotted.

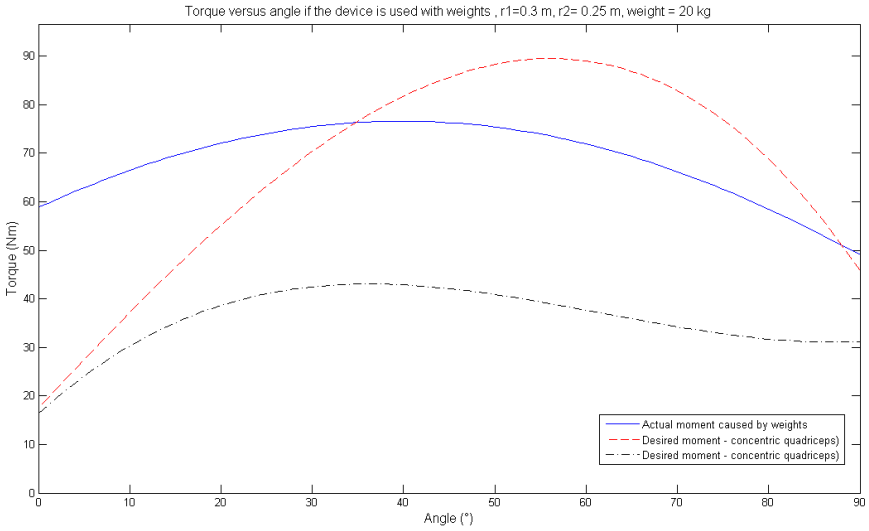

Figure 4.16: Bench Torque if weights are used. Whereas the amplitude of the torque can be changed by changing the weights, it is impossible to vary the shape of the torque-angle curve and meet the desired torque-angle curves for optimal training (concentric Hamstrings and Quadriceps actuation shown, polyfit redraw from [36]).

In the current situation, the torque-angle characteristic is not ideal which leads to the consideration of an alternative approach.

If the weights for torque generation are replaced by an active element (e.g. motor-spring-actuator, variation of r_1 and r_2,...) many different torque-angle patterns can be loaded for different

training situations and patients. It is also possible to apply different profiles for concentric (weight lifting) and eccentric contractions (weight lowering) during exercising which is not possible with conventional exercising devices and can result in a much more effective training regime.

The following section focuses on the description of possible actuator configurations from which one is chosen for a realization.

4.5.1 Pulley Cable System

In this design approach, the basic idea is to replace the force generation with conventional weights by a force generation using a motor-spring combination (e.g. a robotic tendon), which is capable of positive power (concentric actuation, resistance, force direction against the movement direction) and negative power (eccentric actuation, force direction in the same direction as the movement).

Figure 4.17 shows a rough model of the system generated in Matlab. The blue line between point A and B illustrates the moving lever arm. At point B a tendon is attached which is connected via a guide pulley (center point is C) to a motor M that generates a force F along the tendon. The red lines from point B to point D is the first part of the tendon (length l_1) which continues along the guide pulley to the motor.

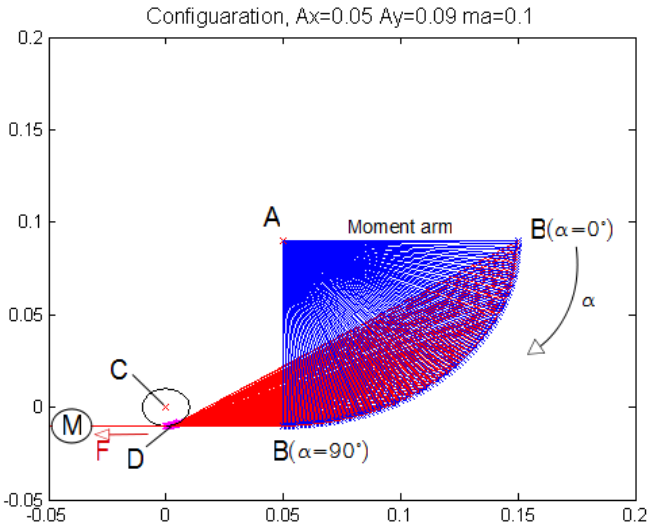

Figure 4.17: Bench Pulley Cable Configuration

In order to determine if this approach is suitable, the different desired torque-angle (from α = 0 to 90°) curves are taken as input curves and recalculated into a force-length relationship to determine the motor position. With the force-length information, a suitable ballscrew-motor

combination can be chosen. At the first point $B = f(\alpha)$, the motor position is calculated:

$$\begin{aligned} C &= \begin{bmatrix} 0 \\ \\ 0 \end{bmatrix} \\ A &= \begin{bmatrix} A_x \\ \\ A_y \end{bmatrix} \\ B &= \begin{bmatrix} A_x + ma \cdot cos(\alpha) \\ \\ A_y - ma \cdot sin(\alpha) \end{bmatrix} \end{aligned} \tag{4.2}$$

The tendon is touching the guide pulley at its tangent connecting points B and D. Point D is at the intersection point of the two circles C_1 and C_2:

$$\begin{aligned} C_1 &: x^2 + y^2 = r^2 \\ C_2 &: (x - \frac{B_x}{2})^2 + (y - \frac{B_y}{2})^2 = \frac{|\vec{B}|^2}{4} \end{aligned} \tag{4.3}$$

Where r is the radius of the guide pulley. Intersecting C_1 and C_2 leads to two points:

$$\begin{aligned} y^2 + y \cdot \underbrace{(-\frac{2r^2 B_y}{|\vec{B}|^2})}_{p} + \underbrace{\frac{r^4 - r^2 B_x^2}{|\vec{B}|^2}}_{q} &= 0 \\ y_{1,2} &= -\frac{p}{2} \pm \sqrt{(\frac{p}{2})^2 - q} \end{aligned} \tag{4.4}$$

The negative solution is chosen:

$$\begin{aligned} D_y &= -\frac{p}{2} - \sqrt{(\frac{p}{2})^2 - q} \\ D_x &= \sqrt{r^2 - D_y^2} \end{aligned} \tag{4.5}$$

The first part of the length change in the tendon is the length between the two moving points B and D:

$$l_1 = |\vec{BD}| \tag{4.6}$$

The second part of the length change in the tendon is the arc length from point D to the point where the tendon leaves the guide pulley horizontally in the direction of the motor:

$$\begin{aligned} \beta &= \arctan \frac{D_x}{D_y} \\ l_2 &= \beta \cdot r \cdot \frac{\pi}{180^\circ} \end{aligned} \tag{4.7}$$

The total change in length during a leg extension or flexion is:

$$l_{total} = f(\alpha) = l_1 + l_2 \tag{4.8}$$

In order to calculate the necessary force F as a function of the desired torque $T_{desired}$, the lever arm ma and the angle α at the the tendon-angle of attack at point B is calculated:

$$\begin{aligned} F_{perpendicular} &= \frac{T_{desired}}{ma} \\ \gamma &= 180^\circ - \alpha - \arctan \frac{B_y}{B_x} \\ F &= \frac{F_{perpendicular}}{\sin \gamma} \end{aligned} \tag{4.9}$$

With the derived information of the force F and the length l, a suitable actuator can be chosen. In order to determine if a spring in series with a motor is a suitable choice, the stiffness of the system is calculated. As only discrete values are available, instead of the derivative the difference from one angle-step to the next is used for this calculation:

$$\begin{aligned} Stiffness &= \frac{dF}{dl} \\ Stiffness_i &\approx \frac{\Delta F}{\Delta l} = \frac{F_i - F_{i-1}}{l_i - l_{i-1}} \end{aligned} \tag{4.10}$$

Figure 4.18 shows the force-length dependency and stiffness-dependency for a concentric Quadriceps torque-angle curve. For the calculations a lever arm of 0.1 m, a guide pulley radius of 0.01 m and a position of the point A=(0.05/0.09) m was assumed.

With this configuration, a maximum force F=1004 N occurs and the total length change is 0.13 m. The stiffness plot shows a negative Stiffness between 0 and 40° and a positive stiffness above 40° and no constant areas which makes it difficult to choose a suitable spring in order to compensate e.g. the non-linearities of the system.

If a speed of 30 °/sec is assumed, an angular speed of 5 RPM is calculated and a respective

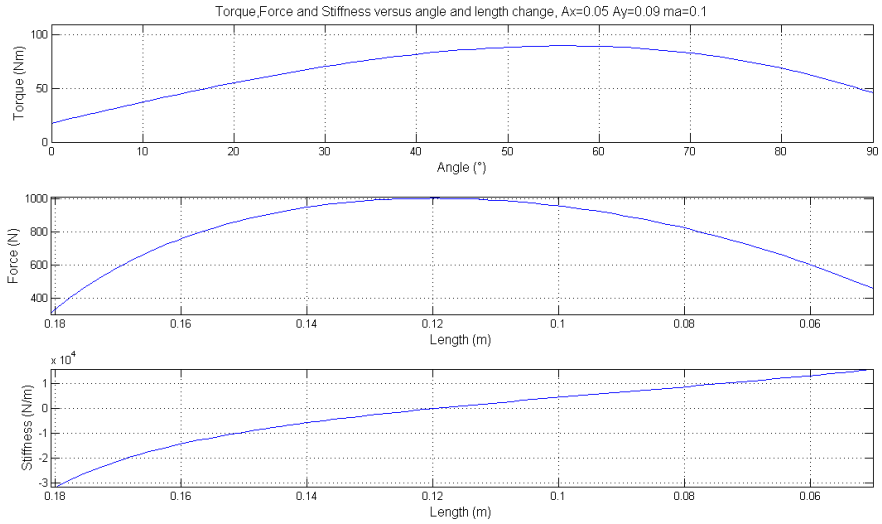

Figure 4.18: Pulley Cable Approach: Force Length Change, Stiffness

linear speed v of 0.0524 m/s. If furthermore a ballscrew with a lead of 1.27 mm is assumed to convert the linear movement at the motor into a rotation and a gearbox with a ration of 3.9:1 is integrated, the maximum motor requirements are calculated as follows:

$$\begin{aligned} T_{Gearbox} &= \frac{F \cdot l}{2\pi} \\ \dot{\theta}_{Gearbox} &= \frac{v}{lead} \\ T_{Motor} = \frac{T_{Gearbox}}{ratio \cdot \eta} &= 0.116Nm \\ \dot{\theta}_{Motor} = \dot{\theta}_{Gearbox} \cdot ratio &= 8657RPM \\ P_{Motor} = T_{Motor} \cdot \dot{\theta}_{Motor} &= 105W \end{aligned} \tag{4.11}$$

Where η is the overall system efficiency which is assumed to be 0.5. With the maximum requirements $T_{Motor} = 0.116$ Nm, $\dot{\theta}_{Motor} = 8657$ RPM e.g. a Maxon RE40 is a possible choice.

If this solution is chosen, a lot of non linearities have to be considered (changing angle of attacks during movement), as described before and also the the large translational range of motion and high forces on the system (e.g. on the guide pulley) have to be considered making this system quite complicated. In order to reduce non linearities of this pulley cable system, it is possible to use a cam with a varying radius instead of the circular guide pulley which is considered in the previous analysis, but the system is still complex.

4.5.2 Variation of the Lever Arms

A different approach for varying the torque-angle curves is an active variation of the lever arms r_1 and r_2 which are shown in figure 4.15. At $\alpha = 0°$ only r_1 is effective and at $\alpha = 90°$ only r_2, and the mass influences magnitude of the generated torque.

Between 0 and 90 degrees, the torque generated calculated:

$$T = m \cdot g \cdot (r_1 \cos(\alpha) + r_2 \sin(\alpha)) \tag{4.12}$$

The idea in this approach is to use variable lever arms e.g. by using a motor-ballscrew combination. In order to evaluate if such an approach is possible, a desired torque-angle characteristic for concentric Quadriceps actuation of an 80 kg person is assumed. For the torque generation a mass of 40 kg is used. The lever arm r_1 is held constant and in a fully extended position ($\alpha = 90°$) only r_1 is affecting the torque. r_1 is calculated as:

$$r_1 = \frac{T(\alpha = 0°)}{m \cdot g} = 0.05m \tag{4.13}$$

The length of r_1 equals 0.05 m which is very low. An actual device probably needs a longer lever arm and lower weight. In order to reach the desired torque, r_2 is calculated:

$$r_2 = \frac{\frac{T}{mg} - r_1 \cos(\alpha)}{\sin(\alpha)} \tag{4.14}$$

Figure 4.19 shows a evaluation of the lever arm variation approach with a mass of 40 kg, $30°/sec$ for concentric Quadriceps actuation for an 80 kg person. To reach an optimized range of motion, forces, speeds and powers, the lever arm r_1 should be varied during the movement as well.

Subplot 1 shows the desired torque for concentric Quadriceps actuation for an 80 kg person (starts with 90 degrees and ends with 0 degrees). A polyfit function is used to approximate the curve. The range of motion shown in subplot 2 is between 0.12 and 0.29 m. From the speed and force along the lever arm, the necessary power can be calculated.

$$\begin{aligned} v_i &\approx \frac{\Delta r_2}{\Delta t} \\ F_i &= mg\cos(\alpha) \\ P_i &= F_i \cdot v_i \end{aligned} \tag{4.15}$$

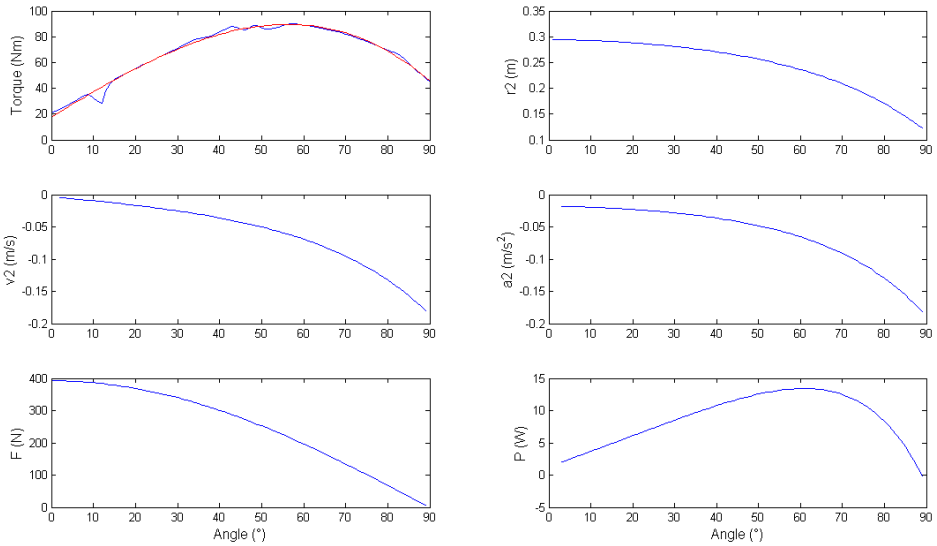

Figure 4.19: Variation of r1 and r2 Approach: An evaluation with a weight of 40 kg for concentric Quadriceps actuation results in a maximum speed of 0.17 m/s, maximum force of 392.4 N and a maximum power of 13.4 W

The evaluation shows a maximum speed of 0.17 m/s, maximum force of 392.4 N and a maximum power of 13.4 W. The large range of motion (approximately 0.4 m) and also a minimum value for the lever arms of less than 0.1 m makes it hard to realize a device that varies the lever arms.

4.5.3 Magnetic Brake

As electrical motors have problems with high torques at low speeds which leads to gearboxes with a high ratios, in this approach the idea is to use a magnetic brake. For this consideration, magnetic particle brakes from the company Placid Industries Inc. are used [7].

As a magnetic particle brake is only capable of generating positive power (force against movement, resistance), with this design approach it is only possible to generate concentric actuations for Hamstrings or Quadriceps.

According to the data sheet of the magnetic brake B220 from Placid Industries Inc. it would be possible to use this brake e.g. with a 5:1 timing belt arrangement to generate a peak torque of 120 Nm needed for eccentric Quadriceps exercises for an 80 kg person without exceeding the maximum heat dissipation of 110 W in the brake. Because only concentric actuations are possible, this approach was determined to not be desirable.

4.5.4 Combination: Magnetic Brake, Weights and Lever Arm Variation

As a magnetic brake shows promising characteristics but it is only capable of generating a resistance, the idea to combine weights with certain lever arms r_1 and r_2 and a magnetic particle brake emerged. Similar to conventional machines, weights are used, but the torque-angle characteristic can be actively changed to the desired characteristics using a magnetic brake.

For concentric contraction (force against the movement direction), the goal in this approach is, to have a lower than desired torque caused by the weights, as the brake torque can increase the total torque at the knee:

$$T_{total} = T_{weights} + T_{brake} \tag{4.16}$$

On the other hand for eccentric contraction (force along the movement direction), the torque caused by the weights has to be higher than the desired one as the brake reduces the actual torque at the knee:

$$T_{total} = T_{weights} - T_{brake} \tag{4.17}$$

An evaluation of this approach is shown in figure 4.20 for four different torque-angle characteristics for an 80 kg person. The lever arms $r_1 = 0.15$ m and $r_2 = 0.25$ m are constant for all four cases, but the mass added to the device is changing.

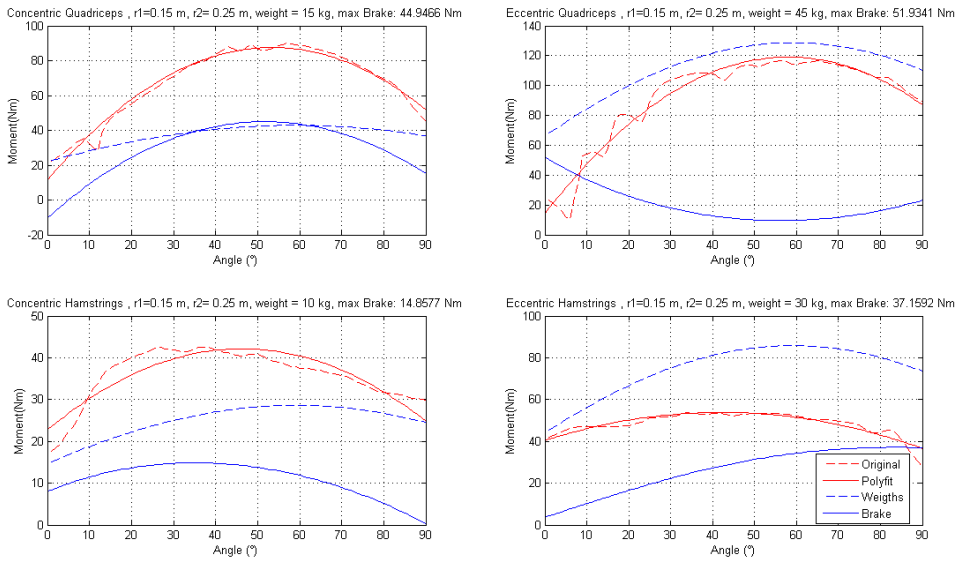

Figure 4.20: Bench design approach: Combination of a magnetic particle brake and weight variation. $r_1 = 0.15$ m and $r_2 = 0.25$ m. Four different desired torque curves for an 80 kg person. Polyfit approximated curves are used. Conc quad: 15 kg, ecc quad: 45 kg, conc ham: 10 kg, ecc ham 30 kg.

As the brake is only generating the difference from the weight generated torque curve to the desired torque curve, the maximum torque occurs at the eccentric contraction for the Quadriceps muscles at approximately 52 Nm.

Thus with a 10:1 ratio transmission a torque of 6 Nm at 50 RPM occurs at the brake which results in a heat dissipation of [7]:

$$P_{heat} = RPM \cdot torque(Nm) \cdot 0.106 = 32W \tag{4.18}$$

32 W is lower than the maximum heat dissipation of 50 W in a magnetic particle brake B60 from Placid Industries Inc. [7].

In a future project instead of varying the weight, varying the lever arms would work (if r_1 and r_2 are doubled, the same torque curve is achieved with half of the weight).

As the system needs a magnetic brake, a variation of the lever arms and a variation of the weights it is too complicated because motors and brakes are needed for this solution.

4.5.5 Combination: Motor-Spring-Cam

This approach attempts to use a motor in combination with springs. The system is a combination of a motor in series with a spring and an additional spring parallel to it. The whole motor with parallel and serial springs is connected to a cam with a varying radius as shown in figure 4.21.

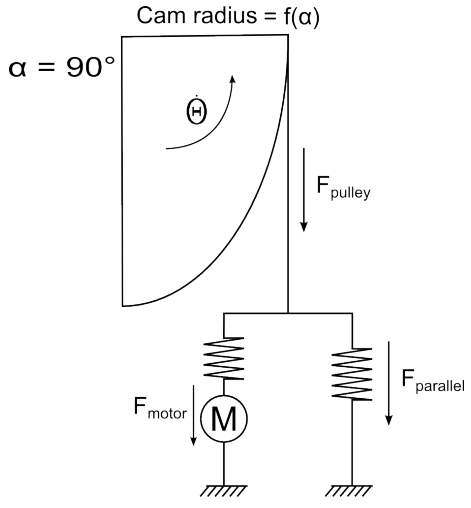

Figure 4.21: Design approach: motor spring cam combination

In order to always guarantee tension in the springs, additionally a pre-tension for both springs is applied. To alter the necessary pulley force, a cam with a varying radius is integrated in the system. For the upcoming calculations only Quadriceps actuations (for an 80 kg person)

are considered, because the torque values are higher than the ones for Hamstrings actuations. The torque at the cam is the acting force times the lever arm (parallel spring not taken in the consideration):

$$T_{des} = F \cdot r = (K_s \cdot s_o + K_s \cdot r \cdot \Theta) \tag{4.19}$$

Which results in the following cam calculation:

$$r = -\frac{s_o}{2\Theta} + \sqrt{\frac{s_0^2}{4\Theta^2} + \frac{T_{des}}{K_s \cdot \Theta}} \tag{4.20}$$

Where r is the cam radius, K_s the serial springs stiffness, s_o the offset for the pre-tension, T_{des} the desired torque and Θ is the varying knee/device angle. For the serial spring, six parallel springs with a stiffness of 3.21 lb/in each are assumed which results in a total serial stiffness of 3373 N/m.

Figure 4.22 shows the resulting cam radius for concentric and eccentric Quadriceps actuation. For most angle positions the eccentric actuation shows a larger radius, these values are used for the following analysis. (It was determined that two cam profiles was not valid as only one cam part would be machined. The radius of the cam has to be the same for both concentric and eccentric actuation for simplicity.

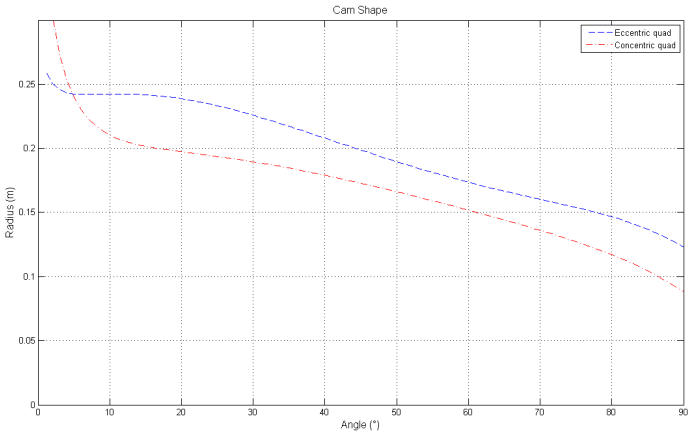

Figure 4.22: Cam radius for the motor spring cam combination. For most angle positions, the eccentric actuation has a larger radius and these values are taken for the following analysis.

The necessary pulley forces are calculated by dividing the desired torque T_{des} by the cam radius r:

$$F_{pulley} = \frac{T_{des}}{r} \tag{4.21}$$

In order to reduce these necessary forces, a parallel spring is integrated in the system. For the parallel spring, three parallel springs with a stiffness of 3.21 lb/in each are assumed which results in a total parallel stiffness K_p of 1687 N/m.

The necessary forces at the input side F_{motor} of the spring (motor side) are calculated by subtracting the parallel spring force $F_{parallel}$ from the pulley force F_{pulley}:

$$\begin{aligned} x_p &= s_o + \alpha \cdot r \\ F_{motor} &= F_{pulley} - K_p \cdot x_p \end{aligned} \tag{4.22}$$

Where x_p is the spring deflection of the parallel spring depending on the offset s_o, α and the cam radius r.

The necessary pulley and motor forces are shown in figure 4.23. The blue lines are for eccentric actuation and the red lines for concentric actuation. The figure shows the necessary pulley (dotted) and the necessary motor forces (solid). The difference is due to the force in the parallel spring.

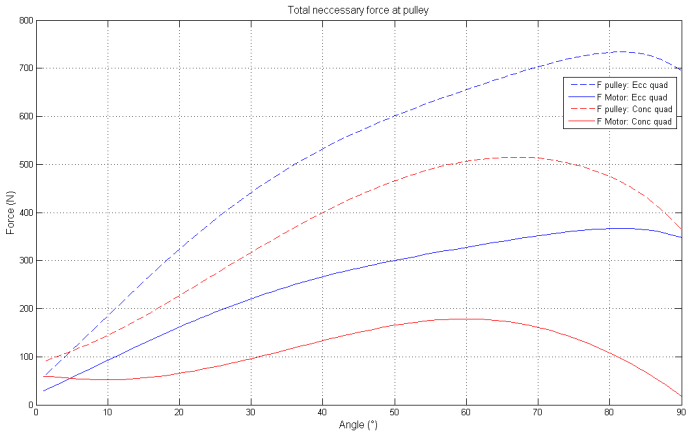

Figure 4.23: Necessary forces for the motor spring cam combination. The blue lines represent the eccentric Quadriceps contraction and the red lines show the necessary forces for concentric Quadriceps contraction for an 80 kg person. The necessary forces provided by the motor are smaller because of the parallel spring.

The necessary serial spring input position (motor position) r is calculated (assuming a constant radius for the arc length calculation $r \cdot \alpha$):

$$r = \frac{F_{motor}}{K_s} - r \cdot \alpha \tag{4.23}$$

The necessary motor position varies between zero and 188 mm for concentric Quadriceps

actuation. The necessary motor speed is approximately:

$$v_{motor} \approx \frac{\Delta r}{\Delta t} \tag{4.24}$$

The necessary motor power is calculated by:

$$P = F_{motor} \cdot v_{motor} \tag{4.25}$$

The necessary motor power for concentric and eccentric Quadriceps actuation for an 80 kg person varies between -11 W and 16 W and is shown in figure 4.24.

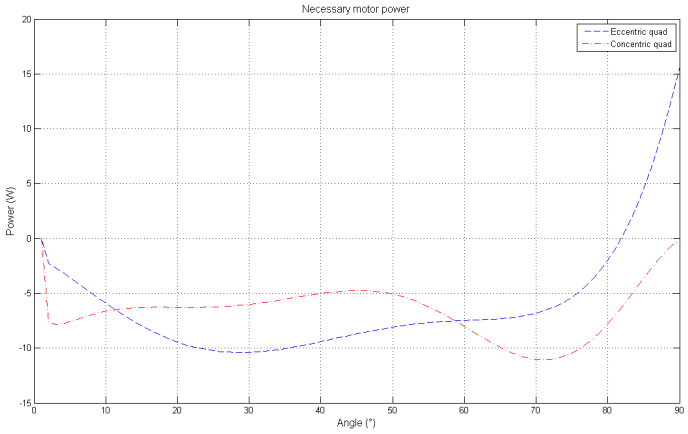

Figure 4.24: Necessary motor power for the motor spring cam combination. Necessary motor power for concentric and eccentric Quadriceps actuation for an 80 kg person varies between -11 W and 16 W.

If a motor pulley radius of 0.45 m is assumed this results in a maximum motor torque of 0.17 Nm and a maximum motor rotation speed of 2900 rpm. Thus a suitable motor is quite easy to find.

Despite a possible solution with the described combination of a motor, two springs (one in series and one parallel to the motor) and a cam with a varying radius, this system seems to be quite complicated to prototype and many separate parts and and their influences have to be considered. Thus, this system will not be realized during this project, but it should be possible with the described configuration to realize this system.

4.5.6 Motor directly attached with Gearbox

As all previous design concepts had either issues with complexity or with consuming too much power or only able to resist loads, this final approach tries to attach a motor directly to the rotating

axis of the bench. Between the bench and the motor is a gearbox to convert the high torques and low speeds of the human into low torques and high speeds which is more suitable for an electrical motor.

The approach is only described roughly in this chapter as a more detailed description follows in the chapter "Realization". As mentioned the basic idea is to connect the motor directly to the rotating axis of the bench with a gearbox. One gearbox is attached directly to motor (gear ratio 64:1) and an additional worm gearbox (gear ratio 10:1) connects the motor gearbox directly to the rotational axis of the leg extension/flexion bench, which results in a total gear ratio of 640:1. An important criteria of both gearboxes is that they are backdrivable in order to apply a more comfortable feeling for the user.

The gear ratio influences the inertia felt by the user of the system. In order to evaluate the inertia, the rotational inertia of the motor RE40 is used, as no rotational inertia of the purchased CIM motor is available:

$$J_{total} = J_{motor} \cdot ratio^2 = 13.8 \cdot 10^{-6} kgm^2 \cdot 640^2 = 5.6 kgm^2 \tag{4.26}$$

The inertia felt by the user is quite high. In order to get a feeling if this value is too high, it is compared with the inertia of the existing leg extension/curl bench with weights as described before:

$$J_{weights} = m \cdot radius^2 = 40kg \cdot (0.3m)^2 = 3.6 kgm^2 \tag{4.27}$$

Thus the inertia felt by the user for both systems is in the same order of magnitude. A large inertia is a problem if the user tries to change the velocity or tries to change the movement direction quickly.

Figure 4.25 shows the four possible modes of operations of a motor [33]. For the operation of the motor, two quadrants are relevant for this project. One is in quadrant one "motor mode", which means that the motor is operated in forward direction and the torque is acting against the movement direction (concentric contraction of the muscle). The second mode of operation is in quadrant four "generator mode", were the motor is moving in reverse direction and the torque is going in the same direction direction as the movement, which is called "regenerative braking" [33] (eccentric contraction of the muscle). When changing the mode of operation from quadrant one to four, the current has the same sign (current is proportional to the torque and thus the force

direction), but the voltage has a negative sign (voltage sign depends on the turning direction). Thus from quadrant one to four the force has the same direction, but the movement direction changes which describes our case.

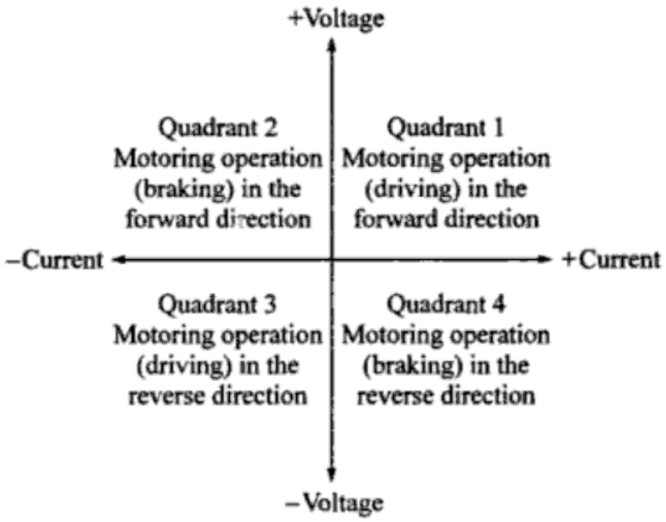

Figure 4.25: Four quadrant operation of a motor [33]. For this project quadrant one and quadrant four are relevant.

We believe, that this solution is the most realistic and practical approach and thus it is realized which is described in the following chapter.

5 Realization

As mentioned earlier, the motor has to be controlled in quadrants one and four which leads to two different approaches. The first approach is the usage of a state-of-the-art four quadrant controller in combination with a regulated power source. A disadvantage of this approach is the need for a regulated power source leading to a higher price for the power supply and the controller, larger dimensions and also for very high power the electronic parts may not exist. In our system large power spikes are not the case for the slow knee movements that we will rehabiliate. Also e.g. for a stand alone system with battery power, the burning of the negative energy can be a less complicated alternative to charging the batteries with the generated power as less electronics are required, but of course there is a disadvantage of energy loss.

In the second, alternative approach instead of using a regulated power supply and four quadrant control, it could be easier and cheaper to use a one quadrant controller for powering the motor (quadrant 1) and a resistor to burn the energy in the generator mode (quadrant 4). In order to vary the loads (varied desired torque) with the generator, the value of the resistor can be varied by a pulse-width modulation (PWM) scheme.

5.1 PWM Testing

In order to evaluate if such a PWM approach is possible, a bench test was performed. The test arrangement consists of two motors coupled together. One motor drives the other one and thus simulates the input torque of the user. The second motor acts as a generator and is connected to a resistor where the energy is burned. In order to vary the load of the system (later the desired torque), the resistor is switched on and off with a PWM modulation scheme.

Figure 5.1 shows the basic electronic test circuit. The generated current flows through a Hall sensor to measure the current and is switched on and off with a MOSFET. The controlling of the driving motor, PWM signal generation and evaluation of the generated current I and voltage Vm is done in Matlab/Simulink with the xPC Target toolbox.

For the dimensioning of the circuit the following considerations were made:
An update of the pulse width shall be done every 0.1 s (PWM period time T)and thus the resistance and respectively the torque that the user has to overcome is also updated every 0.1 s. Depending on motor constants, turning speed and chosen resistor to burn energy, a minimum power (0 % pulse width) and a maximum power (100 % pulse width) are possible. The resolution r between minimum and maximum shall be 100 which makes it possible to vary the power in 1 % steps which

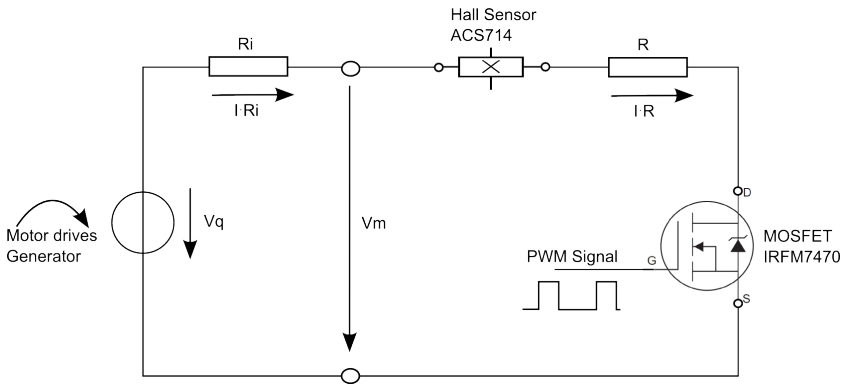

Figure 5.1: PWM Test: Schematic. A PWM signal controlled MOSFET switches a resistor on and off causing a variable resistor, current and thus a variable torque.

leads to a necessary PWM update frequency f of 1 kHz.

$$\begin{aligned} T &= 0.1s \\ r &= 100 \\ f &= \frac{1}{\frac{T}{r}} = 1000Hz \end{aligned} \tag{5.1}$$

Depending on the length of the executed code and thus the execution time, the existing xPC target system (described in more detail later) is capable of approximately a 2 kHz system frequency. Thus, it should be possible to generate the PWM signal with this system and test it.

The generator used for this test is a RE25 Maxon Motor with the following motor constants:

Table 5.1: Maxon RE25 motor constants

Nominal speed	n	8240 rpm
Torque constant	K_t	115 mNm/A
Speed constant	K_v	828 rpm/V
Inner ohmic resistance	R_i	0.517 Ω

For the pulse width generating, the desired resistor R_{des} needs to be calculated:

$$\begin{aligned} P &= T \cdot \omega \\ I &= \frac{T}{K_t} = \frac{P}{\omega \cdot K_t} \\ R_{des} &= \frac{V}{I} = \frac{V \cdot \omega \cdot K_t}{P} \\ R_{des} &= \frac{n^2 \cdot K_t \cdot \Pi}{K_v \cdot P \cdot 30} \end{aligned} \tag{5.2}$$

The necessary pulse width PW in percent is calculated with the desired and the actual resistor R_{act}:

$$PW = \frac{R_{act}}{R_{des}} \cdot 100\% \tag{5.3}$$

The actual resistor of the circuit is a sum of the serial resistors in the circuit. The resistor $R_{DS(on)}$ of the MOSFET and the resistor of the Hall sensor are neglected.

$$R_{act} = R_i + R = 0.517\Omega + 10.69\Omega = 11.21\Omega \tag{5.4}$$

In order to evaluate if the digital outputs of the system are capable to provide the necessary current, the input capacity C_{ISS} of the MOSFET must be checked. For the chosen MOSFET, IRF7470 $C_{ISS} = 3.43nF$. To get a rough idea, the necessary current is approximately:

$$I_{out} \approx C_{ISS} \frac{\Delta U}{\Delta t \cdot 2} = 0.43mA \tag{5.5}$$

The Schmitt Trigger ICs 74HC14 at the output of the system are capable of 25 mA and thus are easily capable of providing the necessary current.

Figure 5.2 shows results of the PWM testing. It shows the desired and actual turning speed, the generated motor voltage, current, and the generated power. At the time of 6 s the pulse width is increased from 45 % before 6 s to 56 % after 6 s.

The actual turning speed of the motor speed shows a variation between approximately 8600 rpm and 7700 rpm instead of a constant rated turning speed of 8240 rpm. The reason for that is that the controller of the driving motor is not capable of compensating the turning speed from idle running to rated power and back in 0.1 s. Also, the resistance of the connections and wires to the resistor are not considered in this test. These two inaccuracies result in combination with other

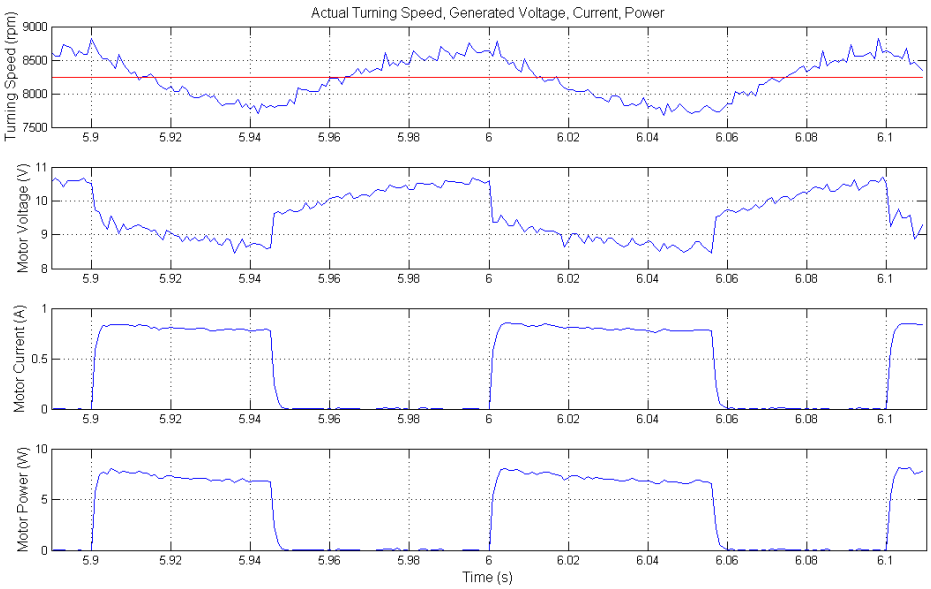

Figure 5.2: PWM Test: Generated voltage and pulsed current and power. The turning speed varies between 8600 rpm and 7700 rpm instead of 8240.

factors to a small difference from the rated and actual power shown in figure 5.3. The generated power is increased from 0 W to 8 W by varying the the pulse width.

The evaluation of this test shows promising results which makes a further investigation of the PWM approach possible. The problem of quickly varying the turning speed will be much smaller in the actual bench device, as the inertia due to the bigger motor and gearboxes will be much higher. Also the switched-on-time can be changed from one block and distributed over the whole period time (e.g. 10 times switching for PW/10), which should reduce this effect.

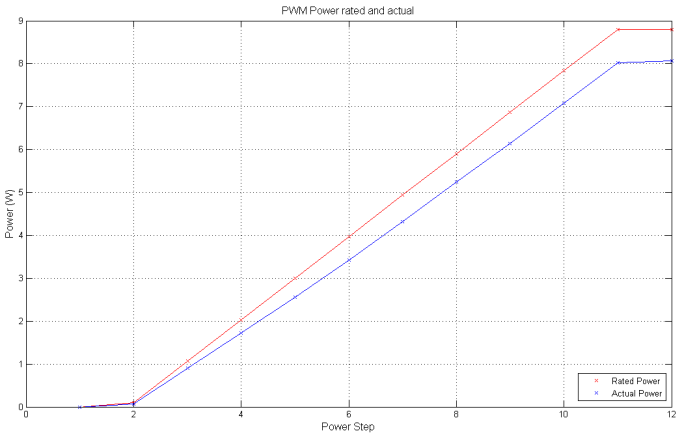

Figure 5.3: PWM Test: Rated and generated power. A difference between rated and actual power occurs due to a varying turning speed, the ignored resistance of the power lines and other reasons, but the test shows that the PWM approach principle is working as expected and works with a linear behavior.

5.2 Mechanical Design Test Arrangement

5.2.1 System Configuration

In a first step, only the actuation part of the system is built which means that the motor is connected via two gearboxes to a turning shaft which in the future would be connected to the bench. In order to evaluate if the system works properly, a lever arm is connected to the rotating shaft where an absolute encoder measures the angle. At the lever arm, the necessary force versus the "knee-angle" is evaluated. After these tests show promising results, the whole system can be connected to the training bench in the future.

Figure 5.4 shows the test arrangement. The motor gearbox combination drives the turning shaft and the lever arm where a weight of 26.6 kg is attached. The picture shows the weight in the low position ($\alpha = 0°$). During the testing procedures, the motor drives the lever arm up to a position of 90°(horizontal). If the position is reached, the motor controller is switched off and PWM signal generation is started. The lever arm is pulled down by the gravitational force acting at the weight.

Table 5.2 shows a list of the necessary material to set up the test arrangement.

A defined weight is connected to the lever arm which is shown schematically in figure 5.6. The lever arm $r_1 = 0.471m$, $r_2 = 0.223m$ and the weight $m = 26.6kg$ generate a torque at the turning shaft.

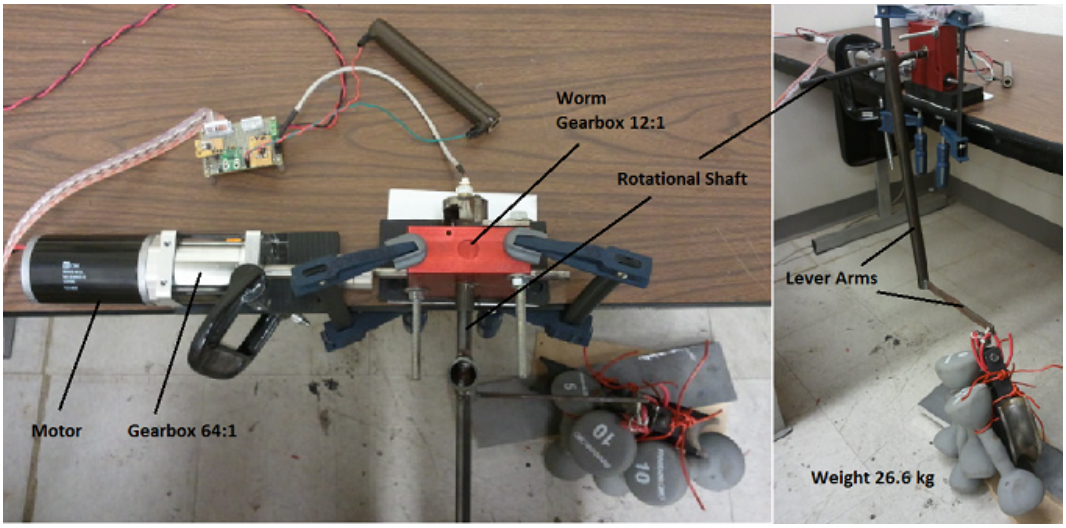

Figure 5.4: Test Arrangement: Mechanical. A motor is connected via two gearboxes to a rotational shaft which is connected to a lever arm where a weight is attached to generate a simulated knee torque.

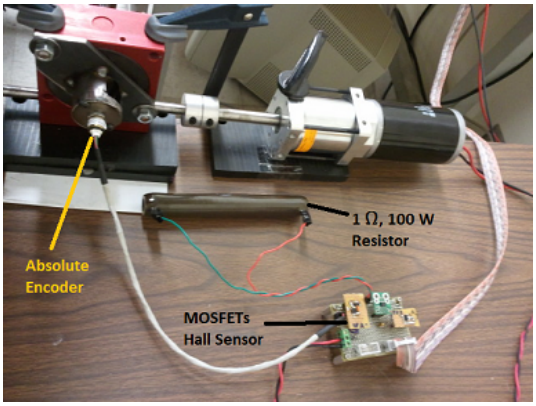

Figure 5.5: Test Arrangement: Electrical, An absolute encoder connected to the rotational shaft, the two MOSFETs, a Hall sensor and a 1 Ω, 100 W resistor are connected to an IO board.

Table 5.2: Material List

Label	Short description	Article number
Mechanical		
CIM Motor	150W, brushed, 12V, 5310 RPM	M4-R0062-12
CIM Gearbox	64:1	P80K-444-0005
Worm Gearbox	10:1	-
Coupler	10 mm - 0.5 in	U-CPRC32-L10-R0.50
Rotary Shaft	12 mm, key groove, end tapped	SFMKRT12-300.0-M5-KA15-A50
Electrical		
Motor Controller	Peak Current 40 A, 20 A cont.	AZBE40A8
Mounting Card	IO Board for MC	MC1XAZ01-HR
2 MOSFETs	I_{DS} 10A and 30A, V_{GS} 5 V	IRF7470 and SI4456DY
Current Sensor	0 - 30 A	ACS715
Resistor	1 Ω, 100 W	L100J1R0E
Encoder	Absolute, 5 V	MA3-A-B8
xPC Target System	PC104, digital and analog IOs	-
Diode	Shottky	1N5819
2 Power supplies	12 V, 24 A in series (24 V)	IF24-12

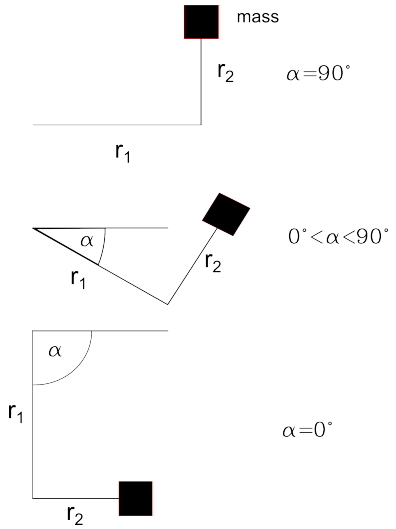

Figure 5.6: Test Arrangement: Lever arms for different angles. At $\alpha = 90°$ only $r_1 = 0.471$ m is effective and at $\alpha = 0°$ only $r_2 = 0.223$ m is effective. The mass $m = 26.6$ kg influences the generated torque.

The generated torque is calculated as:

$$T_{human} = mass \cdot g \cdot (r_1 sin(\alpha) + r_2 cos(\alpha)) \tag{5.6}$$

The torque generated by the weight of the lever arms itself is neglected. Figure 5.7 shows the weight of the test arrangement generated by the lever arms and the weight which is acting at the turning shaft of the system. The maximum torque occurs at 65°with 136 Nm.

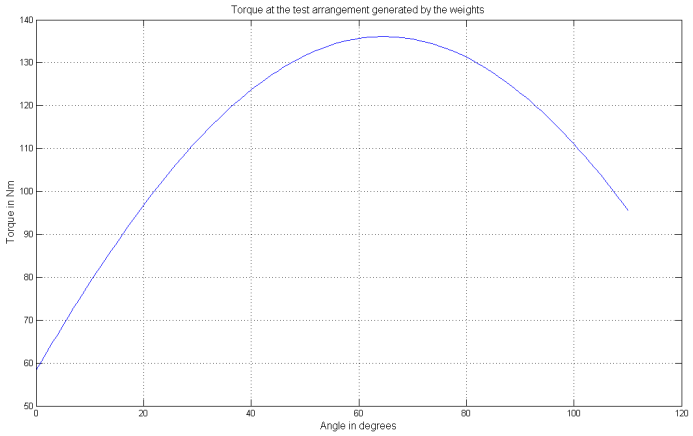

Figure 5.7: Test arrangement: Torque generated by the lever arms and the weight versus the angle of the system.

5.2.2 Motor

For the final design, the RE25 motor used for the PWM testing bench testing could not be used because it does not have enough power. Because efficiency of the system was not a main focus in this project, a cheap brushed DC motor is sufficient. The motor constants for the chosen motor "FIRST CIM Motor" are shown in table 5.3.

Table 5.3: FIRST CIM Motor Constants

Nominal speed	n	5310 rpm
Torque constant	K_t	18.2 mNm/A
Speed constant	K_v	443 rpm/V
Inner ohmic resistance	R_i	not defined

The motor through two gearboxes is directly attached to the turning shaft of the bench. For the pulse width calculation of the PWM signal and the set current of the motor controller, the

inner resistance, power line resistance and the mechanical friction torque of the system need to be determined. The mechanical friction torque is composed of the friction torque of the motor and the torque due to the friction in the gearboxes and the friction in the bearings at the shaft holding the lever arm. As none of these values are given in the data sheets, measuring these values is necessary. In order to measure the inner ohmic resistor, a small voltage was applied to the coils of the motor and the resulting current was measured which is shown in table 5.4. As the voltage is varied in a low range, the rotor of the motor does not turn and thus only the ohmic behavior of the motor that is affecting the current is measufred. A better model is described in more detail later. In the Matlab model for the pulse width calculation the evaluated average ohmic resistance of 175 $m\Omega$ is used.

Table 5.4: Inner Ohmic Resistance CIM Motor

Voltage mV	Current A	Resistance $m\Omega$
18.3	0.1	183
66	0.366	180.3
158	0.917	172.3
231	1.42	162.7
	Average	**175**

5.2.3 System Friction

As the whole system is supposed to be turned either by the motor or by the user, the motor and the two gearboxes have to be backdrivable. The mechanical friction of the system also needs to be measured, which can be done by applying a torque at the turning shaft of the bench to measure how much torque is necessary to move the device consisting of the the two gearboxes and the motor. Also, it is possible to run the motor with different speeds and measure the necessary current and conclude the part due to friction, assuming that the ohmic resistor is known, This method is helpful to evaluate if the friction torque is constant or varying for different turning speeds. Due to a lack of time, the necessary friction torque is not measured for different turning speeds and it is assumed to be constant for different driving speeds. This assumption is relaxed in later sections.

In order to start the movement from standing still a torque of approximately 83 Nm is necessary, which is a value for the static friction of the system. More interesting for the calculation is the

rolling friction of the system which is at approximately 60 Nm, which is a higher value than expected, but it is still possible to run the tests. For future work, a better motor/gearbox system must be purchased.

5.3 Electronics - Controls

All models created in Simulink and Matlab for the test arrangement are included in "Appendix A: Test Arrangement Simulink, Matlab Code".

5.3.1 xPC Target

For the controlling the test arrangement, a xPC Target system is used. Using Matlab, a xPC Target toolbox, Real-Time Workshop, and a C/C++ compiler (e.g. Visual C/C++ Compiler), the system allows one to generate executable C/C++ code. The code is generated on a host PC and downloaded via an Ethernet cable to the target PC. On the target PC, a xPC Target real-time kernel is running. The target PC is a small embedded PC with PC/104 IO boards. For the IO boards, a Sensoray 526 provides 16-bit analog in- and outputs and four 24-bit quadrature encoder inputs and eight digital IO channels which can be used to sense and control the test system [1].

The system provides a very fast and convenient way to export and execute Matlab/Simulink control algorithms. The average execution time for the downloaded model was at 0.13 ms, which makes a minimum cycle time of approximately 0.5 ms or a 2 kHz sample rate possible. In order to run the system with some reserves the sample rate of the test arrangement is set to 1 kHz.

5.3.2 Schematic

Figure 5.8 shows a schematic circuit of the test arrangement. Depending on the turning direction (concentric or eccentric) and the turning speed either the motor controller or one of the two MOSFETS is enabled.

A Hall Sensor is used to measure the actual current during the generator mode, which is read in by an analog input ($I_{measured}$). The actual voltage ($V_{measured}$) at the PWM block is measured with an analog input. Two MOSFETs are necessary as depending on the desired torque and turning speed of the motor/generator different current amplitudes are necessary to achieve the desired torque, which is described in more detail in the generator mode section.

As described earlier and shown in figure 4.25, the motor/generator is used in quadrant one and four. Quadrant one (motor mode) is driving in the forward direction which is achieved by

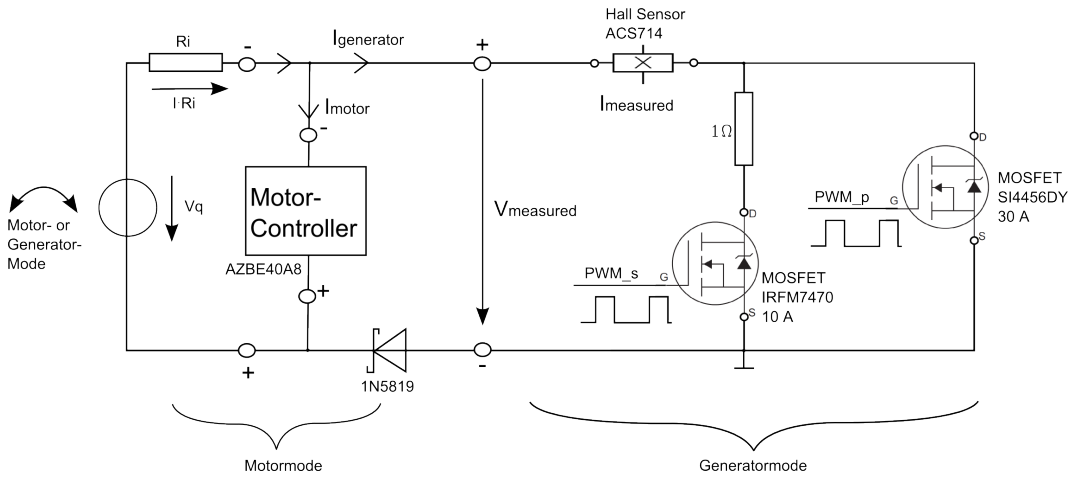

Figure 5.8: Test arrangement: Schematic, Motor controller and MOSFETs

giving the motor controller a defined set current. Quadrant four (generator mode) is braking in the reverse direction. Thus, between these two quadrants, the turning direction changes which is the case for this application. For design of the circuit, one can see that the current direction is the same in both quadrants, but the voltage direction changes, which is the reason why the plus and minus connection of the motor controller and the PWM-generator-block need to be commutated.

The diode is necessary to generate a galvanic isolation between the mass connection of the PWM - connection and the plus output of the motor controller. Without this diode a shortcut would occur during motor mode as the minus output of the motor controller is internally connected to the signal mass of the system. The voltage drop at the diode and the inner resistance have to be considered in the pulse width calculation which is described in more detail in the section generator mode. For the test arrangement, the shottky diode 1N5819 was used. Shottky diodes have a low forward voltage dropout and a fast switching times because a metal-semiconductor junction is used. For the final design of a bench device, a diode capable of higher continuous forward currents needs to be chosen, as the continuous forward current of the IN5819 with 1 A is too low for durable usage in this configuration.

5.3.3 Mode Control

In order to simulate a training session of a human user, the two modes of alternating concentric contraction (weight lifting) and eccentric contraction (weight lowering) must be tested in an alternating fashion. In contrast to the actual leg extension/flexion bench, the test arrangement switches the link between weight lifting/lowering and concentric/eccentric contraction as the weights in this test arrangement simulate the torque generated by the user. Thus, as the motor drives the weights

up against the weight-torque respectively, the user-torque is resisting against the torque generated by the motor, which is similar to eccentric contraction described before.

For example in the generator mode, one of the two MOSFETs is switched on and a current is flowing causing a proportional "resistance-torque" against the movement caused by the weight-torque respectively. This resistance to the user-torque is similar to concentric contraction described before.

The mode control block in the Simulink model (see appendix A) is generating either an enable signal for the motor controller or an enable signal for the pulse width generation. The test procedure itself starts at a lower position where the motor controller is activated causing a motor-torque higher than the friction-torque plus the weight-torque resulting in an upward movement of the weight. When the system reaches the upper position ($\alpha = 95°$), the motor controller is deactivated and with a small time delay to avoid shortcuts, the PWM generation is activated. As the motor torque is switched off and the weight-torque is higher than the friction-torque, the lever arm starts to move back down causing a voltage generation in the coils of the motor/generator.

If no MOSFET is switched on and thus no current is flowing, the only resistance against the movement is the friction-torque, which is assumed to be constant, but if during the downward movement, a PWM signal switches the MOSFETs on and off, theoretically the weight-torque is varied. This modulated resistance simulates the resistance that the user has to overcome. The variable torque is controlled by the xPC target system.

When the system reaches the lower position ($\alpha = 20°$), the PWM generation is deactivated and again with a time delay the motor controller is activated and the cycle starts from the beginning. As a safety precaution a pushbutton is integrated which deactivates the system automatically as soon as the pushbutton is not pressed anymore. Also mechanical end stops are integrated to stop the system if something goes wrong with the control system.

5.3.4 Motor Mode

Motor mode of the test arrangement corresponds to eccentric contraction of the human muscle groups, which means that the external force is acting in the movement direction. For the testing of the system, the torque generated by the user is replaced by the torque generated by the weight and lever arms. The motor moves the system upwards and the weight torque is resisted simulating the torque that the human must resist. The torque reaching the user is the actual motor-torque minus friction.

If the motor controller is activated (motor mode), it sets the current through the motor to the desired value depending on the weight and angle of the system. In the test arrangement the set current is calculated by evaluating the actual position and the desired torque. The necessary current through the motor is calculated as:

$$T_{Motor}(\alpha) = \frac{T_{Human} + T_{Friction}}{ratio} \cdot f_{move} \tag{5.7}$$

$$I_{Motor}(\alpha) = \frac{T_{Motor}(\alpha)}{K_t} \tag{5.8}$$

Where the friction torque $T_{friction} = 60$ Nm is added to the necessary torque as it also needs to be overcome by the motor. The torque at the turning shaft divided by the system $ratio = 640$ results in the necessary motor torque. The movement factor $f_{move} = 1.1$ gives an additional torque in order to allow movement of the system. The necessary motor current is calculated by dividing the necessary motor torque by the torque constant $K_t = 18.2$ mNm/A, which is assumed for all calculations to be constant and linear over the whole motor speed and torque range.

During the motor operation, the actual angle of the system is evaluated with the absolute encoder and depending on its position, the necessary torque is written to the motor controller via an analog output of the xPC target system. The motor controller regulates the actual current to the desired value. Unfortunately the friction and torque factor are not exactly linear and vary slightly for different speeds and torques, which results in a varying torque at the rotating shaft and thus there is a rough and not very smooth operation. An improvement for this situation could be an additional torque or force sensor. With the actual torque information, a feedback control loop can provide an an exact torque, which is also described in the section "Future Work" in the conclusion chapter.

5.3.5 Generator Mode

Generator mode of the test arrangement corresponds to concentric contraction of the human muscle groups, which means that the external force is acting against the movement direction. Thus, the weight-torque simulating the user-torque has to overcome the friction torque and the variable PWM generated torque. Due to the high friction of the system, the minimum torque which is possible with this configuration is approximately 60 Nm, which is already higher than e.g. the desired torque for hamstring actuation, but it is still possible to prove if the system is

working as expected. Additional to the friction-torque, a variable torque can be added by the PWM generation as described before.

The desired behavior of the system is a variable torque based on angular position of the knee joint, and as the torque at the motor is proportional to the current, also a variable current is desired. The flowing current depends on the turning speed, the speed constant of the motor which results in a generated voltage, and the ohmic resistance of the system. Whereas the first two constants remain the same, the ohmic resistance of circuit is varied by switching on and off periodically. By varying the resistance, the actual current and thus the actual torque is varied, which is the goal of the project.

For the calculation of the pulse width, the following calculations have to be made:

$$T = \frac{P}{\omega} \tag{5.9}$$

The torque T at the motor is its power P divided by its angular velocity ω and the current I is the torque divided by the torque constant K_t, which results in:

$$I = \frac{T}{K_t} = \frac{P}{\omega K_t} \tag{5.10}$$

The ohmic resistance R of a system is the voltage V, which is the motor speed n divided by the speed constant K_v, divided by the current which can be rewritten as:

$$R = \frac{V}{I} = \frac{V\omega K_t}{P} = \frac{\frac{n}{K_v}\omega K_t}{T\omega} = \frac{nK_t}{TK_v} \tag{5.11}$$

As the speed constants has rotations per minute as its unit, the desired resistance R_{des} of the system can be written as:

$$R_{des} = \frac{60 \cdot nK_t}{T(\alpha)K_v} \tag{5.12}$$

The ohmic inner resistance R of the motor is 175 mΩ and was evaluated earlier. A 1 Ω resistor is added to the system, which including power line resistances equals 1.147 Ω. Additionally the voltage drop at the diode has to be considered, which as measured during operation has a value of 0.52 V at 1.5 A, which is modeled as a constant ohmic resistor R_{diode} with 0.347 Ω (this assumption is not exactly correct but the resistance change of the diode for different currents is neglected in order to reduce complexity of the model). As two MOSFETs are integrated in the system, one causing a current flow through the motor, one shortcutting the motor, two different

nominal resistors need to be considered:

$$\begin{aligned} R_{serial} &= R_i + R_{diode} + R \\ R_{parallel} &= R_i + R_{diode} \end{aligned} \tag{5.13}$$

The second shortcutting MOSFET is needed to increase the range of virtual resistances. Also, if the turning speeds of the generator are lower and thus lower desired resistances occur, the second MOSFET is needed. If the pulse width of the parallel/serial MOSFETs is 100 %, the resulting resistance will be exactly the parallel/serial resistance. If the pulse width is 50 % the circuit is switched off for half of the time, which is virtually increasing the resistance and thus decreasing the current and respectively the resulting torque.

The pulse width calculation itself is calculated as the following:

$$\begin{aligned} PW_{serial} &= round(\frac{R_{serial}}{R_{des}}) \\ PW_{parallel} &= round(\frac{R_{parallel}}{R_{des}}) \end{aligned} \tag{5.14}$$

and rounded to the next full percent as one percent is the desired resolution of the test arrangement. If the pulse width PW_{serial} is shorter than 100 %, the PWM signal for the serial MOSFET is generated and written to the digital output of the xPC target system. If the pulse width of the serial MOSFET exceeds 100 % the parallel MOSFET gets activated and the serial one is deactivated.

In order to show if the actual torque follows a variable desired torque, a desired, sinusoidal-shaped torque is used, which is shown in figure 5.9. The minimum torque of the system is its friction torque with 60 Nm and its maximum is at 90 Nm. During a movement from 0 to 90° the torque profile shows a sinusoidal-shape. If the system follows the desired torque, arbitrary torque profiles can be loaded as a desired torque profile (the minimum value is always the friction torque).

The voltage signal of the absolute encoder which is proportional to the angle of the rotational shaft showed a high noise level, which made the use of average filters necessary, as the information of the angle and the derivation of the angle to determine the speed of the system is needed in realtime for the calculations during the test cycles. In Simulink "Weighted Moving Average" filters with a length of 500 are used to smooth the angle and motor speed signal. This may cause a short delay between the real angle of the system and the measured angle, but without these filters the evaluation of the actual angle and speed did not work.

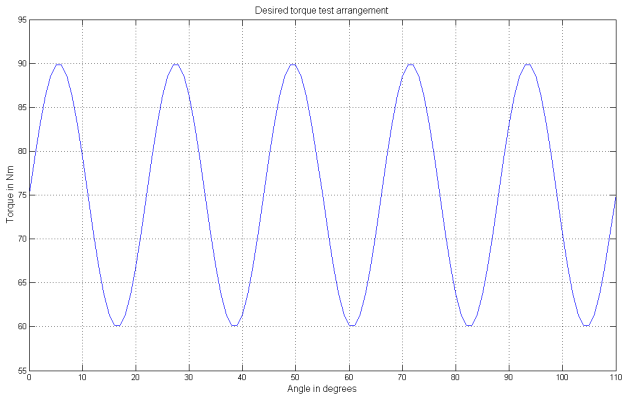

Figure 5.9: Test Arrangement: Desired Torque. Minimum torque is at 60 Nm, which is the friction torque of the system and the maximum torque is at 90 Nm.

5.3.6 Test Cycle

In order to summarize the test procedure, figure 5.10 shows one cycle of the test procedure. In the left picture, the motor mode is activated, where the motor generates a torque 10 % higher (solid blue) than the torque caused by the weight (dotted red). As the motor torque is higher than the weight torque, an upward movement from 20°to 95°will occur.

Once an angle of 95°is reached, the motor mode is deactivated and the generator mode is activated shown the right picture. There the weight torque (dotted red) is higher than the desired sine-shaped torque (solid blue). As the weight torque is higher than the desired torque, a downward movement will occur until the lower position of 20°is reached. Then the next cycle starts.

5.4 Results

Figure 5.11 shows an overview of a testrun with eight cycles. The plot shows the system in alternating motor mode (angle is increasing) and generator mode (angle is decreasing) showing the generated voltage, current, angle and speed of the motor.

For the following plots only one PWM cycle is analyzed in detail, which is cycle four of the overview. Figure 5.12 shows the pulse width during cycle four, which depends on the speed of the generator and the desired torque at each certain angle. At the beginning and at the end of the cycle, the desired resistor was lower than R_{serial} resulting in an activation of the parallel MOSFET, which is mainly due to the lower speed at the beginning and end of the cycle. In the beginning, the system needs to accelerate from zero rps and at the end the generated weight-torque becomes lower as the influence of the longer lever arm r_1 is getting smaller, causing the system

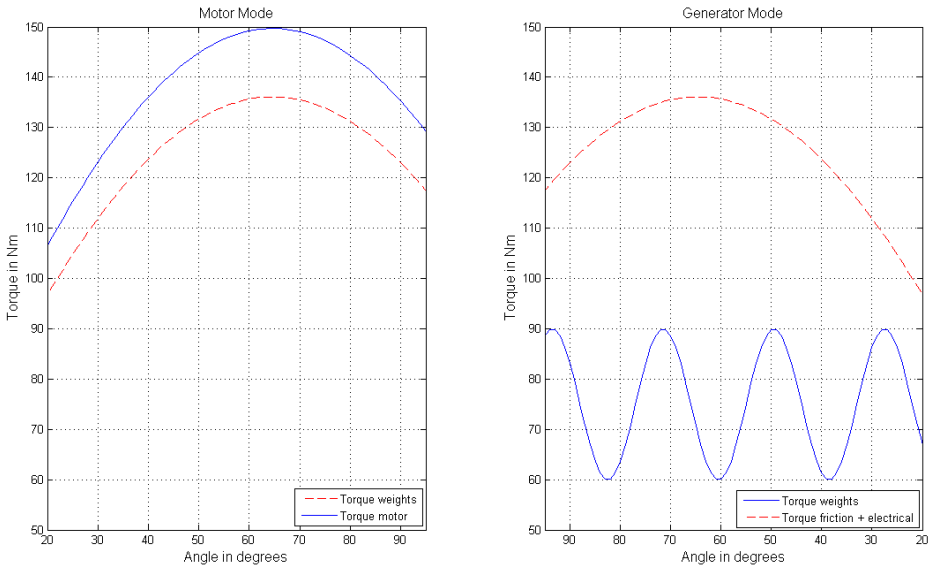

Figure 5.10: Test Arrangement: Motor - Generator - Cycle. In motor mode on the left a motor torque (solid blue) which is higher than the weight torque (dotted red) causes an upward movement. In generator mode on the right, the weight torque is higher than the desired sine-shaped torque, causing a downward movement.

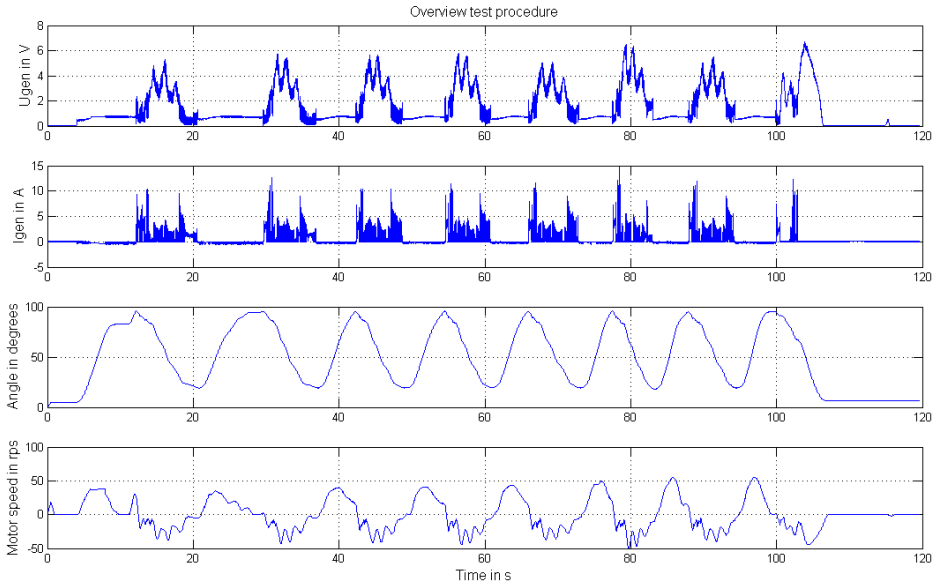

Figure 5.11: Results: Overview Test Procedure. Generated voltage, current, angle and motor speed for a testrun with eight cycles.

to decelerate. Thus, it can lead to the situation that the pulse width of the parallel MOSFET is 100 % because the speed is very low, but the 100 % pulse width itself is creating a high torque slowing the system down even more. For the controlling in combination with a leg extension/curl bench this behavior needs to be considered.

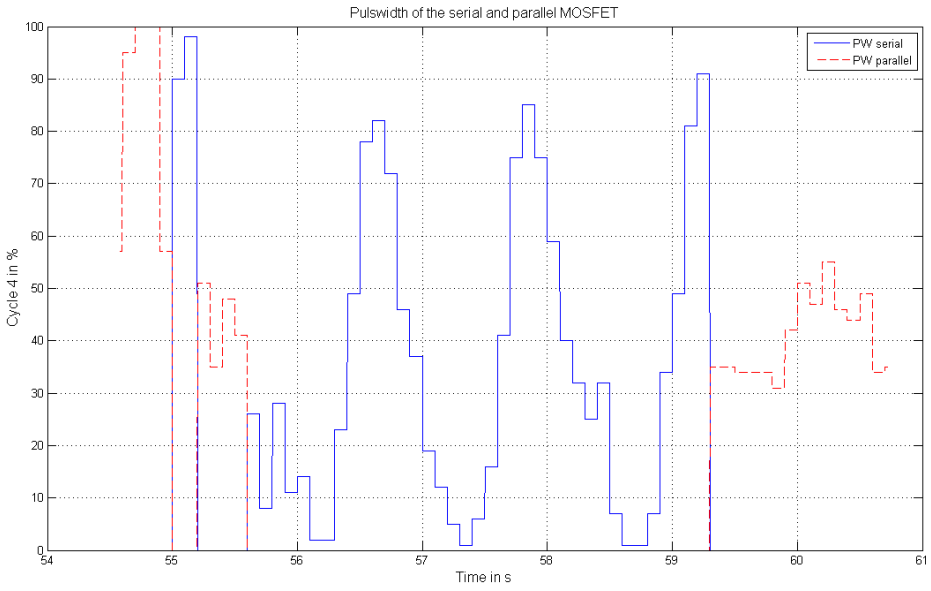

Figure 5.12: Results: Actual Pulse Width Cycle 4. Due to a lower speed at the beginning and the end of the system, the parallel MOSFET needs to be activated in these areas.

Proportional to the turning speed of the motor, a voltage is generated by the motor/generator, which is shown in figure 5.13. If no current is flowing (MOSFETs are switched off), the generated voltage is proportional to the turning speed n times the speed constant K_v:

$$V_{gen} = V_{measured} = n \cdot K_v \tag{5.15}$$

As soon as a MOSFET is switched on, the measured voltage drops immediately, as the voltage drop at the inner ohmic resistor of the motor/generator and at the diode is not part of the voltage measurement.

$$V_{gen} \neq V_{measured} = n \cdot K_v - I \cdot R_i - V_{diode} \tag{5.16}$$

Voltage drops at the hall sensors and MOSFETs are very small and thus neglected and the ohmic resistance of the power lines is already included in the resistor values of the measured inner ohmic resistor of the motor and the measured actual resistance of the 1Ω Resistor equals (1.147Ω).

In the second subplot in figure 5.13, one can see the changing of the actual pulse width over cycle 4. At the beginning and the end of the cycle, higher current peaks occur as the motor is short-wired by the parallel MOSFET during the pulses as described before. In between the pulses, current flows through the 1Ω resistor causing lower current peaks.

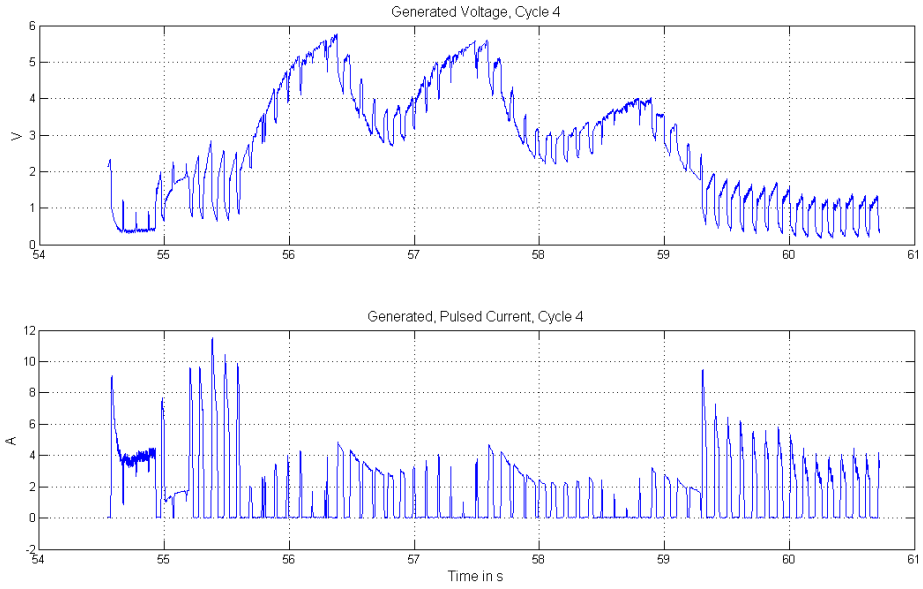

Figure 5.13: Results: Generated Voltage and Pulsed Current.

Figure 5.14 shows the pulsed torque of cycle 4. The upper plot shows the whole cycle and the lower plot shows a detail. The actual pulsed torque T_{act} is the measured current times the torque constant K_t.

$$T_{act} = I \cdot K_t \tag{5.17}$$

One can see that the period time is the desired 0.1 s and the pulse width is changing from one pulse to the next. The average torque is calculated from one rising edge of the pulsed torque to the next resulting in the step function plotted in red in the figures.

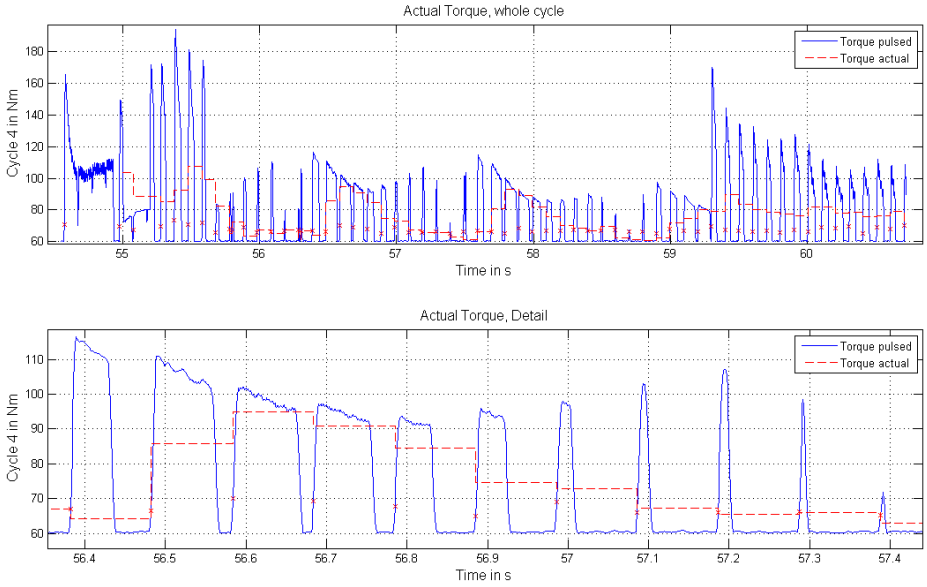

Figure 5.14: Results: Pulsed Torque. The actual pulsed torque is the pulsed current times the torque constant K_t. From one rising edge of the torque to the next, the average torque is calculated and plotted as a red dotted step function.

5.4.1 Torque Angle Characteristic

More interesting than the actual torque versus time is the actual and desired torque versus the angle during the movement, which is shown in figure 5.15. The plot shows the actual and desired torque during a downward movement of the test arrangement versus the actual angle. The actual torque follows the desired sinusoidal-shaped torque in a promising manner, which proves, that it is possible with the a motor, gearboxes and pulsed resistors to vary the actual torque in the desired manner. Using even better motors and gearboxes with less friction, we expect the results to improve.

However, as a torque of 60 Nm is necessary to overcome friction, which is already higher than the average torques for Hamstring actuation, the motor and gearboxes used in this test arrangement are not ideal for a use with an actual leg extension/curl bench, where a system with less friction needs to be built.

5.4.2 Model Verification

During the calculations, several assumptions and linearizations were made. In order to evaluate if the model is still sufficient, a short look at input and output powers is analyzed. Errors are most likely caused by the assumption that the diode has a constant ohmic resistor and that the friction

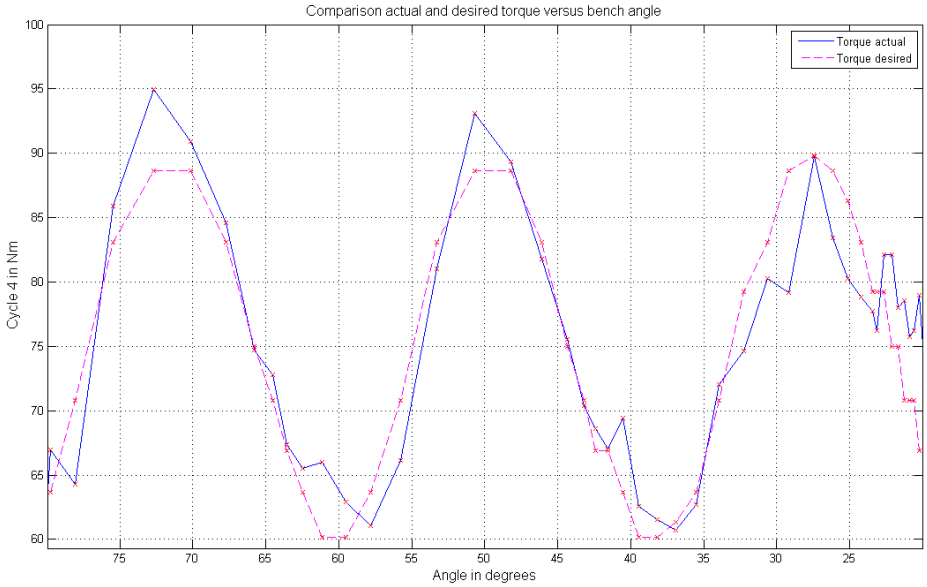

Figure 5.15: Results: Comparison Actual and Desired Torque. The actual torque in blue follows the desired torque in dotted magenta in a promising manner, which is a proof that it is possible to vary the actual torque as desired.

torque is constant at 60 Nm for all speeds:

$$T_{frict} = 60Nm = const \tag{5.18}$$

The input power P_{inp} is calculated by using the weight-torque caused by the weights and lever arms shown in figure 5.7 times the actual angular velocity of the configuration:

$$P_{inp} = T_{human}(\alpha) \cdot \omega_{human} \tag{5.19}$$

The output power P_{out} is the power caused by friction P_{frict} plus the power caused by the current flow P_{el}:

$$\begin{aligned} P_{out} &= P_{frict} + P_{el} \\ P_{out} &= T_{frict} \cdot \omega_{human} + I_{generated} \cdot V_{generated} \\ P_{out} &= T_{frict} \cdot \omega_{human} + I_{measured} \cdot (V_{measured} + V_{diode} + I_{measured} \cdot R_i) \end{aligned} \tag{5.20}$$

Where the constantly assumed friction-torque T_{frict} times the actual angular velocity of the configuration ω_{human} is the friction-power and the electrical Power P_{el} is the generated current times

the generated voltage. The generated current equals the measured current and the generated voltage is the measured voltage plus the voltage drop at the inner resistance and the diode, which is assumed to be constant.

Figure 5.16 shows the result of the input and output power calculation. The red dashed line is the electrical power, the black doted line shows the power caused by a constant friction torque and the blue dash-dot line is the sum of these two curves. Ideally, the input power and output power would match approximately. Most likely, there is a difference caused by the assumption that the friction torque is constant for different speeds. One can see, that at the end of the cycle, where the system slows down as the generated torque is decreasing, the input and output power match almost exactly. The torque of the system was evaluated at these low turning speeds which corroborates this theory. Effects of the unknown rotational inertia of the system are not considered in this power comparison. Also, it is possible that motor constants like the speed constant k_v or the torque constant k_t are not exactly linear over the whole speed and torque range.

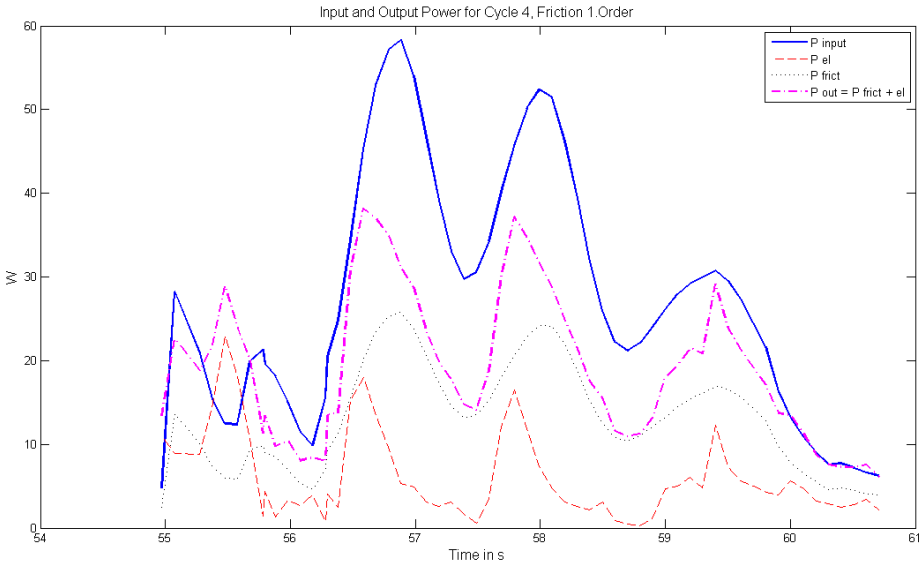

Figure 5.16: Results: Input and Output Power Comparison. The input power, caused by the weight torque, and the output power caused by the friction torque and the electrical power, match only at low turning speeds. The most likely cause for this discrepency is the fact that the friction torque varies based on turning speed.

Additionally a time delay of approximately 0.3 s occurs between the peak electrical power and the peak input power, which is not a mistake of the model. As the electrical power is changing, due to changes in the pulse width, the speed at the rotational shaft is delayed because of the large mechanical time constant due to a high rotational inertia. By evaluating this time delay, using

a step response signal, the mechanical time constant and inertia of the test arrangement can be evaluated, which was not done due to a lack of time.

As an alternative approach, the friction is modeled as a second order polynomial increasing with the turning speed to evaluate if a better model can be achieved as compared to a model with a constant friction. Again the friction is assumed to be 60 Nm at 10 rps motor speed:

$$T_{frict} = T_0 + k \cdot \dot{\alpha} \tag{5.21}$$

With a torque $T_0 = 57.7$ Nm and $k = 0.23$ Nm/rps, a better friction power is calculated and the input and output powers match better, which is shown in figure 5.17.

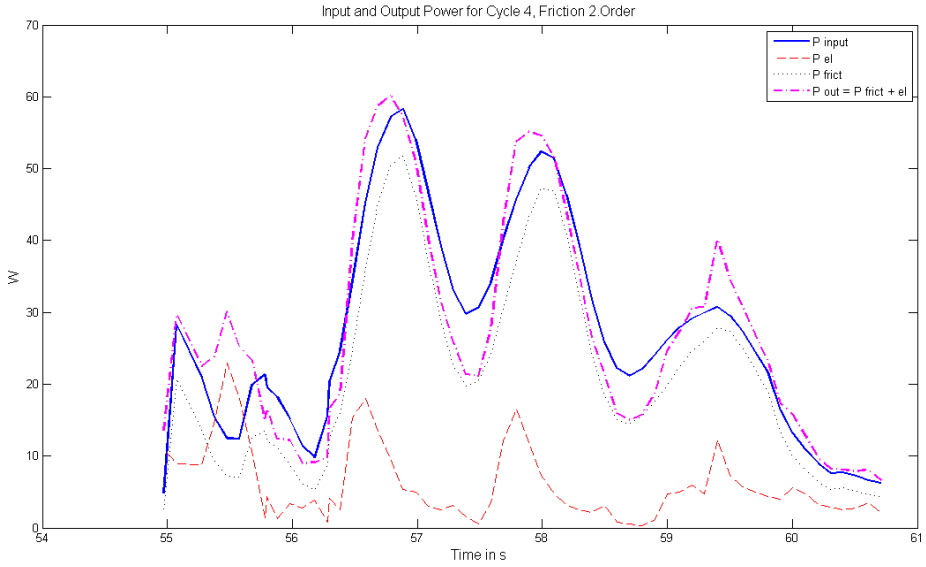

Figure 5.17: Results: Input and Output Power Comparison with the friction modeled as a function that depends on the speed. The input and output power still do not match perfectly.

Even modeling the friction as s function of speed, the input power and output power do not match exactly, but also in reality input and output power can not be exactly the same as, the system is accelerating and decelerating. A better way to evaluate is to calculate the energy input and output over one cycle. As the speed at the beginning and at the end of the cycle is approximately zero, no kinetic energy is released or stored in the system. Thus, the input and

output energy should be approximately the same:

$$E = \int_0^{\infty} P(t)\,dt \simeq \sum_{i=0}^{n} P_i \cdot \Delta t = \Delta t \cdot \sum_{i=0}^{n} Pi$$
$$E_{input} = \Delta t \cdot \sum_{i=0}^{n} P_{input} = 159.04J \tag{5.22}$$
$$E_{outpu} = \Delta t \cdot \sum_{i=0}^{n} (P_{frict} + P_{el}) = 159.004J$$

With the friction modeled with a second order polynomial, the energy input and output match exactly, which is not a proof, that it is exactly correct, but it is an improvement compared with the model that the friction torque is constant for all speeds. Thus, for a future project it is suggested to model the friction with second order polynomial or higher. Also, for more exact results, the inertia can be modeled as well especially if higher turning speeds are used.

In addition other parameters of the system, like torque and speed constants, the exact behavior of the diode and the rotational inertia, need to be more investigated for the actual leg extension/curl device, which can be done after a system with lower friction is chosen and built.

Also a system with a faster reaction time would be desirable as high power/torque steps from one cycle to the next occur. The pulse width actualization time in the test arrangement is at 0.1 s or 10 Hz. With the existing xPC target system, sample rates of approximately 2 kHz causing a pulse width actualization time of 0.05 s or 20 Hz is possible at a pulse width resolution of 1 %. If the desired actualization time is lower, either a different control system with a faster sample rate or the a coarser level of resolution need to be chosen. Lastly, a PC104 board could be purchased that is dedicated to generating a fast PWM signal.

Another solution to control for the unknown effects of not exact and not exactly linear parameters would be the use of a torque or force controller for the test arrangement, which is described in more detail in the section "future work".

6 Conclusion

In the literature review, a large number of on-going knee device research projects are described underlining the need for such devices. Originally, the development of an active knee orthosis was the goal of this research project, but the literature review showed many working prototypes for active knee orthoses, but a lack of knee rehabilitation devices. Existing knee rehabilitation devices capable of providing the user with variable torque-angle characteristics are very expensive, and thus are only available for a small fraction of the people who need it.

A detailed investigation of the human knee describes the anatomic structure, biomechanics of muscles, human gait, and a background on knee rehabilitation. An average knee torque angle characteristic that varies torque based on the angle builds the basis for the following design considerations, as they are designed to meet this characteristic.

Also a new approach to describe the stiffness during gait which is called "Translational Potential Energy at the Knee" is described in the thesis. Muscles and tendons of the human body show an elastic behavior which can be investigated by modeling this behavior with an elastic spring and analyzing the stiffness e.g. during gait. In standard literature usually one side of this spring is assumed to be fixed in position, but this not the case for torque generation at the human ankle and knee as both sides of the "spring" are moving. Allowing both sides to move leads to constant stiffness sectors during human gait (0 - 50 %). If e.g. in an exoskeleton, a compliant actuator with a constant stiffness leads to constant speed phases during gait which is very desirable for motor usage as the necessary peak power decreases and the efficiency increases, which makes smaller motors and gearboxes possible. This behavior has never been described before at the knee to the knowledge of the author. The description and analysis will be important for future knee orthosis projects.

A new compliant actuator concept is described consisting of an elastic band whose length is actively changed by a motor. As the length of the band is changing, it's stiffness is actively changed as well. Some design approaches described in the thesis use such an actuator, but these approaches are modeled and not prototyped. This compliant actuator could be a suitable device for future projects and has never been described before to the knowledge of the author.

A wide design study evaluates different design proposals including possible knee orthoses. A decision in favor of a knee rehabilitation device was made and the focus lies on replacing the passive weights of an existing knee extension/flexion bench by an active element. A large contribution was in the development of six different design proposals which are studied in detail including: pulley

cable systems, variation of lever arms, magnetic brakes, a combination of a motor with springs, and finally a motor directly attached to the bench with a gearbox that allows the generation of positive power and braking. The final concept was built and tested.

For the realization and development of a prototype, a DC motor directly attached via gearboxes to a knee extension/curl machine, is used. The motor has to be controlled by applying power to it in "motor mode" (eccentric contraction, weight lowering) and dissipates electricity in "generator mode" (concentric contraction, weight lifting). Therefore an alternative approach to a standard four quadrant H-Bridge controller in combination with a regulated power source is used. In motor mode, a simple one quadrant controller with a simple power source can be used. Whereas for the generator mode, the generated energy is burned in high power resistors. In order to actively vary the necessary torque for the user, the resistor is switched on and off with a MOSFET controlled by a pulse width modulated signal calculated from one of the actual desired torque-knee angle curves. The advantages of this approach, besides the simplicity, is a possibility of charging a battery source which can be important e.g. for an exoskeleton project. In our online research, no projects using this PWM approach for varying the resistance of a generator were found.

After preliminary tests with the PWM generator mode showed promising results, a test arrangement was designed and built. The goal of the test arrangement was to evaluate if a leg extension/flexion bench using two controllers with a single motor is a suitable choice. One motor controller is used for motor mode and one is used for generator mode by varying a PWM generation based controller. For controlling of the device, a xPC Target system is used. Matlab/Simulink code and models can be used to generate C code, and a xPC target PC104 system is used to run the controlling algorithm in realtime.

The results of the tests on the arrangement show that a motor/generator combined with gearboxes can provide the desired variable torque-angle characteristics. The actual torque, generated by a MOSFET controlled by a PWM signal, followed the desired torque in a promising manner.

6.1 Future Work

As the test arrangement showed promising results, the next logical steps are building up a system where the actuation part is connected to a leg extension/curl bench. Once the system is built, tests with subjects can be started and comparisons between a conventional and a variable concept rehabilitation program can be started.

For the mechanical design, a different motor-gearbox combination with lower friction must

be chosen, as the necessary friction torque to move the system is already higher than the desired torque for hamstring actuation of an average 80 kg person. Also the model of the motor/generation system needs to be evaluated in detail as the test arrangement proved the function but several non-linearities and constants are not known in detail.

Because the current model-based calculation of the mechanical torque at the bench is based on several constants which are not exactly correct and linear and thus create errors between the model and reality, a different control structure could be used to improve the accuracy of torque generation. A much easier control approach for a future project could be a torque/force controller instead of the realized current controller. If the torque and not the current is controlled, several non linearities of the system are compensated by the control structure. With the knowledge of the actual torque or force at the user, used in a closed loop control architecture, the controlling algorithm can be simplified and would be more accurate. The new system would require a torque sensor at the output of the leg extension/curl bench.

All design considerations in this work focused on torque-angle (length) characteristics of the human knee muscles, but additionally the force-velocity characteristics could be considered. In the chapter section "Force-Velocity-Characteristics", it was shown that the maximum tension of human muscles varies significantly with different movement speeds and directions. Thus, also torque-velocity influences should be considered in a future project as well.

References

[1] Matlab r2007b documentation, 2007. xPC Target, Sensoray 526.

[2] C-leg product specifications. www.ottobockus.com, December 2010. Otto Bock Healthcare, Inc.

[3] Free walk orthosis and e-mag active product specifications. www.ottobock.de, December 2010. Otto Bock Healthcare, Inc.

[4] Funktionelle knieorthesen. www.Ossur.com, December 2010. Ossur Health care, Inc.

[5] Biodex multi-joint system-pro, setup/operation manual. www.biodex.com, April 2011. Biodex Medical Systems Inc.

[6] Body and solid inc. www.bodysolid.com, May 2011. Powerline Leg Extension and Curl Machine PLCE165X.

[7] Placid industries inc. www.placidindustries.com, May 2011. Magnetic Particle Brake - Specifications.

[8] Robowalker. www.yobotics.com/robowalker/robowalker.html, March 2011. 2000-2009 Yobotics, Inc.

[9] Springactive inc. www.springactive.com, April 2011. Copyright (C) 2010 SpringActive, Inc.

[10] Tutorial for biodex system multi-joint testing and rehabilitation system. www.biodex.com, April 2011. Biodex Medical Systems Inc.

[11] M. Albohm. Understanding and preventing noncontact anterior cruciate ligament injuries: A review of the hunt valley ii meeting, january 2005. *The American Journal of Sports Medicine*, 34(9):1512–1532, -09-30 2006.

[12] CL Baker. Cost effectiveness of anterior cruciate ligament reconstruction in young adults. *Clinical orthopaedics and related research*, (367):272–282, -10-01 1999.

[13] P. Beyl, J. Naudet, R. Van Ham, and D. Lefeber. Mechanical design of an active knee orthosis for gait rehabilitation. In *Rehabilitation Robotics, 2007. ICORR 2007. IEEE 10th International Conference on*, pages 100 –105, june 2007.

[14] A. Boehler. *Mechanics, control and testing of a robotic ankle foot orthosis for stroke rehabilitation.* 2008. Masters Thesis. Arizona State University.

[15] Jinzhou Chen and Wei-Hsin Liao. Design and testing of assistive knee brace with magnetorheological actuator. In *Robotics and Biomimetics, 2008. ROBIO 2008. IEEE International Conference on*, pages 512 –517, feb. 2009.

[16] A.M. Dollar and H. Herr. Design of a quasi-passive knee exoskeleton to assist running. In *Intelligent Robots and Systems, 2008. IROS 2008. IEEE/RSJ International Conference on*, pages 747 –754, sept. 2008.

[17] C. Fleischer and G. Hommel. A human exoskeleton interface utilizing electromyography. *Robotics, IEEE Transactions on*, 24(4):872 –882, aug. 2008.

[18] R. Flynn. The familial predisposition toward tearing the anterior cruciate ligament. *The American Journal of Sports Medicine*, 33(1):23–28, -01-01 2005.

[19] M. Frind. Brief overview of anatomy and physiology of the knee. factotem.org/library/database/Knee-Articles/Knee-anatomy-physiology.shtml, March 2008. On-Line Knee Library.

[20] L. Y. Griffin. *Rehabilitation of the injured knee.* Mosby, 1995.

[21] W. HERZOG. Lines of action and moment arms of the major force-carrying structures crossing the human knee-joint. *Journal of anatomy*, 182:213–230, -04-01 1993.

[22] J. K. Hitt. *A robotic transtibial prosthesis with regenerative kinetics.* PhD thesis, Arizona State University, 2008.

[23] M. A. Holgate. *Control of a robotic transtibial prosthesis.* 2009. PhD Thesis. Arizona State University.

[24] K. W. Hollander. *Design and control of wearable robot actuators.* PhD thesis, Arizona State University, 2005.

[25] P. Holzach. Epidemiology of knee injuries in alpine skiing activities. *Helvetica chirurgica acta*, 60(4):531–537, 1994.

[26] R.W. Horst. A bio-robotic leg orthosis for rehabilitation and mobility enhancement. In *Engineering in Medicine and Biology Society, 2009. EMBC 2009. Annual International Conference of the IEEE*, pages 5030 –5033, sept. 2009.

[27] J. Kragh. Gender differences in anterior cruciate ligament injury vary with activity. *The American Journal of Sports Medicine*, 35(10):1635–1642, -10-01 2007.

[28] M. Majewski. Epidemiology of athletic knee injuries: A 10-year study. *The knee*, 13(3):184–188, -06-01 2006.

[29] A. S. McIntosh, K. T. Beatty, L. N. Dwan, and D. R. Vickers. Gait dynamics on an inclined walkway. *Journal of Biomechanics*, 39(13):2491–2502, -01-01 2006.

[30] T. Nakamura and K. Kosuge. Model-based walking support system with wearable walking helper. In *Robot and Human Interactive Communication, 2003. Proceedings. ROMAN 2003. The 12th IEEE International Workshop on*, pages 61 – 66, oct.-2 nov. 2003.

[31] T. Nakamura, K. Saito, and K. Kosuge. Control of wearable walking support system based on human-model and grf. In *Robotics and Automation, 2005. ICRA 2005. Proceedings of the 2005 IEEE International Conference on*, pages 4394 – 4399, april 2005.

[32] J. Nikitczuk, B. Weinberg, P.K. Canavan, and C. Mavroidis. Active knee rehabilitation orthotic device with variable damping characteristics implemented via an electrorheological fluid. *Mechatronics, IEEE/ASME Transactions on*, 15(6):952 –960, dec. 2010.

[33] B. Paul. *Industrial Electronics and Control*. Prentice-Hall Of India Pvt. Ltd., 2004.

[34] J.E. Pratt, B.T. Krupp, C.J. Morse, and S.H. Collins. The roboknee: an exoskeleton for enhancing strength and endurance during walking. In *Robotics and Automation, 2004. Proceedings. ICRA '04. 2004 IEEE International Conference on*, volume 3, pages 2430 – 2435 Vol.3, april-1 may 2004.

[35] Bellman R. *Design and Control of a Wearable Robot to Actuate the Knee*. Human Machine Integration Laboratory, Arizona State University.

[36] G. Smidt. Biomechanical analysis of knee flexion and extension. *Journal of Biomechanics*, 6(1):79–80, -01-01 1973.

[37] J.S. Sulzer, R.A. Roiz, M.A. Peshkin, and J.L. Patton. A highly backdrivable, lightweight knee actuator for investigating gait in stroke. *Robotics, IEEE Transactions on*, 25(3):539 –548, june 2009.

[38] K. Suzuki, Y. Kawamura, T. Hayashi, T. Sakurai, Y. Hasegawa, and Y. Sankai. Intention-based walking support for paraplegia patient. In *Systems, Man and Cybernetics, 2005 IEEE International Conference on*, volume 3, pages 2707 – 2713 Vol. 3, oct. 2005.

[39] H. van der Kooij, J. Veneman, and R. Ekkelenkamp. Design of a compliantly actuated exo-skeleton for an impedance controlled gait trainer robot. In *Engineering in Medicine and Biology Society, 2006. EMBS '06. 28th Annual International Conference of the IEEE*, pages 189 –193, 30 2006-sept. 3 2006.

[40] J. A. Ward, T. G. Sugar, and K. W. Hollander. Optimizing the translational potential energy of springs for prosthetic systems. *Submitted to Robotics in Medicine - Advances and Challenges*, 2011.

[41] M. Whittle. *Gait analysis: an introduction*. Butterworth-Heinemann, Oxford; Boston, 2002.

[42] D. A. Winter. *The biomechanics and motor control of human gait :normal, elderly and pathological*. University of Waterloo Press, Waterloo, Ont., 1991.

[43] D. A. Winter. *Biomechanics and motor control of human movement*. John Wiley and Sons, Hoboken, N.J., 2005.

[44] J. Withrow. Biomechanics of knee ligaments. *The American Journal of Sports Medicine*, 27(4):533–543, -08-01 1999. doi: pmid:.

[45] R. Wright. Anterior cruciate ligament tear. *The New England journal of medicine*, 359(20):2135–2142, -11-13 2008.

[46] A.B. Zoss, H. Kazerooni, and A. Chu. Biomechanical design of the berkeley lower extremity exoskeleton (bleex). *Mechatronics, IEEE/ASME Transactions on*, 11(2):128 –138, April 2006.

Glossary

ACL ..... Anterior Cruciate Ligament

AKROD ..... Active Knee Rehabilitation Orthotic Device

BLEEX ..... Berkeley Lower Extremity Exoskeleton

CAD ..... Computer Aided Design

CPM ..... Continuous Passive Motion

DARPA ..... Defense Advanced Research Projects Agency

DC ..... Direct Current

DOF ..... Degrees Of Freedom

EMG ..... Electromyography

HAL ..... Hybrid Assistive Limb

LOPES ..... Lower Extremity Powered Exo-Skeleton

MOSFET ..... Metal Oxide Semiconductor Field Effect Transistor

PAFO ..... Powered Ankle Foot Orthosis

PWM ..... Pulse Width Modulation

SPARKy ..... Spring Ankle with Regenerative Kinetics

Sworn Declaration

I hereby declare under oath that this master's thesis is the product of my own independent work. All content and ideas drawn directly or indirectly from external sources are indicated as such. The thesis has not been submitted to any other examining body and has not been published.

Place, date and signature of the student

APPENDIX

A Test Arrangement Simulink, Matlab Code

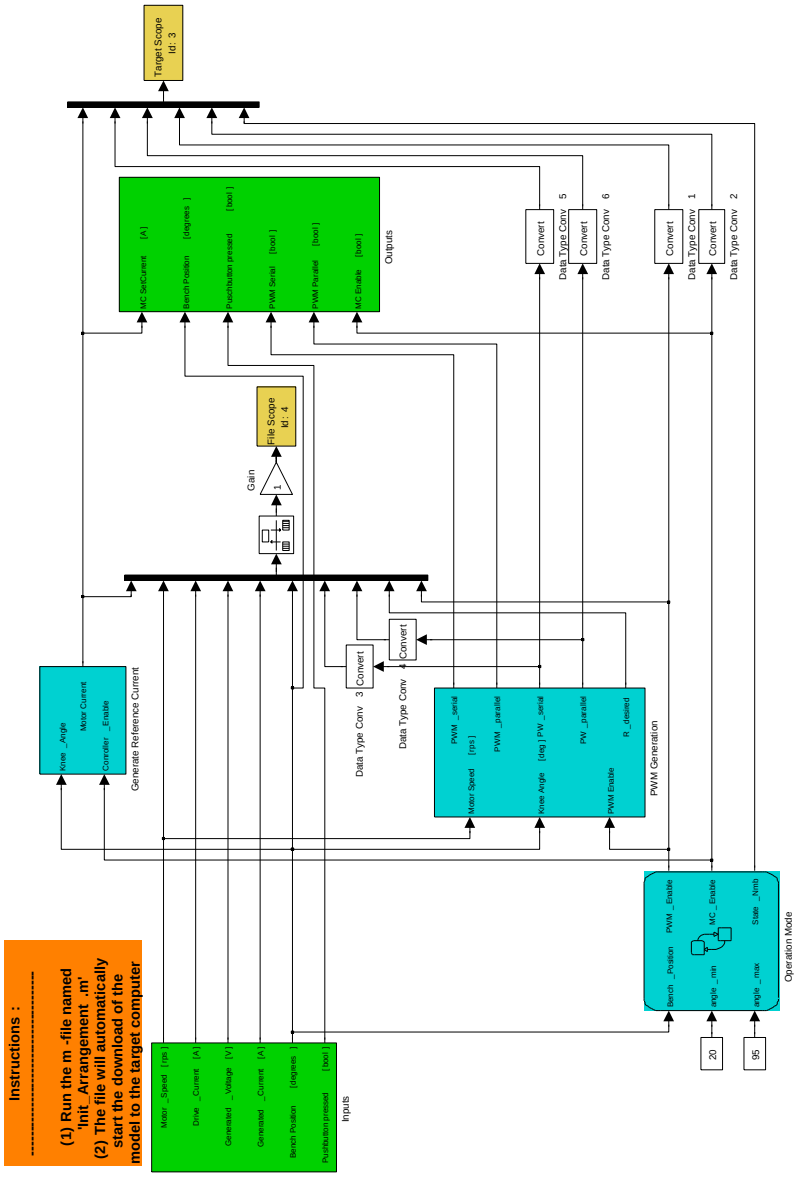

Figure A.1: Test Arrangement Control: Main

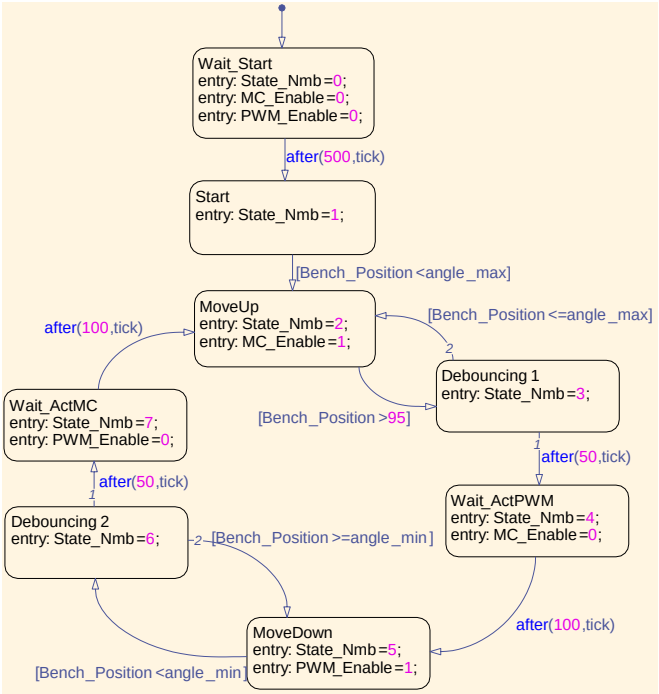

Figure A.2: Test Arrangement Control: Mode Control

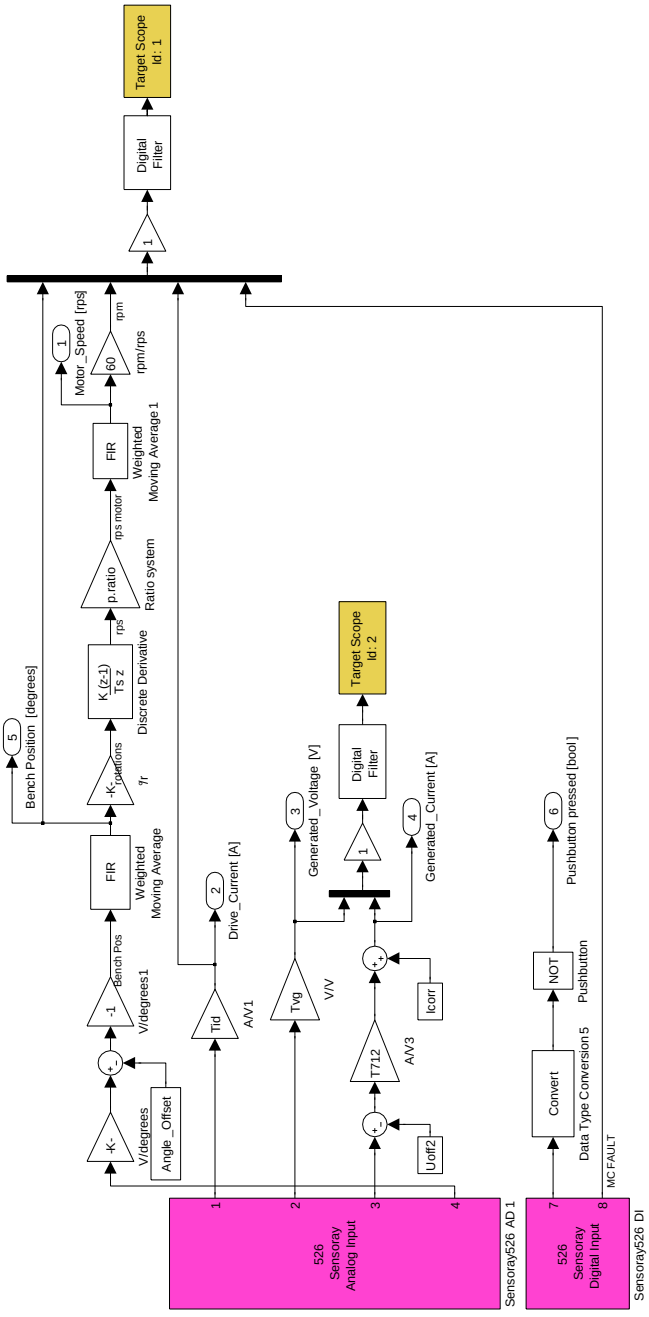

Figure A.3: Test Arrangement Control: Inputs

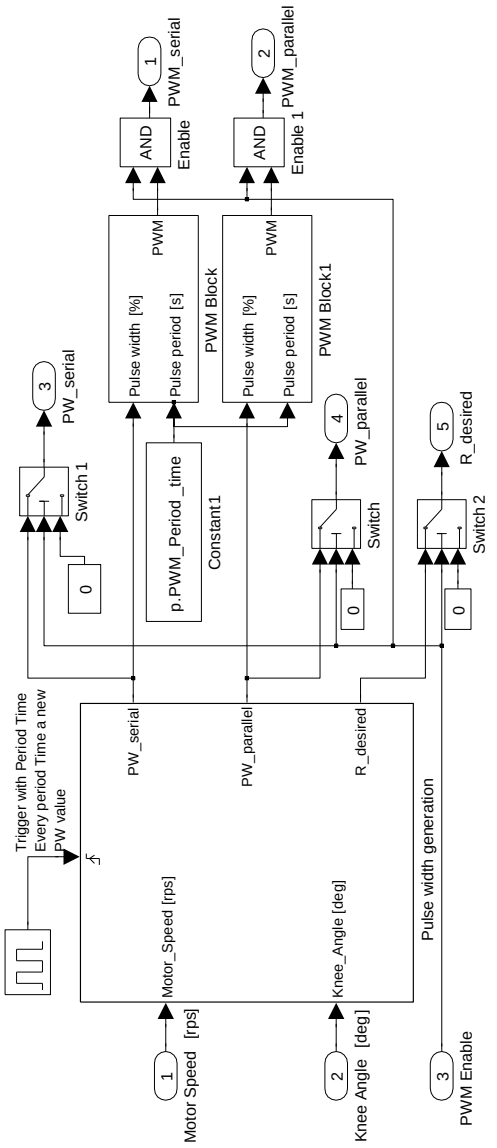

Figure A.4: Test Arrangement Control: PWM Generation 1

```
function [PW_serial, PW_parallel, R_desired] = PW_Generation(rps_motor, Knee_Angle,↙
Torque_Generator,Kt,Kv,R_serial, R_parallel)
% This block supports the Embedded MATLAB subset.
% See the help menu for details.
% Calculate new pulse width (PW) Signals every 0.1 s


% Desired index
index = round(Knee_Angle)+1;

% Index too high?
if (index) > length(Torque_Generator)
    index = length(Torque_Generator); % Override angle to the highest possible
end

% Take the actual Torque
Torque_Gen = Torque_Generator(index);

% Desired ohmic resistor
if Torque_Gen>0
    R_desired = abs(rps_motor) * 60 * Kt/(Kv*Torque_Gen);
    % Calculate pulse width
    PW_serial = round(R_serial/R_desired*100);
    PW_parallel= round(R_parallel/R_desired*100);
else
    R_desired = 0;
    % Calculate pulse width
    PW_serial = 0;
    PW_parallel = 0;
end

% Limit Pulsewidth between 0% and 100%
if PW_serial<0
   PW_serial = 0;
elseif PW_serial>100
   PW_serial = 100;
end
if PW_parallel<0
   PW_parallel = 0;
elseif PW_parallel>100
   PW_parallel = 100;
end

% Only one Mosfet will be triggered
if PW_serial<100
    PW_parallel = 0;
else
    PW_serial = 0;
end
```

Figure A.5: Test Arrangement Control: PWM Generation Function

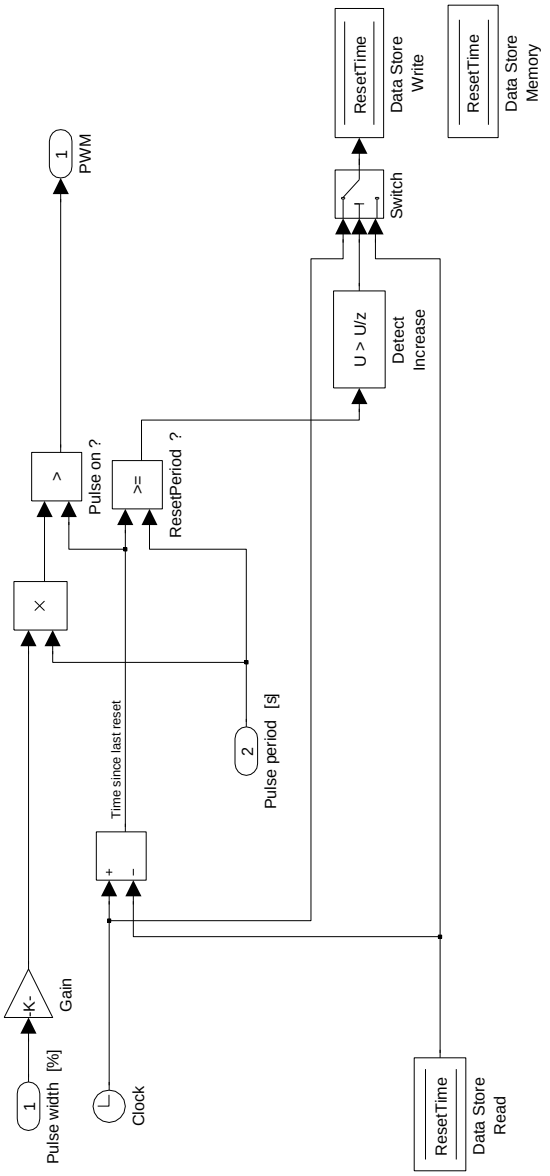

Figure A.6: Test Arrangement Control: PWM Generation Timer

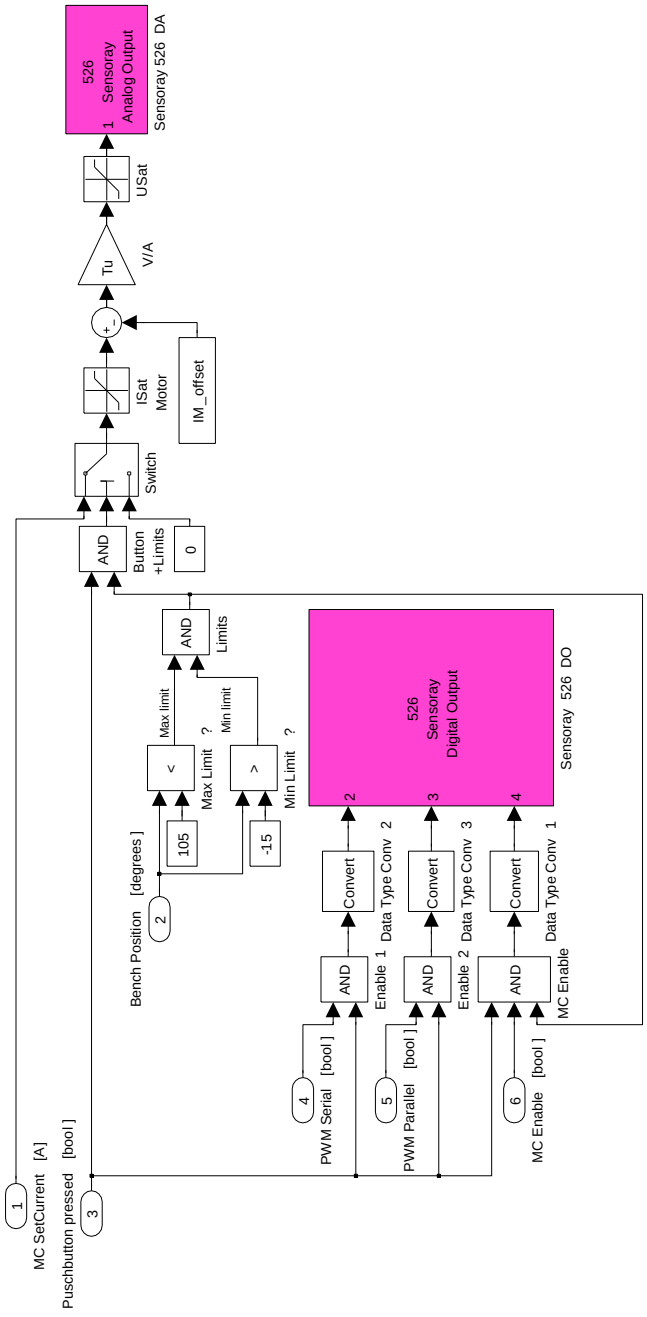

Figure A.7: Test Arrangement Control: Outputs

```
function p=parameters
% Parameteres for Test Arrangement

%% Input Parameters FIRST CIM Motor
p.Kt = 0.0182; % Nm/A
p.Kv = 443; % RPM/V

p.Ri = 0.175; % measured
p.R_nominal = 1.147; % Ohm
p.R_Power_lines = 0; % Assumed to be in the measured Resistors!
p.U_diode = 0.52;
p.R_diode = p.U_diode/1.5; % = 0.347 Ohm, assued to be constant Voltage and Current↙
at Shottky Diode 1N5819
p.R_serial = p.Ri+p.R_nominal+p.R_Power_lines+p.R_diode;
p.R_parallel = p.Ri+p.R_Power_lines+p.R_diode;

p.Imax_Motor = 19.8; % Datasheet motor
p.Imin_Motor = -2; % mass is helping moving dowm

%% Motor gearbox + worm gearbox
ratio_motor_GB = 64;
ratio_worm_GB = 10;
p.ratio = ratio_motor_GB*ratio_worm_GB;
p.Friction_Torque_Human = 60; %60 Nm

%% Define torque profile
p.alpha = linspace(0,110,111); % Have to start with zero!! simulink

p.m = (28.7+30)*0.4535; % kg
p.g = 9.81; % m/s^2

% Lever arms, test arrangment
p.r1 = 0.471; % m
p.r2 = 0.223;
```

Figure A.8: Test Arrangement Control: Parameters 1

```
Torque_1 = p.m*p.g*p.r1*sin(p.alpha*pi()/180);
Torque_2 = p.m*p.g*p.r2*cos(p.alpha*pi()/180);
p.Torque_Human = Torque_1 + Torque_2; % Torque generated by the weights

p.Friction_Torque_Motor = p.Friction_Torque_Human/p.ratio;

% Desired motor and generator torque
Torque_fact_motor = 1.1; % In order to get a movement up
%Torque_fact_generator = 0.3; % In order to get a movement down
p.Torque_Motor = (p.Torque_Human + p.Friction_Torque_Human)/p.↙
ratio*Torque_fact_motor;
p.Current_Motor = p.Torque_Motor/p.Kt;
%p.Torque_Generator = (p.Torque_Human - p.Friction_Torque_Human)/p.↙
ratio*Torque_fact_generator;

% Generate Sinus pattern
sinus_x_values = linspace(0,10*pi(),111);
sinus_y_values = (sin(sinus_x_values)+1)*15;
p.Torque_Generator  = sinus_y_values/p.ratio;

% Period Time for PWM
p.PWM_Period_time = 0.1; % sec

% Desired torque for Human
p.Torque_desired_Human= p.Torque_Generator*p.ratio;
```

Figure A.9: Test Arrangement Control: Parameters 2

```
% This function initializes all variables for the
% corresponding model file.
% ------------------------------------------------------------------------
% Created: 04/11/2011
% Author: Alexander Boehler addapted for PWM TEST ARRANGEMENT Sebastian Bereuter
% Spring Active
% Doc. No.: T0005-02-1-0100
% Last Revised: 05/03/2011
% Version: 1.00
% Change History: -
% ------------------------------------------------------------------------

clc;
clear all;
close all;

% Load parameters
p=parameters();

modelfile='Test_Arrangement';

disp('SIMULINK INITIALIZATION FILE')
disp('-----------------------------------------------------')
disp(sprintf('Supported Model: %s\n',modelfile))

% Fundamental Sampling Time [s]
Tsa=1e-3;

% Data Sampling Time [s]
Tsd=1e-3;

% End of Execution [s]
Tex=5*60;

% Raw Data Directory
rdata_dir='D:\Master_Thesis\Control\Laboratory\Data';
```

Figure A.10: Test Arrangement Control: Init Arrangement 1

```
%% MA3 Encoder Analog [V/°]
% Range 0 - 5 V --> 0 - 360 degrees
T_MA3 = 360/5;
Angle_Offset = 243+9-7-20-10-5-8-5; % Degrees due to encoder offset
Angle_Average_Filt_Nmb = 500;
Angle_Average_Filt= linspace(1/Angle_Average_Filt_Nmb,1/Angle_Average_Filt_Nmb,↙
Angle_Average_Filt_Nmb);
Speed_Average_Filt_Nmb = 500;
Speed_Average_Filt= linspace(1/Speed_Average_Filt_Nmb,1/Speed_Average_Filt_Nmb,↙
Speed_Average_Filt_Nmb);

%% Conversion from current command to A/D volts [V/A]
% AZBE40A8 Imax=40A, Ref=+/-10V
IM_offset = 0.4; % 0.4 A offset!
Tu=0.25*.7166;%*0.7166 from test

%% Maxon ADS50/10 Current Monitor Conversion Constant [A/V]
Tid=-13.3; % 13.3 A/V datasheet

%% ACS712 Conversion Constant [A/V]
T712=1/0.133; %A/mV
Uoff2=0.52;%2.478; % Sebastian
Icorr = 0.01;% -0.03; %0.08; % Offset Sebastian

%% Generated Voltage Divider Circuit [V/V]
Tvg=2;

%% Filter for Display on Scope
wf=3;%5;
[numF,denF]=butter(2,wf*(Tsa*2),'low');

%% Download to Target

disp('Starting build...')
pause(2)

rtwbuild(modelfile)
```

Figure A.11: Test Arrangement Control: Init Arrangement 2